THE PALEOECOLOGY AND FIRE HISTORY
FROM CRATER LAKE, COLORADO:
THE LAST 1000 YEARS

By Charles T. Mogen

A Thesis

Submitted in Partial Fulfillment

of the Requirements for the Degree of

Master of Science

in Environmental Science and Policy

Northern Arizona University

August 2018

Approved:

R. Scott Anderson, Ph.D., Chair

Nicholas P. McKay, Ph.D.

Darrell S. Kaufman, Ph.D.

Abstract

High-resolution pollen, plant macrofossil, charcoal and pyrogenic Polycyclic Aromatic Hydrocarbon (PAH) records were developed from a 154 cm long sediment core collected from Crater Lake (37.39°N, 106.70°W; 3328 m asl), San Juan Mountains, Colorado. Several studies have explored Holocene paleo-vegetation and fire histories from mixed conifer and subalpine bogs and lakes in the San Juan and southern Rocky Mountains utilizing both palynological and charcoal studies, but most have been at relatively low resolution. In addition to presenting the highest resolution palynological study over the last 1000 years from the southern Rocky Mountains, this thesis also presents the first high-resolution pyrogenic PAH and charcoal paired analysis aimed at understanding both long-term fire history and the unresolved relationship between how each of these proxies depict paleofire events.

Pollen assemblages, pollen ratios, and paleofire activity, indicated by charcoal and pyrogenic PAH records, were used to infer past climatic conditions. Although the ecosystem surrounding Crater Lake has remained a largely spruce (*Picea*) dominated forest, the proxies developed in this thesis suggest there were two distinct climate intervals between ~1035 to ~1350 CE and ~1350 to ~1850 CE in the southern Rocky Mountains, associated with the Medieval Climate Anomaly (MCA) and Little Ice Age (LIA) respectively. The MCA was a period of increased aridity, temperature, and regional fire activity, whereas the LIA was wetter, cooler and experienced decreased regional fire activity. The paired charcoal - pyrogenic PAH record indicates that these paleofire proxies follow similar general trends in regional fire patterns (i.e. indicate increased or decreased fire activity, respectively), but that peak concentrations do not correspond to each other. This suggests that these two paleofire proxies record different paleofire events. The vegetation and fire history inferred from Crater Lake sediments

demonstrate that centennial and sub-centennial scale climate variability can be determined from high elevation pollen assemblages, pollen ratios, plant macrofossil, charcoal, and pyrogenic PAH proxies.

Table of Contents

List of Figures

List of Tables

List of Appendices

Acknowledgements

Financial support for this project was provided by the Northern Arizona University College of International Education, the NAU School of Earth Sciences and Environmental Sustainability Quaternary Studies Fund, the Tom and Rose Bedwell Earth Physics Scholarship, the University of Glasgow Biomarkers for Environmental and Climate Science (BECS) Laboratory, and the Wyss Scholars Foundation.

In addition to the generous financial support I received, this project would not have been possible without the help, guidance, and support of so many wonderful people. I would like to wholeheartedly thank Dr. R. Scott Anderson for giving me the opportunity to continue my education at NAU in the Lab of Paleoecology, and for invaluable guidance he provided every step of the way during this project. I would also like to express my deepest gratitude to both Dr. Nicholas P. McKay and Dr. Darrell S. Kaufman who served as thesis committee members throughout this project, and whose thorough and thoughtful reviews of my manuscript were indispensable to this project. Additionally, if it were not for Dr. McKay's invitation to join him and a fellow student on a Fall 2015 trip to the San Juan Mountains, this project at Crater Lake may never have materialized.

In addition to my committee members I would like to thank Dr. Jaime Toney at the University of Glasgow for allowing me to utilize her lab facilities and other resources to complete pyrogenic PAH analysis. To Harry Jackson, the BECS laboratory technician, and lab members Dr. Julien Plancq and Philippe Nauny, who took time out of their busy schedules to guide me through the laboratory processes and PAH analysis, I cannot thank you all enough for your assistance. I would like to extend a special thank you to Katherine Whitacre in the Sedimentary Records of Environmental Change Lab at NAU who helped with radiocarbon sample preparation and processing. I also want to thank Cody Routson and his beautiful family. They helped me to recover the sediment core that was used in this study, and Cody graciously provided data that helped me interpret my own. A very big thank you to Ethan Yackulic who partnered with me in the field and in the lab to collect and analyze some prime high altitude lacustrine Colorado mud, and for his thoughtful insights where both of our thesis projects overlapped. To Cole Edward Webster, thank you for sharing many hours and even more laughs in the lab as we worked through or respective projects. To Hannah Kolus, thank you for all of your help running programs in MATLAB and R, without which I would have lost my mind, and for all of your helpful suggestions as I prepared to defend and write my final manuscript.

To Ryan Lima, Katie Junghans, Jesse Webber, Aaron Weintraub, Tyler and Casey Jones, Michael Meihaus, Steph Arcusa, Andrew Platt, Danny and Bryan Foley, and so many others: Thank you! I have been incredibly fortunate to have found such an amazing, eclectic, supportive group of friends here in Flagstaff. You have made me feel at home from day one, and there is never a dull moment with this crew. For that I cannot thank you enough.

Last but not least I want to thank my incredible parents and my four amazing brothers Philip, Will, Walker, and Sam. You have supported me not only throughout the duration of this project, but also in every step leading to it. Mom and Dad, thank you so much for giving me every opportunity to explore beyond our little neck of the woods in rural Virginia. You helped me to see how big and exciting this world is and have inspired me to explore as much of it as I can. To my brothers, thank you for always challenging me and inspiring me to be a better person. One day I hope to achieve the same reading level as all of you! I love you all.

Chapter 1: Introduction

1.1 Introduction

Rapid ecosystem transformations associated with anthropogenic global climate change and land surface disturbances pose critical challenges to researchers, land managers, and policy makers around the world. Average annual temperatures are rising around the globe as a result of increased concentrations of greenhouse gases in the atmosphere, and these temperature increases are observed to have been amplified at high latitude sites (Rangwala et al., 2013; Pepin et al., 2015). The same may hold true for mountainous, high elevation sites, even at mid-latitudes, where many ecosystems are confined to specific altitudinal zones (Beniston et al., 1997; Rangwala et al., 2013; Pepin et al., 2015). Mountainous regions, such as the southern Rocky Mountains, therefore, provide an ideal location for studying the effects and impacts of climate change on vegetation communities both in the past and the present (Grace et al., 2002; Thompson and Anderson, 2013).

The southern Rocky Mountains of North America host a diverse array of ecosystems and natural resources, including headwaters for both the Rio Grande and the Colorado Rivers (Costigan et al., 2000; Yuan et al., 2013). These river systems currently supply municipal water to over 40 million people in the water limited southwestern United States and northern Mexico (USDI, 2012; IBWC, 2016), and help to irrigate hundreds of thousands of hectares of arid agricultural land (CRWUA, 2017). Annual snowpack in the southern Rocky Mountains is the primary water source for both of these river systems (Seager and Vecchi, 2010), and is expected to decrease dramatically by the middle of the 21st century (Nydick et al., 2012). In addition to having a major impact on the high elevation ecosystems that harbor the majority of this moisture, future climatic changes will likely lead to a major water crisis for the large human populations that now inhabit the region.

As the Southwest becomes increasingly arid as a result of climate change, documenting how past climatic fluctuations have affected vegetation, fire, and other disturbance regimes provide researchers with a better understanding of the processes that will shape and influence ecosystem changes in the future (Anderson et al., 2015). Quaternary paleoecologic proxies provide essential baseline information for many investigations of contemporary ecosystems, as well as modern environmental issues and problems (Dietl and Flessa, 2011; Wingard et al., 2017). Although past environmental changes as determined by paleoecologic and paleoclimate proxies are not perfect analogues for future changes, paleoecologic studies allow for a more complete understanding and interpretation of longer term environmental and climatic changes than is currently available through limited historic records (Jackson et al., 2009). They also provide valuable information for estimating the impacts of future climate change and the potential extinction rates of modern species (Anderson et al., 2000; Elias, 2007; Jackson et al., 2009). Additionally, these studies provide evidence concerning how species adapt under a wide range of environmental conditions that differ from those of the present day, how climatic changes might affect the geographical dispersion of numerous flora and fauna species, and how climatic changes influence disturbance regimes such as wildfire frequency. They also provide an important tool with which to test and validate computer generated models that assess and project future changes to the biosphere and atmosphere (Husar et al., 1991; Elias, 2007; Dietl and Flessa, 2011).

Our knowledge of former environments of the San Juan Mountains, a sub-range of the southern Rocky Mountains of Colorado, has advanced greatly over the last four decades due to a large catalogue of work compiled by researchers across multiple disciplines, including palynology (Markgraf and Scott, 1981; Fall, 1992; Petersen, 1994; Vierling, 1998; Jiménez-

Moreno et al., 2010; Jiménez-Moreno and Anderson, 2012; Johnson et al., 2013), charcoal analysis (Toney and Anderson, 2006; Allen et al., 2008; Anderson et al., 2008a), geomorphology (Johnson et al., 2011), geochemistry (Routson et al., 2016), and dendrochronology (Allen et al., 1998; Grissino-Mayer et al., 2004; Routson et al., 2011), among others. As the southwestern United States experiences increased stress on both water and other natural resources as a result of population growth and a warming and increasingly arid regional climate, understanding how climatic fluctuations will affect vegetation and fire regimes is essential for researchers, land managers, and policy makers (Yuan et al., 2013; Chylek et al., 2014).

1.2 Research Objectives and Questions

1.2.1 Thesis Research Objectives

The objectives of the research presented here are (1) to reconstruct the vegetation and fire histories of the Crater Lake watershed in order to infer, based on responses by modern analogous ecosystems, how subalpine ecosystems were influenced by climatic variability over the course of the last 1000 years, and (2) to investigate the relationship between sedimentary charcoal and pyrogenic Polycyclic Aromatic Hydrocarbons (PAHs) as fire history proxies, and whether or not they record the same fire events. Although numerous palynological studies have been conducted at low temporal resolution from sites in the southern Rocky Mountains (Toney and Anderson, 2006; Allen et al., 2008; Anderson et al., 2008a, 2008b; Johnson et al., 2013; Herring et al., 2014), none have combined both high-resolution pollen and charcoal records on decadal scales like the data presented in this thesis. The impact of the Medieval Climate Anomaly (MCA) and Little Ice Age (LIA) climate intervals on vegetation and fire regimes in the southern Rocky Mountains remains unresolved (Dean, 1994), and much can be gained from detailed examination of higher resolution records that explore sub-centennial vegetation and fire history. To this end, this research presents a 1000-year (a) sedimentary pollen record with a resolution of ~30-35 years/sample, (b) sedimentary charcoal record with a resolution of ~7 years/sample, and (c) pyrogenic PAH record with a resolution of ~30-35 years/sample, between ca. 950 CE and 1875 CE. This is the first study to explore pyrogenic PAHs as a paleofire proxy in the southern Rocky Mountains.

Plant macrofossil analyses were also conducted. Analysis of both pollen and plant macrofossils can reduce biases in paleoecological interpretations due to the differences in the production, transportation, deposition and preservation between the two proxies (Anderson et al., 2000). Plant macrofossils are usually deposited close to the producing plant, whereas pollen can be transported over a range of distances, up to several tens or hundreds of kilometers from the source plant (Elias, 2007; Seppä, 2007).

Charcoal and PAH analyses were conducted to determine past fire occurrence in the Crater Lake basin. Several, high-resolution dendrochronological fire records spanning thousands of years have been developed at sites across the western US by examining fire scars on living and dead trees (e.g. Meko et al., 2007; Woodhouse et al., 2010; Marlon et al., 2012). However, these records are typically confined to certain long-lived tree species, specific ecosystem types, and specific well preserved archaeologic sites with post and beam construction. Subalpine spruce (*Picea*) - fir (*Abies*) forests typically experience stand replacing crown fires (Vankat, 2013) leaving few if any trees to be studied using dendrochronology.

Lithological descriptions, magnetic susceptibility (MS) measurements, and sediment accumulation rates (SAR) are also used to determine potential disturbances within the lake basin. Magnetic susceptibility (MS), which measures the ability of sediment to accept an induced magnetic charge (Dearing, 1999; Sandgren and Snowball, 2001), provides an estimate of the abundance of magnetic minerals in a particular sediment sample. Elevated MS and SAR in lake sediments may indicate increased deposition of minerogenic material because inorganic minerogenic sediment typically contains magnetic particles (Thompson and Oldfield, 1986).

1.2.2. Thesis Research Questions

The research presented in this thesis seeks to answer the following questions:

1. **How have the vegetation communities surrounding Crater Lake changed over the course of the last 1000 years?** Fluctuations in pollen percentages would indicate that there have been changes to the vegetation surrounding Crater Lake, as well as indicate changes to surrounding regional ecosystems. Since pollen can be transported several kilometers from the source plant (Elias, 2007; Seppä, 2007), ratios of important pollen taxa are employed to also investigate local and regional vegetation change, expansion and/or contraction of lower elevation species, and potential treeline fluctuations, and also to identify general periods of moisture and temperature change.
2. **What is the relationship between charcoal and selected pyrogenic PAHs that were analyzed from Crater Lake sediments, and do these two proxies record the same or different fire events?** Sedimentary pyrogenic PAH analysis has been utilized in only a handful of published studies to explore fire history (e.g. Page et al., 1999; Denis et al., 2012; Miller et al., 2017). As such, the relationship between charcoal, an established fire history reconstruction proxy, and pyrogenic PAHs remains unresolved in lacustrine sediments. Questions such as whether these two fire history proxies depict the same fire event simultaneously, asynchronously, or different fire events altogether, remain unanswered. The paired charcoal-pyrogenic PAH record presented in this thesis provides an opportunity to explore this novel approach to understanding fire history over long time periods, and how it relates to the well-established method of fire reconstruction using charcoal.

3. **Do the high-resolution pollen and sedimentary fire records presented in this thesis reveal anything unique about the last 1000 years compared to previous studies from mixed conifer to subalpine lakes and bogs in the southern Rocky Mountains?** Despite the lack of high-resolution pollen and charcoal records covering the last 1000 years, numerous paleoproxies (e.g. dendrochronology) have been utilized to study climatic variations across both the southern Rocky Mountains, and the greater Southwest region. Can any of the observed fluctuations in the high-resolution pollen and fire records developed at Crater Lake be ascribed to previously identified climatic variability over the last 1000 years, such as the MCA and LIA, in the southern Rocky Mountains?

1.3 Crater Lake Site Setting

1.3.1 Site Location

Crater Lake (37.39˚N, 106.70˚W; Figures 1.1, 1.2 and 1.3) is an oligotrophic lake located in the northeast corner of Archuleta County, Colorado. It is located at 3323 m asl in a north-facing cirque, immediately west of the continental divide. There are multiple small, seasonal inflows on the south end of the lake, and Crater Creek forms the outlet on the north end. The lake catchment is confined by a continuous bedrock ridge, with its two highest points being Montezuma Peak (4008 m asl) to the south-southeast of the lake, and Long Trek Mountain (3921 m asl) to the east. The catchment area is ~2.7 km^2, and Crater Lake has a surface area of ~0.08 km^2. Only ~0.6 km^2, or 20% of the basin is vegetated (Figure 1.3). The lake lies within 100 m of the upper treeline of an Engelmann spruce (*Picea engelmannii*) – subalpine fir (*Abies lasiocarpa*) forest.

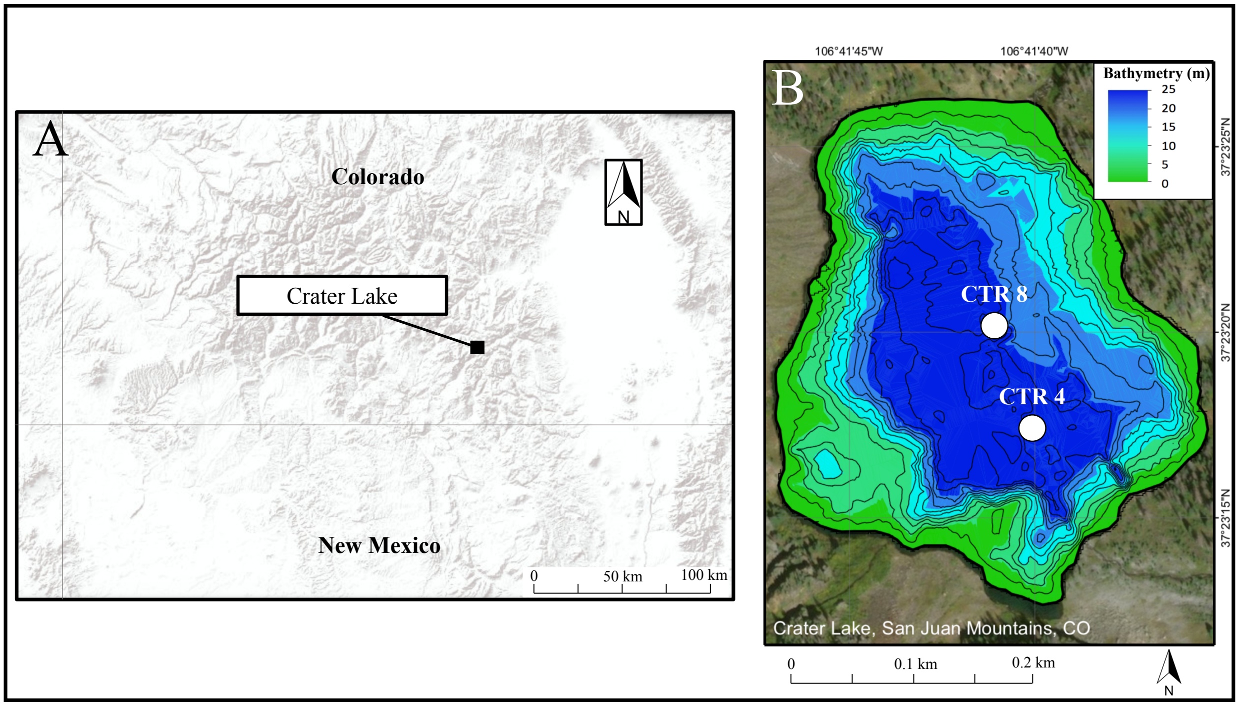

Figure 1.1: A. Location of Crater Lake, San Juan Mountains of southwestern Colorado. The lake occurs within the South San Juan Wilderness Area ~1.5 km west of the continental divide. Topographic relief base layer from Esri, DigitalGlobe, GeoEye, Earthstar Geographics, CNES/Airbus DS, USDA, USGS, AeroGRID, IGN, and the GIS User Community; accessed from databasin.org. **B.** The coring site for CTR 4, CTR 8, and Crater Lake bathymetry with 5 m contours.

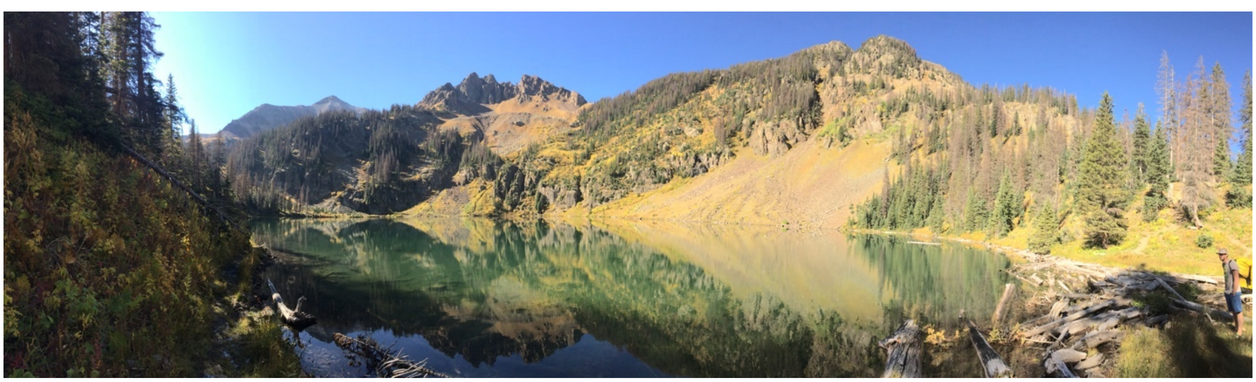

Figure 1.2: A panoramic view of Crater Lake and the catchment looking south-southeast from the lake outflow in September, 2015. The bare summit of Montezuma Peak (4008 m asl) is visible in the distant far left background, with a jagged, unnamed cirque in the central background. Note the numerous dead Engelmann spruce (*Picea engelmannii*) trees, and the steep talus slopes that surround much of the lake.

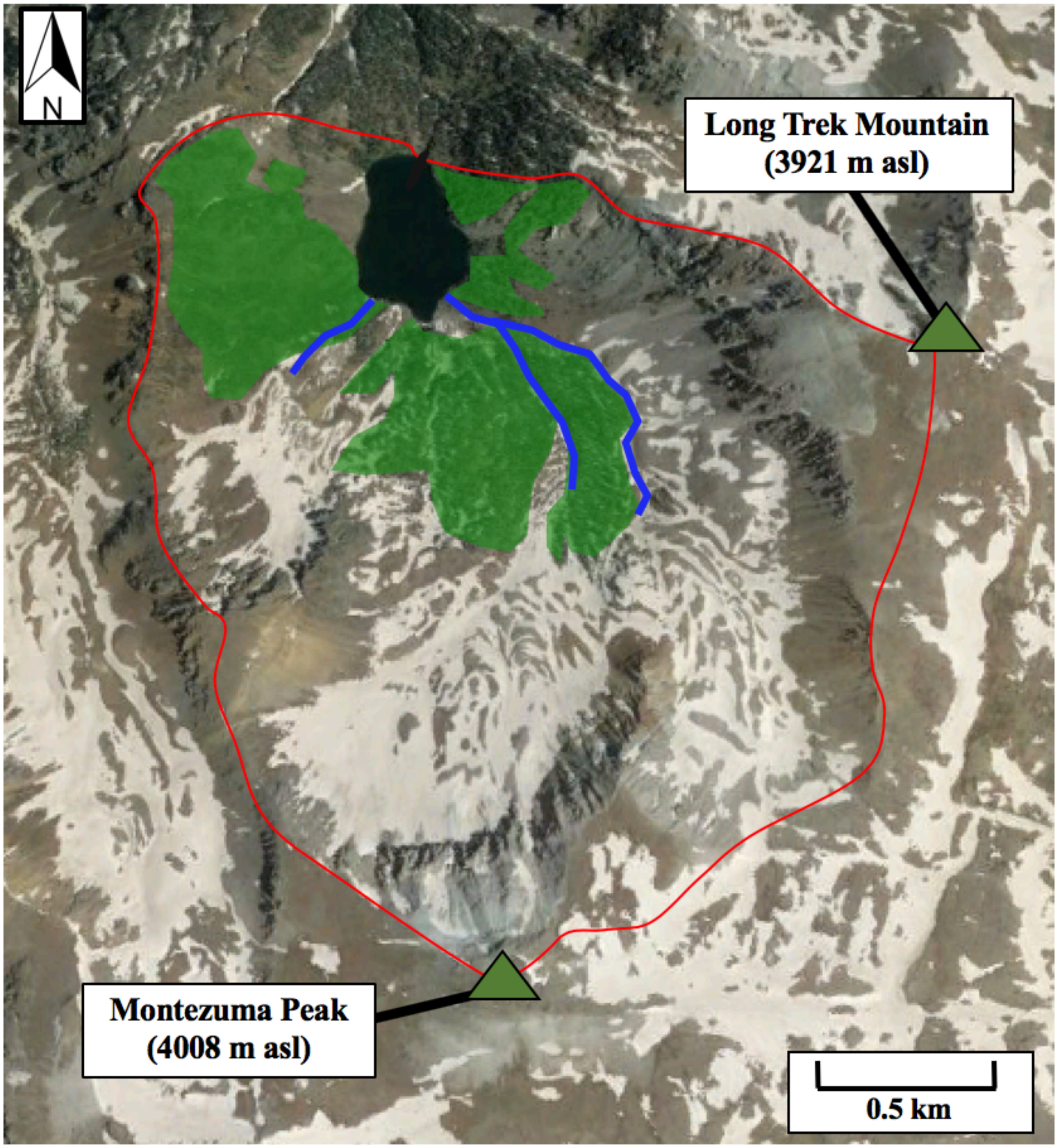

Figure 1.3: Satellite imagery of the Crater Lake catchment, outlined in red line (Google Earth Image, 2018 Digital Globe). Only ~20% (0.6 km^2) of the catchment is vegetated (green polygons), with the majority of the area being exposed talus (gray/brown), and white (snow). The three most prominent lake inflows are shown with blue lines. Montezuma Peak (4008 m asl) and Long Trek Mountain (3921 m asl) are the two most prominent topographic features surrounding the Crater Lake catchment.

1.3.2 Geologic Setting

Crater Lake lies on the western edge of the Summitville and Platoro Caldera Complexes (Lipman, 1975; Lipman et al., 1996). The regional bedrock geology is comprised primarily of hydrothermally altered intrusive intermediate volcanic rocks (Steven et al., 1974). Crater Lake itself is confined by a monzonite stock (known as the Bear Creek stock) and a vent facies of the Conejos Formation (Steven et al., 1974), both of which are Oligocene in age. The slopes immediately surrounding Crater Lake are covered in talus fields comprised of the underlying igneous, and meta-igneous parent material. Rock glaciers are present throughout the San Juan Mountains (Mateo, 2017), including in higher elevation areas at the southern end of the Crater Lake catchment (Figure 1.3).

Deglaciation in the San Juan Mountains occurred at different rates across the range following the end of the last glacial maximum (LGM), but most areas were clear of ice by ~15 ka (Carrara et al., 1984; Elias et al., 1991; Pierce, 2003). Isolated areas, such as north facing cirques, retained remnant alpine glaciers until ~12 ka (Guido et al., 2007; Johnson, 2012). Radiocarbon dates obtained from the bottom of a sediment core (CTR8) indicate that Crater Lake was free of ice prior to ~15.6 ka (Yackulic, 2017).

1.3.3 Modern Climate

The majority of the southern Rocky Mountains, including the San Juan Mountains, receive most of their annual precipitation from winter Pacific frontal storms and summer North American Monsoon (NAM) air masses (Mitchell, 1976; Mock, 1996; Adams and Comrie, 1997; Higgins et al., 1997; Barron et al., 2012). The intensity and amount of moisture associated with winter storms and the resulting annual snowpack, the primary source of water across much of the Southwest (Seager and Vecchi, 2010), is often dependent on Pacific winter storm tracks, as well as variations in El Niño – Southern Oscillation (ENSO), Pacific Decadal Oscillation (PDO), and Atlantic Multi-decadal Oscillation (AMO), which operate on decadal timescales (Mitchell, 1976; Mock, 1996; Higgins et al., 1997; Barron et al., 2012; Nydick et al., 2012; Chylek et al., 2014). Temperatures are moderated by elevation and moisture differences (Mitchell, 1976; Pase and Brown, 1994). Snowfall during the winter can exceed 5 m, and commonly persists into the late spring (Chambers and Holthausen, 2000), and summer rainfall associated with the NAM helps to maintain a cool and wet climate year-round (Adams and Comrie, 1997; Nydick et al., 2012).

Climate data are unavailable for the Crater Lake catchment. However, the mean annual temperature at 3353 m elevation in the eastern San Juan Mountains as derived from two subalpine spruce-fir SNOTEL sites (SNOwpack TELemetry; ~30 m higher in elevation than Crater Lake), each located 13.4 km from Crater Lake, is 1.08˚C (1984 – 2016). The monthly averages of both temperature and precipitation data at these sites were calculated and combined in R-Studio ignoring missing values (Figure 1.4). More information about the Lily Pond (37.38˚N, 106.55˚W, 13.4 km east of Crater Lake; http://wcc.sc.egov.usda.gov/nwcc/site?sitenum=580) and Wolf Creek Summit (37.29˚N, 106.48˚W, 13.4 km north of Crater Lake; https://wcc.sc.egov.usda.gov/nwcc/site?sitenum=874), including raw precipitation and temperature data, can be found at their respective SNOTEL websites listed above.

Average annual precipitation (1981-2016) from these two sites is 102.7 cm (Figure 1.4). Average monthly precipitation averages ~12.5 cm from November through March, but drops sharply during April and May, before reaching a minimum in June at approximately 2.5 cm. Beginning in July the area experiences increased precipitation associated with NAM, and average monthly precipitation exceeds 8 cm in August. Average precipitation declines again in September, before increasing in October leading into the wettest average season between November and March.

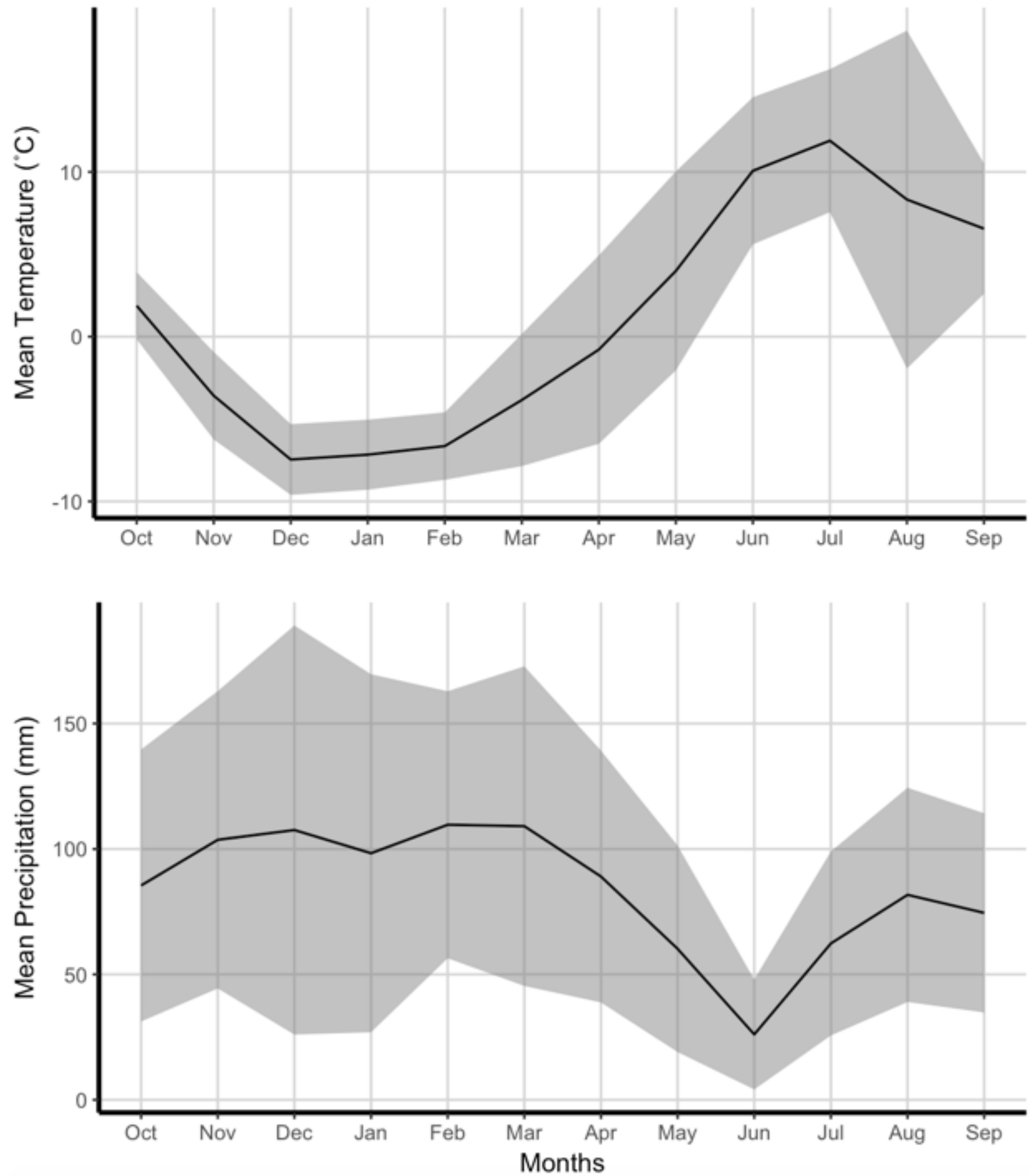

Figure 1.4: Mean monthly temperature (top) and mean monthly precipitation (bottom) data with one standard deviation ranges (shaded area) above and below the mean (black line) from two SNOTEL sites (Lily Pond and Wolf Creek Summit) both located 13.4 km from Crater Lake, Colorado.

1.3.4 Modern Vegetation

The lake lies within the Engelmann spruce-subalpine fir forest, dominated by *Picea engelmannii*. *Picea engelmannii – Abies lasiocarpa* forests in Colorado inhabit elevations between 2700-3600 m asl in the southern Rocky Mountains (Romme et al., 2009a). *P. engelmannii* generally dominates stands over *A. lasiocarpa* in the absence of disturbance (e.g. fire, blowdown, biotic agents; Vankat, 2013; Andrus, 2015). Other common arboreal species in the spruce-fir forest of the San Juan Mountains are quaking aspen (*Populus tremuloides*), Rocky Mountain bristlecone (*Pinus aristata*) and limber (*Pinus flexilis*) pines (Vankat, 2013), and at lower elevation sites, white fir (*Abies concolor*) and Colorado blue spruce (*Picea pungens*). Tree growth rates are slow due to long winters, and poorly developed soils (Pfister, 1972; Andrus, 2015).

Avalanches, blowdown events, bark beetle outbreaks, forest fires, and human influences are the primary disturbances that impact subalpine forests (Kulakowski and Veblen, 2007; Vankat, 2013; Andrus, 2015). These disturbances operate under widely different spatial and temporal scales, and produce heterogeneous forest composition and structure (Andrus, 2015). Avalanches operate on an annual basis, prohibiting forest development in established avalanche chutes (Veblen et al., 1994). Blowdown events occur as the result of wind storms and can range in areal extent from a single tree to multiple hectares (Veblen et al., 1989). Blowdown events increase the risk of both fire and fire severity (Kulakowski and Veblen, 2007).

Large wildfire events and widespread bark beetle outbreaks are infrequent and likely operate on centennial scales (Veblen et al., 1994). Although the natural fire regime of spruce-fir forests in the Southwest remains unresolved (Allen, 2002; Vankat, 2013), the relatively cool and wet climate reduces the threat of frequent forest fires but generates large quantities of biomass that accumulate on the forest floor, which, when burned, can produce large, high severity, stand-replacing crown fires (Sibold et al., 2006; Margolis et al., 2007, 2011). Sedimentary charcoal records have indicated that stand replacing crown fires occurred every 100 – 200 years throughout much the Holocene (Anderson et al., 2008a). However, some research indicates that mixed severity fires may also occur in spruce-fir forests, particularly at lower elevations in transitional stands with mixed-conifer forests (Abolt, 1997; Fulé et al., 2003; Vankat, 2013). Although fire suppression has been practiced in forests across the western US for nearly a century, it does not appear to have affected the natural fire regime of subalpine forests (Sibold et al., 2006). There is no evidence of recent fire (e.g. fire scars, charred tree trunks, etc.) in the Crater Lake basin.

Virtually all of the mature *P. engelmannii* trees in the lake basin are dead as a result of a regional spruce beetle (*Dendroctonus rufipennis*) outbreak that began in the early 2000s (Figure 1.2; Andrus, 2015). Spruce beetles preferentially attack large diameter spruce, killing most of the dominant canopy trees, while leaving smaller diameter healthy understory trees (DeRose and Long, 2007; Andrus, 2015). No *Abies lasiocarpa* was identified at the lake, however, it is present in the forests immediately surrounding the basin and as krummholz at treeline outside of the basin along the continental divide.

In addition to *Picea engelmannii*, other species identified on August, 17, 2017, within the lake basin include, but are not limited to, mountain gooseberry (*Ribes montigenum*), blueberry (*Vaccinium* sp.), elderberry (*Sambucus microbotrys*), Queen Anne's lace (*Daucus carota*), poison hemlock (*Conium maculatum*), thick-leaf ragwort (*Senecio crassulus*), common dandilion (*Taraxacum officianale*), fleabane (*Erigeron* sp.), rose crown sedum (*Sedum rodanthum*), green gentian (*Frasera speciosa*), Richardson's geranium (*Geranium richardsonii*), corn lily (*Veratrum californicum*), fireweed (*Chamerion angustifolius*), yellow monkeyflower (*Mimulus guttatus*), wild strawberry (*Fragaria virginiana*), monkshood (*Aconitum columbianum*), subalpine larkspur (*Delphinium barbeyi*), Poaceae (grasses, including *Phleum*), alpine sorrel (*Oxyria digyna*), penstemon (*Penstemon* sp.), Fendler meadowrue (*Thalictrum fendeleri*), Colorado columbine (*Aquilegia coerulea*), and willow (*Salix* sp.) (terminology after Weber and Wittmann, 2012). A full list of plant species identified at Crater Lake can be found in Appendix 1.

The Southwest is defined by its diverse array of contrasting landscapes with unique biotic communities. Vegetation distributions in the Southwest are controlled primarily by elevational gradients and moisture availability (Daubenmire, 1938; Nydick et al., 2012; Vankat, 2013). Grassland and desert communities (below 1500 m asl), piñon pine (*Pinus edulis*)- juniper (*Juniperus*, Cupressaceae) woodlands (1500-2600 m asl), ponderosa pine (*Pinus ponderosa*; 2100-2600 m asl) forests, and mixed-conifer forests (2400-2900 m asl) are the primary vegetation communities that surround the spruce-fir forests of the southern Rocky Mountains at lower elevations (Romme et al., 2009a; Vankat, 2013). Table 1.1 provides a summary of these other regional ecosystems and the primary species that inhabit each.

1.4 Previous Research in the San Juan Mountains

1.4.1 Background

Vegetation distributions in the Southwest are controlled primarily by elevational gradients (Daubenmire, 1938; Nydick et al., 2012; Vankat, 2013). The regional expansion and contraction of vegetation communities at different elevations over time is therefore indicative of changes in regional climate. Much of our knowledge of former vegetation and fire regimes has come from sites within the mixed conifer and subalpine spruce (*Picea*) – fir (*Abies*) forests due to the greater abundance of small lakes and bogs that effectively preserve sediments at these high elevation locations. In addition to their relative abundance, paleoecologic records from subalpine sites are extremely useful to researchers because they are sensitive to fluctuations in treeline as a response to climatic changes (Grace et al., 2002; Thompson and Anderson, 2013). Records from subalpine lakes near treeline can detect elevational changes in vegetation regimes on a scale of hundreds to thousands of meters (Lynch, 1996).

Vegetation Type	Elevation (m)	Dominant Species
Grasslands - Desert	below 1500	Sagebrush (*Artemisia* sp.), saltbush (*Atriplex* sp.), bunch grasses (Poaceae spp.), mountain mahogany (*Cercocarpus* sp.), cliffrose (*Purshia* sp.), Mormon tea (*Ephedra* sp.), snowberry (*Symphoricarpos* sp.)
Piñon-Juniper Woodlands	1500 - 2600	Piñon pine (*Pinus edulis*), juniper (Cupressaceae spp.), oak (*Quercus* sp.), sagebrush (*Artemisia* sp.), saltbush (*Atriplex* sp.), bunch grasses (Poaceae spp.), mountain mahogany (*Cercocarpus* sp.), cliffrose (*Purshia* sp.), Mormon tea (*Ephedra* sp.)
Ponderosa Pine Forests	2100 - 2600	Ponderosa pine (*Pinus ponderosa*), juniper (Cupressaceae spp.), Gambel's oak (*Quercus gambelii*), bunch grasses (Poaceae spp.), mountain mahogany (*Cercocarpus* sp.), cliffrose (*Purshia* sp.), sagebrush (*Artemisia* sp.)
Mixed Conifer Forests	2400 - 2900	Douglas-fir (*Pseudotsuga menziesii*), ponderosa pine (*Pinus ponderosa*), white fir (*Abies concolor*), blue spruce (*Picea pungens*), southwestern white pine (*Pinus strobiformis*), limber pine (*Pinus flexilis*), aspen (*Populus tremuloides*), Gambel's oak (*Quercus gambelii*), sagebrush (*Artemisia* sp.)
Spruce-fir Forests	2700 - 3600	Engelmann spruce (*Picea engelmannii*), subalpine fir (*Abies lasiocarpa*), aspen (*Populus tremuloides*), Rocky Mountain bristlecone pine (*Pinus aristata*)
Riparian	below 3600	Willow (*Salix* sp.), alder (*Alnus* sp.), birch (*Betula* sp.), sedges (*Carex* sp.), rushes (Juncaceae spp.), corn lily (*Veratrum californicum*), fireweed (*Chamerion angustifolius*), green gentian (*Frasera speciosa*), Richardson's geranium (*Geranium richardsonii*)
Tundra Vegetation	above 3600	Lichens and forbs, such as ragwort (*Senecio* sp.) and cinquefoil (*Potentilla* sp.); krumholtz *Picea engelmanni*, *Pinus aristata* and *Abies lasiocarpa* can also be present

Table 1.1: Summary of regional vegetation life zones and the dominant plants (primarily arboreal) that inhabit each plant belt. Many species grow in multiple zones (e.g. *Quercus*, *Artemisia*, *Pinus ponderosa*) because environmental conditions, including moisture availability, can vary considerably across elevation gradients. Table adapted and augmented from Romme et al. (2009a).

Researchers have used a combination of pollen, plant macrofossil and charcoal stratigraphies to determine vegetation change and fire event history since the end of the LGM across the San Juan Mountains (Betancourt, 1990; Toney and Anderson, 2006; Anderson et al., 2008a; Jiménez-Moreno et al., 2010; Johnson et al., 2013). Dendrochronological and fire scar studies have also played a pivotal role in our understanding of regional climatic and fire history from sites located in lower elevation ponderosa pine (*Pinus ponderosa*) and mixed conifer forests, to high elevation bristlecone pine (*P. aristata*) stands at treeline (Forman et al., 2006; Meko et al., 2007; Pierce and Meyer, 2008; Woodhouse et al., 2010; Routson et al., 2011).

Virtually all of the published palynological and charcoal records from the San Juan Mountains explore changes through the entire Holocene with millennial and centennial scale resolution (Toney and Anderson, 2006; Anderson et al., 2008a; Jiménez-Moreno et al., 2010; Johnson et al., 2013). High-resolution studies that focus on centennial to decadal scale events, such as the Medieval Climate Anomaly (MCA) and the Little Ice Age (LIA), however, are rare. Although this review includes a brief overview of the vegetation and fire history of the San Juan Mountains since deglaciation, the primary focus is on the last 1 ka. This timeframe includes both the MCA and LIA climate intervals as defined by Masson-Delmotte et al. (2013). In addition, this introduction provides an overview on Polycyclic Aromatic Hydrocarbons (PAHs), which can potentially provide fire history researchers with a powerful new tool with which to study past fire events.

1.4.2 LGM to the Late Holocene in the Southern Rocky Mountains

During the LGM the San Juan Mountains were the southernmost range in the Rocky Mountains to support an ice cap with a reconstructed total volume of 5000 km^3 (Elias et al., 1991; Pierce, 2003; Guido et al., 2007). Deglaciation in the San Juan Mountains occurred at different rates across the range following the end of the LGM, but most areas were clear of ice by ~15 ka (Carrara et al., 1984; Elias et al., 1991; Pierce, 2003). Deglaciation likely ended by

~12.3 ka (Guido et al., 2007), with isolated areas, such as north facing cirques, retaining remnant alpine glaciers until ~12 ka (Guido et al., 2007; Johnson, 2012). As a result of deglacial timing, paleoecologic records across the southern Rocky Mountains vary in length, but only a handful extend into the late Pleistocene and beyond (e.g. Legg and Baker, 1980; Short and Elias, 1987; Anderson et al., 2014).

Following deglaciation, most sites were colonized first by tundra and/or steppe vegetation. The full glacial pollen record from Devlins Park on the Front Range of Colorado (Legg and Baker, 1980) revealed sagebrush (*Artemisia*) pollen dominated from ~22-12 ka with minor amounts of grasses (Poaceae), pine (*Pinus*), spruce (*Picea*), and juniper (*Juniperus*). These data, and low pollen concentrations, indicated that treeline during the late Pleistocene, following the onset of deglaciation, was much lower than modern elevation (Legg and Baker, 1980). In the San Juan Mountains, treeline is estimated to have been nearly 650 m lower than its modern elevation following deglaciation (Carrara, 2011).

During the Pleistocene-Holocene transition (~12-10 ka), vegetation at many sites shifted from steppe and open *Picea* parkland vegetation to increasingly dense *Picea-Abies* forests very similar to modern ecosystems (Toney and Anderson, 2006; Anderson et al., 2008a; Carrara et al., 2011; Johnson et al., 2013). Some sites also show an increase in fire events as recorded by charcoal concentrations (Toney and Anderson, 2006; Anderson et al., 2008a, 2008b). Anderson et al. (2008a) suggested two explanations for the increase in fire event frequency (FEF) during this time; (1) climate changes driven by orbitally induced shifts in insolation; and (2) rapid ecosystem changes as increasing numbers of arboreal species began to colonize higher elevation sites. Multiple sites in the southern Rocky Mountains also indicate higher lake levels during this timeframe, associated with warmer, wetter conditions (Jiménez-Moreno and Anderson, 2012; Johnson et al., 2013).

Despite multiple pollen analyses indicating a brief period of colder conditions between 11-9 ka that was dominated by winter precipitation (Vierling, 1998; Jiménez-Moreno and Anderson, 2012; Johnson et al., 2013), the early Holocene in the southern Rocky Mountains is interpreted as warming, and likely wetter, climatic conditions. Early Holocene warming occurred due to changes in solar insolation that also led to wetter summer conditions as a result of a strengthened NAM (Friedman et al., 1988; Anderson et al., 2008a; Jiménez-Moreno et al., 2011). These conditions allowed for the establishment of dense *Picea* and *Abies* dominated high elevation forests and led to an increase in treeline across the region (Carrara, 2011).

These *Picea*-*Abies* forests persisted through the mid-Holocene (~8.2-4.2 ka; Toney and Anderson, 2006; Anderson et al., 2008a; Johnson et al., 2013; subdivisions of the Holocene after Walker et al., 2012). Due to monsoonal precipitation, pines also expanded down-elevation during this period (Markgraf and Scott, 1981; Anderson et al., 2008a), as well as upward in elevation (Elias et al., 1991; Carrara, 2011). However, during the Holocene climatic optimum (HCO; ~9-5 ka), several sites across the southern Rocky Mountains experienced a dry interval that lasted for centuries to millennia. For example, lowered lake levels within Little Molas Lake, Colorado, ~6 ka (Toney and Anderson, 2006) and drying of the wetlands at Chihuahueños Bog, New Mexico, from ~8-6.5 ka (Brunner-Jass, 1999; Anderson et al., 2008b) are indicative of increased effective evaporation or reduced precipitation. Shuman et al. (2009) found similar results at lakes across the Rocky Mountains during the mid-Holocene, including at Hidden Lake, in northern Colorado, where mid-Holocene shorelines of small lakes (4-110 ha) were about 10 m lower than modern lake shore levels during this interval. Around 9 ka average summer temperatures are estimated to have been over 2°C warmer than present, and between 10.4-6.6 ka treeline was about 80 m higher than present in the San Juan Mountains (Elias et al., 1991; Carrara, 2011).

During the late Holocene (4.2 ka – present; Walker et al., 2012) *Picea*-*Abies* forests remained intact at high elevation sites across the southern Rocky Mountains (Toney and

Anderson, 2006; Anderson et al., 2008a; Johnson et al., 2013). Treeline, however, declined from the mid-Holocene maximum elevation and reached its present-day limits in the San Juan Mountains between 6.2-3.8 ka (Carrara, 2011; Johnson et al., 2011). Benedict et al. (2008) and Jiménez-Moreno et al. (2011) inferred a similar downward shift in treeline between 5-3.5 ka based on pollen and macrofossil analysis, respectively, from sites in northern Colorado. Despite a decline in treeline throughout much of the region during the late Holocene, at Hunters Lake and DeHerrera Lake, Colorado, Anderson et al. (2008a) found that there was an increase of lowland species pollen, such as piñon pine (*Pinus edulis*), in the pollen record. This was interpreted as an elevational range expansion of lowland species (Anderson et al., 2008a; Anderson and Feiler, 2009).

Although treeline declined to present elevations during the late Holocene, there was a brief shift to warmer-drier conditions at some sites around 4 ka, which has been interpreted as a major shift in annual regional precipitation patterns from being dominated by Pacific frontal winter storms prior to 10 ka, to being dominated by summer monsoonal storms until about 4 ka (Markgraf and Scott, 1981; Friedman et al., 1988). Johnson et al. (2011) inferred a decrease in temperature during the late-Holocene from the mid-Holocene, as well as an increase in the frequency of summer precipitation events as the result of a strengthened El Niño-Southern Oscillation (ENSO) cycle in the eastern San Juan Mountains (Johnson et al., 2013). The lack of long-term ENSO records and the poorly understood variability and complexity of the NAM, however, makes interpreting potential impacts on regional climate difficult (Johnson et al., 2013). Although it is clear that the late Holocene has been cooler than the mid-Holocene (Jiménez-Moreno et al., 2011), the relatively low resolution of most pollen and charcoal records make it difficult to determine whether rapid shifts in ecosystems occurred over much of the late Holocene.

1.4.3 The Last 1000 Years: Prominence of the MCA and LIA Climate Intervals

The MCA and LIA describe two climate intervals that occurred in the late Holocene between ~950-1250 CE and ~1450-1850 CE, respectively (Masson-Delmotte et al., 2013). Paleoclimatic and paleoecologic reconstructions, along with computer model simulations, have shown that several external factors such as orbital, solar (Eddy, 1976; Goosse et al., 2012) and volcanic (Mann et al., 1998) forcings, as well as internal variability, contributed to the climatic changes that were experienced during both the MCA and LIA (Masson-Delmotte et al., 2013; Andres and Peltier, 2016). Whereas the geographical extent and the exact causal mechanisms of these two intervals remains a topic of debate, recent research has suggested that there were no globally synchronous warm or cold intervals during the MCA and LIA respectively (PAGES 2k Consortium, 2013).

The scientific community's initial understanding of the MCA and LIA was influenced by and developed from instrumental records and historical accounts from Europe (Matthes, 1939; Lamb, 1965; Grove and Switsur, 1994; Mann, 2002a, 2002b; Mann et al., 2009; White, 2017). Over the past few decades the addition of numerous studies using a variety of paleo-proxies from around the northern hemisphere, as well advances in paleo-proxy data and computer modeling, have changed our understanding of these intervals considerably (Smeardon and Pollack, 2016). Although average temperatures were similar to those experienced today during the MCA (Loisel et al., 2017), and average climatic conditions were cooler during the LIA in Europe (Mann, 2002a), current evidence does not support the conclusion that the MCA and the LIA were intervals of globally synchronous warmer and cooler climatic conditions (Masson-Delmotte et al., 2013; PAGES 2k Consortium, 2013). Instead the MCA and LIA were climatically and spatiotemporally complex in the Northern Hemisphere, including in the Southwest (Hughes and Diaz, 1994; Mann, 2002b; Mann et al., 2009; Masson-Delmotte et al., 2013; Young et al., 2015).

In North America there are a limited number of long instrumental climate records, with the oldest dating only to the 17th century CE (Mann, 2002a; White, 2017). Since the historical period in North America did not begin until the second half of the LIA, and it is impossible to draw conclusions about the climate based on the few extant historical accounts (e.g. Winship, 1896; White, 2017), virtually all of the information available to researchers about both the MCA and LIA come from high-resolution paleorecords (e.g. dendrochronological records). Although spatial and temporal constraints exist, these records can still tell us a great deal about North America during both of these climate intervals. Due to the aridity and a diverse array of contrasting landscapes, the Southwest has numerous relevant paleo-proxies. Additionally, the archaeological record presents an unparalleled opportunity to understand the complex and sophisticated social groups that inhabited the region before the first Europeans arrived, and how these groups were influenced and affected by regional climate despite no written records.

1.4.4 The Last 1000 Years in the Southwest

Dendrochronology and Drought

Arguably the most important tool for reconstructing recent climate history in the Southwest has been dendrochronology, which provides annual climate records reconstructed from long-lived trees, preserved ancient remnant wood, and wood from well-preserved archeological sites. For example, Woodhouse et al. (2010) identified a 12^{th} century CE Southwest drought that was more extensive temporally and spatially than any drought of the instrumental period. This drought greatly affected Colorado River streamflow, suggesting decreased snowpack in the southern Rocky Mountains. Average temperatures during the MCA displayed similar variability to that inferred from northern Europe (Woodhouse et al., 2010), with intervals of above and below average temperatures (Mann, 2002b).

Forman et al. (2006) identified severe regional droughts affecting southern Colorado during the same time interval as the MCA using eolian deposits and dendrochronological records. Using a tree-ring series of Rocky Mountain bristlecone pine (*Pinus aristata*) in the eastern San Juan Mountains, Routson et al. (2011) found that between 1000-1400 CE the region experienced increased aridity and drought frequency, including four of the ten driest 25-year intervals over the last 2.2 ka. The Salzer and Kipfmueller (2005) temperature reconstruction from northern Arizona suggested that MCA droughts were potentially influenced by warmer than average temperatures. Similarly, a high-resolution lacustrine dust record from Fish Lake, San Juan Mountains, suggests increased aridity during the same time interval as the MCA (Routson et al., 2016). Although it is clear that severe droughts were common during the MCA (950-1250 CE), it does not appear that they were exclusive to this time period and occurred during the LIA (1450-1850 CE) as well (Grissino-Mayer and Swetnam, 2000; Salzer and Kipfmueller, 2005; Routson et al., 2011)

Fire Records

Marlon et al. (2012) identified prominent peaks in forest fires from multiple western North American sites that occurred during the MCA, with a noticeable decline in fire activity during the LIA. Pierce and Meyer (2008) identified fire related debris flows in the middle Rocky Mountains during the MCA, and noted that, despite an increased number of low intensity fires, there was an overall decline in fire related debris flows during the LIA. At Hunters Lake, Colorado, and Brazos Ridge Marsh, New Mexico, Anderson et al. (2008a) found an increase in charcoal accumulation rates from ~950 to ~1300 CE, indicating increased regional fire activity during this interval. Increased charcoal accumulation rates might also indicate increased aridity in the southern Rocky Mountains during the MCA, supporting similar conclusions developed by other studies (Forman et al., 2006; Woodhouse et al., 2010; Routson et al., 2016).

However, some fire history records from the southern Rocky Mountains do not show distinct differences between the MCA and LIA periods. Neither Anderson et al. (2008b) nor Allen et al. (2008) identified significant change during the MCA or LIA in fire scar or charcoal records from two bogs in the southern Rocky Mountains of New Mexico. At Prater Canyon, in Mesa Verde National Park, Herring et al. (2014) found higher charcoal concentrations and accumulation rates during the MCA than at any other time period, but noted this could be a function of widespread human habitation of the area during that time. The peak in charcoal at Prater Canyon was followed by a decline, which reached minimum frequency during the LIA. The Mesa Verde area was largely abandoned by Ancestral Puebloans by the end of the MCA, allowing equivocal explanations on whether the Prater Canyon sedimentary changes are related to changes in natural fire regimes or human habitation (Herring et al., 2014).

Pollen Records

The temporal resolution of most pollen records of the region (Toney and Anderson, 2006; Allen et al., 2008; Anderson et al., 2008a, 2008b; Johnson et al., 2013; Herring et al., 2014) is not high enough to provide robust interpretations of decadal scale vegetation change over the last 1000 years. For example, the pollen record developed at Prater Canyon by Herring et al. (2014; ~167 years/sample), did not reveal any significant changes during the MCA or LIA climate intervals. Similarly, at two bog sites in Jemez Mountains of northern New Mexico, Anderson et al. (2008b; ~500 years/sample) did not find any clear indication of change in the pollen during the MCA or LIA climate intervals.

Over the last ~1000 years, most records here (e.g. Toney and Anderson, 2006; Anderson et al., 2008a, 2008b; Johnson et al., 2013) suggest vegetation communities were very similar, if not identical, to modern day *Picea-Abies* ecosystems despite some variability in annual precipitation and temperature from 3 ka to present day. Petersen (1994), however, examined high-resolution pollen (~55 years between samples) records from two sites in the adjacent La Plata Mountain range. Fluctuations in spruce (*Picea*)/pine (*Pinus*) and conifer/nonarboreal pollen ratios, as well as piñon pine (*Pinus edulis*) concentrations, were interpreted as climate driven changes during the MCA and the LIA (Petersen, 1994; Wright, 2006).

Archaeological Record

The considerable number of well-preserved archaeological sites throughout the Southwest provides us with another tool to explore past environment - human interactions. In fact, some of the strongest evidence for a variable MCA in the Southwest comes from the archaeological record. During this period, Ancestral Puebloans on the southeastern Colorado Plateau undertook massive building projects. For example, during this period the great houses in Chaco Canyon (850-1150 CE; Lekson, 1999a, 1999b), the large pueblos in the San Juan Basin of New Mexico (1090-1280 CE), and the iconic cliff dwellings near Mesa Verde, Colorado (1150-1285 CE; Benson and Berry, 2009; Schwindt et al., 2016) all took place. By the mid-12th century CE, however, sites such as Chaco Canyon were abandoned, and populations shifted north towards the San Juan Basin and Mesa Verde (Lekson, 1999a, 1999b; Benson and Berry, 2009). Here, communities continued to grow until the end of the 13th century CE, when virtually all sites in the Four-Corners region were abandoned (Plog, 1997; Schwindt et al., 2016).

Abandonments at many sites appear to have coincided with severe droughts during the MCA (Benson and Berry, 2009; Woodhouse et al., 2010; Schwindt et al., 2016). Following the MCA, populations from the Four-Corners had dispersed into new regions. By the onset of the LIA most sites were abandoned and protohistoric groups, whom the Spanish contacted during the mid-16th century, were becoming established (Plog, 1997).

Petersen (1994) and Wright (2006) argued that during the MCA the region was much more conducive to successful dry-land farming due to a longer growing season, increased precipitation in both the summer and the winter, and a larger potential growing zone than exists today. This interval of ameliorated climate came to an end during the LIA (Petersen, 1994; Wright, 2006). Although changes in regional climate were not the only impetus, it does appear to have influenced population dynamics and movements across the Southwest. Many of the peoples who left the Four-Corners region presumably moved towards the Hopi Mesas, the Rio Grande Valley of New Mexico establishing many of the modern pueblos that exist there to this day, and to the Mogollon highlands, which saw a dramatic population increase around this time (Plog, 1997; Monastersky, 2015). Future archaeologic studies and exploration of the topic will help to elucidate what drove native communities to move across the region and help further our understanding on the role climate has played.

Summary of Climate in the Southern Rocky Mountains over the Last 1000 Years

Several studies have explored Holocene paleo-vegetation and fire histories from mixed conifer and subalpine bogs and lakes in the San Juan and southern Rocky Mountains utilizing both palynological and charcoal studies (Figure 1.5). During both the MCA and the LIA climatic conditions varied considerably throughout the Northern Hemisphere (PAGES 2k Consortium, 2013), including in the southern Rocky Mountain region. During the MCA some areas in the southern Rockies experienced increased aridity, fire activity, and slight shifts in vegetation composition (Petersen, 1994; Woodhouse et al., 2010; Marlon et al., 2012; Routson et al., 2011; 2016). During the LIA some areas experienced decreased fire activity and changes in vegetation compositions indicative of decreased aridity (Petersen, 1994; Armour et al., 2002; Anderson et al., 2008a; Bigio et al., 2010; Anderson et al., 2012; Marlon et al., 2012; Johnson et al., 2013; Herring et al., 2014; Loisel et al., 2017). Certain researchers, including Dean (1994), who examined multiple proxy records from the Southwest, have concluded that there is no evidence of significant climate changes during the MCA or LIA. Historical accounts from Spanish expeditions in the region during the LIA suggest that regional climate was defined by arid and cold conditions, including exceedingly harsh winters (e.g. the Rio Grande freezing over), throughout the late 16th century CE (Flint and Flint, 2005; White, 2017), but no instrumental records exist to confirm these accounts. Continued research in the paleoenvironmental conditions in the southern Rocky Mountains using high-resolution pollen and charcoal records, like this study, will increase our understanding about how vegetation responded during the MCA and LIA.

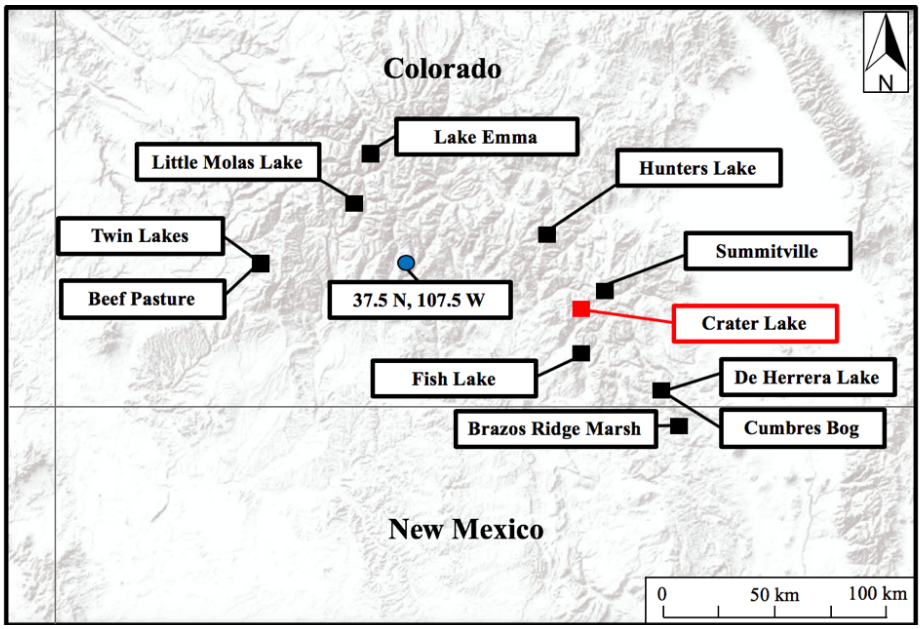

Figure 1.5: The locations of important sites discussed in this thesis. Clockwise, from the left: Beef Pasture and Twin Lakes (Petersen, 1994; Wright, 2006), Little Molas Lake (Toney, 2004; Toney and Anderson, 2006), Lake Emma (Carrara et al., 1984); Hunters Lake (Anderson et al. 2008a), Summitville (Routson et al., 2011), Crater Lake (this study), Fish Lake (Routson et al., 2016), De Herrera Lake (Anderson et al., 2008b) and Cumbres Bog (Johnson et al., 2013), and Brazos Ridge Marsh (Anderson et al., 2008b). The central location of the Cook and Krusic (2004; 37.5 N, 107.5 W) PDSI reconstruction is also included in the map denoted with a blue circle. Topographic relief base layer from Esri, DigitalGlobe, GeoEye, Earthstar Geographics, CNES/Airbus DS, USDA, USGS, AeroGRID, IGN, and the GIS User Community; accessed from databasin.org.

1.5 Pyrogenic Polycyclic Aromatic Hydrocarbons: A Novel Approach to Understanding Fire History

Pyrogenic polycyclic aromatic hydrocarbons (PAHs) are uncharged, non-polar organic compounds consisting only of carbon and hydrogen, that are produced by the combustion of organic matter (e.g. wood) and contain anywhere from two to eight conjugated ring systems (Pampanin and Sydnes, 2013). Three major types of PAHs have been identified: (1) biogenic/diagenetic PAHs, which are generated by biologic processes or the early stages of diagenesis in marine sediments (Page et al., 1999; Stogiannidis and Laane, 2015); (2) petrogenic PAHs, which are related to petroleum, including crude oil and other refined products (Page et al., 1999; Stogiannidis and Laane, 2015); and (3) pyrogenic PAHs, the focus of this thesis, which are generated by the incomplete combustion of fossil fuels and recent organic material such as wood (Neff, 1979; Killops and Massoud, 1992; Jiang et al., 1998; Page et al., 1999; Finkelstein et al., 2005; Nabbefeld et al., 2010; Denis et al., 2012; Stogiannidis and Laane, 2015). Many high molecular weight (HMW) PAHs have been researched as acute environmental toxins (Stogiannidis and Laane, 2015; WDHS, 2015), but a growing body of research shows them to be useful biomarkers in paleoenvironmental studies (Jiang et al., 1998; Finkelstein et al., 2005; Denis et al., 2012; Miller et al., 2017).

Although charcoal has been used to reconstruct past fire occurrence in paleoecologic research, degradation, sediment depositional processes (e.g. mixing), and secondary deposition years after a fire event, can all produce uncertainty (Denis et al., 2012). Few studies have sought to validate the occurrence of pyrogenic PAHs as reliable fire markers in Quaternary sediments (Page et al., 1999; Gabos et al., 2001; Denis et al., 2012; Miller et al., 2017), but pyrogenic PAH analysis may allow for a more complete paleofire reconstruction at a given site by capturing distinct fire events (Denis et al., 2012). For example, Denis et al. (2012) suggested that both low molecular weight (LMW) and HMW pyrogenic PAHs are indicators of fire in lacustrine sediments, but that HMW PAHs (e.g. pyrene) are also indicators of burn intensity or temperature. Additionally, PAHs are attractive paleofire biomarkers because they are resistant to diagenetic processes (Johnsen et al., 2005), possess a structure that is determined by the temperature of the burn event (e.g. hotter fires produce PAHs with more rings and heavier molecular weights; McGrath et al., 2003; Finkelstein et al., 2005; Denis et al., 2012), are produced over a much broader temperature range than charcoal (Conedera et al., 2009; Denis et al., 2012), can reveal the source (i.e. arboreal species) of the combusted material (Jiang et al., 1998; Finkelstein et al., 2005; Denis et al., 2012; Stogiannidis and Laane, 2015; Miller et al. 2017), and allow for comparison with both the charcoal records, and historical regional fire records (Denis et al., 2012; Miller et al., 2017).

Chapter 2: Methods

2.1 Field Methods

Numerous sediment cores were collected from Crater Lake between September 2015 and October 2016 (Table 2.1). Three exploratory surface cores were collected from pack rafts in September 2015 using an Aquatic Instruments surface corer. Two more surfaces cores were collected in July 2016 from pack rafts using an Uwitec surface corer. In September 2016, three long cores were taken from a platform, using a percussion-piston corer with PVC tubing. Additionally, Crater Lake bathymetry data was collected in September 2016 using a side-scanning sonar device fixed to the stern of a pack raft. Multiple transects were paddled north-south and east-west, to map the bathymetry of Crater Lake in detail.

CTR 4 was selected for this study because it was one of the longest (180 cm) and earliest (July 2016) cores collected in this series. CTR 4 was collected using an Uwitec surface corer with a 180 cm long, 8 cm diameter PVC core tube. Because a bathymetry map of the lake did not exist at the time CTR 4 was collected, a handheld fish finder was used to locate the deepest parts of the lake. Once extracted from the lake sediments, a polymer gel (Zorbitrol) was added to the top of the core before it was capped to absorb excess water and to stabilize surface sediments to prevent mixing during transport from field to laboratory.

Core Name	Latitude (°N)	Longitude (°W)	Water Depth (m)	Core Length (m)	Coring Instrument	Retrieval Date
CTR 1	37.38813	106.69463	21.4	0.93	Aquatic Instruments surface corer	9/26/15
CTR 2	37.38847	106.69516	19.3	0.81	Aquatic Instruments surface corer	9/26/15
CTR 3	37.38835	106.69480	20.6	0.66	Aquatic Instruments surface corer	9/26/15
CTR 4	37.38806	106.69439	18.8	1.44	Uwitec surface corer	7/19/16
CTR 5	37.38818	106.69517	19.3	0.90	Uwitec surface corer	7/19/16
CTR 6	37.38962	106.69483	15.8	2.92	Percussion corer	9/28/16
CTR 7	37.38833	106.69477	21.1	3.00	Percussion corer	9/28/16
CTR 8	37.38871	106.69491	20.8	4.10	Percussion corer	9/29/16

Table 2.1: Coring locations, water depth (m), core length (m), instruments used for extraction, and retrieval date. CTR 4 was used in the present study.

2.2 Laboratory Methods

All cores collected at Crater Lake were transported back to NAU and subsequently stored in coolers at the Sedimentary Records of Environmental Change Laboratory. In the laboratory, the cores were split longitudinally and the exposed surface was scraped clean before subsamples were collected. All subsampling was completed in the Laboratory of Paleoecology at NAU.

2.2.1. Lithology and Magnetic Susceptibility

CTR 4 was cut into two sections: CTR 4A which consisted of the top 40 cm, and CTR 4B, consisting of the remaining 140 cm. This was done so that each section would fit securely on to a cutting platform designed to stabilize the core tubes while they were split. The sections were then split longitudinally using a circular saw, adjusted on the cutting platform to cut only the plastic tubing. The top and bottom core sections were then separated from each other with a wire, and subsequently measured. Lithology and sediment characteristics were described by visual examination and in reference to the Munsell soil color chart.

After allowing the cores to acclimate to room temperature, MS measurements were taken at every 5 mm along the length of each section using a Bartington MS2E-1 meter and surface probe with an operative frequency of 0.565 kHz. MS analysis was conducted on CTR 4B by Ethan Yackulic in January 2017, and on CTR 4A by Charles Mogen in March 2017. MS data can be found in Appendix 2.

2.2.2. Charcoal and Plant Macrofossils

Charcoal and plant macrofossils were analyzed from the same sediment subsamples taken in CTR 4. One hundred and seventy-three contiguous 1 cm^3 sediment samples down core (every 0.5 cm between 53.5 – 26.0 cm depth) to achieve a high-resolution record. In order to gauge the amount of charcoal in CTR 4, I sampled at 0.5 cm intervals in the upper portion of the core (between 53.5 – 26.0 cm). Because charcoal concentrations were very low, 1 cm intervals were used for the remainder of the core (154 – 53.5 cm and 26.0 – 0.5 cm).

Each sample was soaked in 10% $(NaPO_3)_6$ (sodium hexametaphosphate) for two to five days. Wet-sieving through 250 µm and 125 µm screens provided two sample fractions – particles >250 µm, and particles between 125 µm and 250 µm. Samples were placed into a petri dish, and charcoal particles and plant macrofossils were identified and counted using a dissecting microscope at 50x magnification.

Once charcoal counts were complete, the charcoal influx or charcoal accumulation rate (CHAR; particles/cm^2/yr) was calculated by multiplying the total charcoal sum for each sampled depth (particles/cm^3) by the sedimentation rate at each depth (cm/year). This was calculated to control for the effects of sedimentation rate on charcoal particle concentrations at each sample depth.

CharAnalysis software was used to determine fire return intervals (FRI). CharAnalysis is a set of diagnostic and analytical tools that aids in the reconstruction of local fire histories using sedimentary charcoal records (Higuera et al., 2009). The analyses decompose a charcoal series into low- and high-frequency components (i.e. background and peak components) to separate the signal of specific fire events from background "noise." The background component consists of low frequency CHAR that are not indicative of a fire within the immediate vicinity of the study site, but it may be representative of regional charcoal production and sedimentation. The peak component consists of peaks in CHAR that are large enough to be from fire events within the immediate vicinity of the study site. The program allows the user to choose between a variety of parameters and statistical tools, and to specify age zones within the charcoal record to be analyzed for different characteristics. For the CTR 4 charcoal data, multiple iterations were run using the "local" background charcoal parameter to ensure consistency amongst results given different sets of parameters. The program was set to interpolate 7 years between each sample, because the average number of years between samples was 6.8. Higuera et al. (2009) recommends background smoothing over at least 30 samples, so the smoothing parameter was set at 210 years.

Plant macrofossils were identified to genus or species when possible, with reference to the Laboratory of Paleoecology reference collection and an online guide provided by NSFs Lacustrine Core Facility at the University of Minnesota (https://tmi.laccore.umn.edu/organic/gallery). Plant macrofossils were used to obtain radiocarbon dates at four separate depths and analyzed to determine which plant species were present at various times around the lake. A full list of charcoal counts and identified macrofossils can be found in Appendix 3.

2.2.3. Pyrogenic Polycyclic Aromatic Hydrocarbons (PAHs)

Pyrogenic PAH analysis was supervised by Dr. Jaime Toney in the Biomarkers for Environmental and Climate Science (BECS) laboratory at the University of Glasgow. Thirty-seven, 2 cm^3 samples were taken from CTR 4 (four from CTR 4A and thirty-three from CTR 4B) and analyzed in the BECS laboratory. Thirty-one samples from CTR 4B were analyzed in August 2016; analysis of the remaining six samples, which were subsampled in June 2017, has not yet been completed.

The thirty-one CTR 4B samples were freeze-dried to remove all water content. Samples were processed using a Thermo Scientific: Dionex ASE 350 accelerated solvent extractor (ASE) using a 2:1 solution of DCM: MeOH (dichloromethane: methanol). Blank samples were also run to assure there was no cross-contamination between samples during the solvent extraction process. The total lipid extract (TLE) produced following the ASE step was then treated using acid neutral separation by filtering each sample through a pipette column filled with LC-NH_2 SPE Si-gel using a 2:1 solution DCM: Isopropyl (dichloromethane: isopropyl) to produce a total neutral fraction (TNF) for each sample. To further separate out compounds, the TNF was treated with four separate solutions: hexane, dichloromethane, a 1:3 ratio of Et Ac: hexane, and methanol. Fractions extracted using hexane and dichloromethane were utilized for PAH analyses using a Gas Chromatography-Mass Spectrometer (GC-MS). Each fraction had to be treated with activated copper granules to remove excess sulfur from solution before samples could be processed using GC-MS.

Each sample was then injected into an inert gas stream, which was transferred to a separation tube where samples reacted with a compound. GC-MS produces chromatograms with a series of peaks through a temperature and heat series over time. A total of sixteen standards were prepared by BECS lab technician, Harry Jackson, to test for common pyrogenic PAH types in each sample. The sixteen pyrogenic PAH compounds of interest included both LMW (2-3 benzene rings) PAHs – naphthalene, acenaphthylene, acenaphthene, fluorene, phenanthrene, and anthracene – and HMW (4 or more benzene rings) PAHs – fluoranthene, pyrene, benzo(anthracene), chrysene, benzo(b)fluoranthene, benzo(k)fluoranthene, benzo(a)pyrene, ideno(1,2,3-cd)pyrene, dibenzo(a,h)anthracene, and benzo(g,h,i)perylene.

Pyrogenic PAHs were identified by matching chromatogram peaks produced in each sample with peaks produced by the pre-made standards using the Agilent MassHunter software package. Standards were used to determine the retention time in the gas chromatography column and the ion mass of the molecule by producing chromatograms with specific peak areas. The relationship between the known concentration of the standards and peak areas were then used to construct a calibration curve that quantified unknown concentrations by using their peak area. Concentrations of the constituent PAHs in each sample were determined by integrating the area under the peak. The concentration for each identifiable PAH was then calculated using a calibration curve constructed with the known standard PAH concentrations and peak areas. PAHs that were present with peak areas within the range of the standards (0.2-1.0 mg/L) were recorded and calculated based on linear curves produced by the standards (Miller et al., 2017). This value was then divided by the dry mass of the sample to obtain the ratio of $\frac{ng\ of\ PAH}{g\ of\ dry\ sample}$. After the concentrations of all of the PAHs in the studied samples were determined, the data were organized into LMW and HMW PAHs. Pyrogenic PAH data from CTR 4 can be found in Appendix 4.

2.2.4 Pollen

One cm^3 subsamples were taken at 4 cm intervals throughout the CTR 4 core, providing a total of 40 pollen samples (four from CTR 4A, 36 from CTR 4B). Based upon the resulting age model (see below), this resulted in a 30- to 40-year sampling resolution.

Prior to processing, two *Lycopodium* tracer tablets were added to each sediment subsample (Batch # 1031; mean concentration 20,848 spores/tablet) to enable calculation of pollen concentrations for pollen percentages. Subsequent processing followed a modified Faegri and Iversen (1989) technique, beginning with suspension in 10% KOH to disperse humic acids, then sieving through 180 µm screens to remove large organic and inorganic fragments. Dilute 10% HCl was then used to remove carbonates, followed by 48% HF to remove silicates. Each sample was subsequently treated with acetolysis solution ($C_4H_6O_3$ and H_2SO_4) and placed in a hot water bath to remove the remaining organics. Following chemical treatments, each sample was stained with safranin-O dye, and dehydrated using successive treatments of ETOH and TBA (tert-Butyl alcohol). Silicone oil (5000 cs) was added to suspend each sample for storage and mounting on laboratory slides.

Pollen was identified and counted using a compound light microscope at 400x magnification. Each count contained a minimum of 300 terrestrial grains (trees, shrub, and herb pollen). Wetland species (e.g. *Alnus, Salix,* Cyperaceae, Liliaceae) were not included in the minimal count of 300. Pine (*Pinus*) grains were subdivided into diploxylon large (e.g. *Pinus ponderosa*), haploxylon small (e.g. *Pinus edulis*), haploxylon large (e.g. *Pinus aristata*, *Pinus flexilis*, and *Pinus strobiformis*), and undifferentiated. Pine grains were classified as haploxylon if verrucae were present on the leptoma area between the sacci. If verrucae were not present, the grain was classified as diploxylon. Grains less than 65 µm were considered "small," while those that were greater than 65 µm microns were considered "large." If the leptoma could not be sufficiently examined, or the grain was otherwise deteriorated so as to prevent further identification, including fragmented corpi and sacci, it was classified as undifferentiated. Likewise, Asteraceae grains that could not be identified to a particular genus were classified and counted as "other Asteraceae." The pollen reference collection in the Laboratory of Paleoecology, and published keys (e.g. Moore and Webb, 1978) were used to aid identification. Pollen percentages, and cluster analysis (CONISS) were then calculated and plotted using the TILIA software package (Grimm, 2005). Pollen data, including raw pollen counts and percentages, can be found in Appendices 5 and 6.

Pollen Ratios

In addition to pollen percentages, pollen ratios were calculated to explore both paleoenvironmental (e.g. treeline fluctuations) and paleoclimatic (e.g. temperature and aridity) change. Pollen ratios have been used by numerous previous studies (Maher, 1961, 1972; Markgraf and Scott, 1981; Carrara et al., 1984; Fall, 1992, 1997; Cour et al., 1999; Reasoner and Jodry, 2000; Turney et al., 2004; Toney and Anderson, 2006; Mensing et al., 2007; Jiménez-Moreno et al., 2008, 2011; Johnson et al., 2013; Anderson et al., 2014) to extract additional information on local paleoecosystems and climates. The *Picea/Pinus* percentage ratio is a measure of treeline position (Fall, 1992). Anderson et al. (2014) determined that in Colorado *Picea* dominated forests below ~3500 m asl, the *Picea*/*Pinus* pollen percentage ratio is typically ~0.4, it is always < 0.3 within the *Picea* krummholz (i.e. treeline), and < 0.2 above treeline in the alpine zone where no trees are present.

Above treeline, pollen traps tend to record higher percentages of *Pinus* pollen, whereas *Picea* and *Abies* appear in lower percentages despite pollen sources existing in closer proximity to treeline than the majority of *Pinus* species (Fall, 1992). Above treeline, *Pinus* pollen percentages are comparable to samples collected within the *Pinus*-dominated forests (Fall, 1992); this is likely due to the more efficient wind transportation of these pollen grains due to their size and architecture. *Picea* and *Abies* pollen percentages are generally higher within subalpine spruce-fir forests themselves. *Picea/Artemisia* (Jiménez-Moreno et al., 2011; Johnson et al., 2013) and *Pinus/Artemisia* (Johnson et al., 2013) pollen ratios have been used to study both upper treeline and lower treeline fluctuations in Colorado and to indicate warmer or cooler climatic conditions, with higher ratios indicating both increased treeline and average temperature. Cyperaceae/Poaceae pollen ratios can also be used to study shifts between wetter and drier climate conditions (Cour et al., 1999; Turney et al., 2004; Mensing et al., 2007), with higher values indicating wetter conditions (Jiménez-Moreno et al., 2008).

The *Picea/Pinus* and Cyperaceae/Poaceae ratios were calculated using a simple ratio. *Picea* pollen percentages were divided by *Pinus* total pollen percentages, and Cyperaceae pollen percentages were divided by Poaceae pollen percentages at each depth. *Picea*/*Artemisia* ((P-A)/(P+A)) and *Pinus*/*Artemisia* ((Pi-A)/(Pi+A)) were calculated using compound ratios as used by Johnson et al. (2013). All pollen ratio data can be found in Appendix 7.

2.2.5. Age Determination

An age model was developed for CTR 4 using $^{239+240}Pu$ and ^{14}C dating. For plutonium dating, 20 samples from CTR 4 were extracted at unfixed intervals to cover the entirety of the modern period (five samples from CTR 4A, and 15 samples from CTR 4B). Levels with obvious Zorbitrol at the top of the core (CTR 4A) were not taken; the first sample was taken at 4.5 cm from the mud/Zorbitrol interface. Plutonium measurements were made by Dr. Michael Ketterer (Metropolitan State University of Denver) in July of 2017.

Four ^{14}C samples were taken from CTR 4B at depths of 76 cm, 112 cm, 134 cm, and 152 cm in May and June 2017. Radiocarbon samples were combusted and analyzed at the University of California Irvine's Accelerator Mass Spectrometer facility. Radiocarbon ages were calibrated, and age depth models were developed using the Bayesian age-depth modeling R software package BACON 2.3.3. BACON uses Bayesian statistics to model accumulation histories for deposits using radiocarbon and other dates (Blaauw and Christen, 2011). BACON uses the assumption that sedimentation rates are within a range characterized by a long-tailed probability distribution, and that radiocarbon ages are in stratigraphic order (Blaauw and Christen, 2011). CALIB 7.1 (Stuiver et al., 2018) was used to generate calibrated ages and uncertainties.

Chapter 3: Results

3.1 Sedimentology

3.1.1 Lithology

Three lithological units were identified in the CTR 4 sediments. Unit 1 (154 – 110 cm) is composed of dark olive, dark to olive gray, and black clay and silt (Munsell colors 5Y/3/2, 5Y/4/2, and 5Y/2.5/2) with sub-cm-scale to mm-scale laminations. Abundant organics are present throughout. A large angular clast at 154 cm prevented a longer core from being extracted. There is no distinct contact between Unit 1 and Unit 2. Unit 2 (110 – 37 cm) is composed of dark olive, pale olive, black and light gray organic rich silt and clay (Munsell colors 5Y/2.5/1, 5Y/3/2, 5Y/6/4, and 5Y/5/1) with cm-scale diffuse bedding. An unidentified stick fragment cross-cuts intact bedding planes between 100 – 97 cm. Abundant needle fragments are present from 76 – 70 cm. There is no distinct contact between Unit 2 and Unit 3. Unit 3 (37 – 0 cm) is composed of sandy mud with organics between 37 – 30 cm. There is a single gray clay bed at 10 cm. Between 9 – 0 cm the sediments are composed of a massive black gyttja (Munsell color 5Y/2.5/12).

There were three instantaneously deposited sediment packages (IDSP – 1, 148-141 cm; IDSP – 2, 126-119 cm; IDSP – 3, 30.5-18.5 cm) interpreted from the CTR 4 sediments. Identification of IDSPs was based on lithologic characteristics (described below). Additionally, the CTR 4 plutonium profile helped to identify IDSP – 3 (Figure 3.1). Both IDSP – 1 (148 – 141 cm) and IDSP – 2 (126 – 119 cm) are composed of subangular and angular pebbles and granules in a poorly sorted sandy mud that differ from the surrounding lithological unit (Unit 1). There was no graded bedding present in either IDSP – 1 or IDSP – 2. IDSP – 3 (30.5 – 18.5 cm) is composed of a sandy mud and contains abundant organics. A subangular clast was present at 24 cm. The disruption of the CTR 4 plutonium profile curve (figure 3.1) further aided in the interpretation of this bed. Graded bedding is present in IDSP – 3. For the remainder of the thesis I omit data collected in these sections from the discussion as they were interpreted as instantaneous deposits and not included in the age model.

In addition to the three IDSPs, there are two sections that contain drop stones. These sections are between 84.5 – 78 cm and 52 – 47.5 cm. Each section consists of a large drop stone (>2 cm diameter), with associated subangular pebbles, granules, and organics. Both of these sections are surrounded by preserved diffuse bedding found in lithological Unit 2.

3.1.2 Chronology

The chronology for the CTR 4 core is based on $^{239+240}Pu$ in the upper portion of the core and ^{14}C dating of sediments below 76 cm (Figures 3.1, 3.2, and 3.3). A plutonium profile analysis was used to date the upper sediments because radiocarbon dating is generally only effective and used to date sediments older than ~400 years (Bradley, 1999). This is due to large fluctuations in atmospheric ^{14}C over the last ~400 years that make it hard to accurately date organics from this time period (Bradley, 1999). This issue has been compounded by the Suess and atomic bomb effects of the last ~100 years (Taylor, 1987; van der Plicht, 2007). Although the amount of atmospheric ^{14}C has varied through time, the proliferation of fossil fuel combustion in the late 19th and early 20th centuries (i.e. the Suess effect) and the onset of nuclear testing in the middle of the 20th century (i.e. the atomic bomb effect) have had a significant effect on the atmospheric ^{14}C concentrations, making it very difficult to assign unambiguous calendar dates to recent ^{14}C samples (Taylor, 1987; van der Plicht, 2007).

A classic sedimentary Pu profile displays a single $^{239+240}Pu$ peak associated with the height of atmospheric thermonuclear testing in 1963, followed by a sharp decline that reaches minimal values by the 1990s (Olivier et al., 2004; Zheng et al., 2008; Waters et al., 2015). The plutonium profile from CTR 4 shows multiple peaks, however (Figure 3.1 and Table 3.1). The irregular nature of the CTR 4 profile, in conjunction with lithological changes, suggests there was an instantaneous deposition event (IDSP-3) that disrupted the profile with an influx of sediment, complicating the interpretation of these data. The sediments between 30.5 – 18.5 cm were not considered in the final age model. After IDSP-3 was removed, two separate peaks remained. Recent research has suggested there might be a smaller peak in plutonium prior to 1963 associated with the early 1950s (personal communication, Dr. Michael Ketterer; Olivier et al., 2004; Waters et al., 2015). Given (1) the absence of a defined peak and subsequent decline in the CTR 4 plutonium profile that would allow for the identification of 1963, (2) the first nuclear devices were not detonated until 1945, (3) the unlikelihood of radioactive material leeching into older sediments and contaminating material deposited prior to 1945 (Olivier et al., 2004), and (4) the possibility of an initial, small peak associated with atmospheric testing ca. 1950, the small peak at 43 cm was considered to date to ~1950. The surface of the core (0 cm) was assigned a date of 2016.

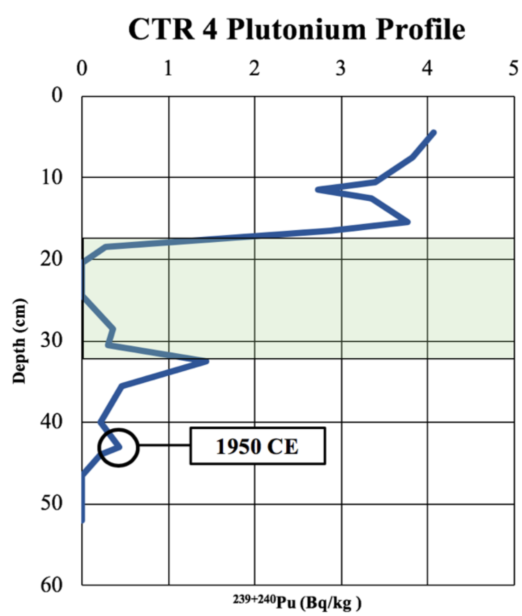

Figure 3.1: Plutonium profile from CTR 4. The sediments between 30.5 – 18.5 cm (highlighted with light green horizontal bar) were not considered in the final age model after being identified as an instantaneous deposit based on lithological descriptions (IDSP - 3). Recent research has suggested there might be a smaller peak in plutonium prior to 1963 associated with the early 1950s (Olivier et al., 2004; Waters et al., 2015; oral communication, Dr. Michael Ketterer, 2017). The small detection peak at 43 cm below lake level was inferred to correspond with 1950.

Core	Depth (cm)	Activity (Bq/kg)	Bq/kg sd	Age (cal BP)
CTR 4A	4.5	4.06858	0.12981	-56
CTR 4A	7.5	3.8208	0.12354	-50
CTR 4A	10.5	3.39326	0.10765	-43
CTR 4A	11.5	2.73054	0.02178	-41
CTR 4A	12.5	3.34595	0.23483	-39
CTR 4B	15.5	3.77169	0.163	-33
CTR 4B	16.5	2.87766	0.21483	-30
CTR 4B	18.5	0.26561	0.05604	removed
CTR 4B	20.5	< 0.05	0	removed
CTR 4B	22.5	< 0.05	0	removed
CTR 4B	24.5	< 0.05	0	removed
CTR 4B	28.5	0.36119	0.06268	removed
CTR 4B	30.5	0.30575	0.01516	removed
CTR 4B	32.5	1.44396	0.12628	-24
CTR 4B	35.5	0.45828	0.03274	-18
CTR 4B	40	0.21153	0.00432	-8
CTR 4B	43	0.43754	0.02333	-1
CTR 4B	44	0.21184	0.02127	7
CTR 4B	46.5	< 0.05	0	29
CTR 4B	52	< 0.05	0	87

Table 3.1: Plutonium data from CTR 4 core, Crater Lake, Colorado. Included are depths from the surface of CTR 4 to the middle of each sample (cm), plutonium measurements (Bq/kg), standard deviation (sd) plutonium measurements, and calibrated BP dates. The six sample depths, highlighted in gray (32.5-24.5 cm), were excluded from calculation of the final age model due to their association with an instantaneous deposition event.

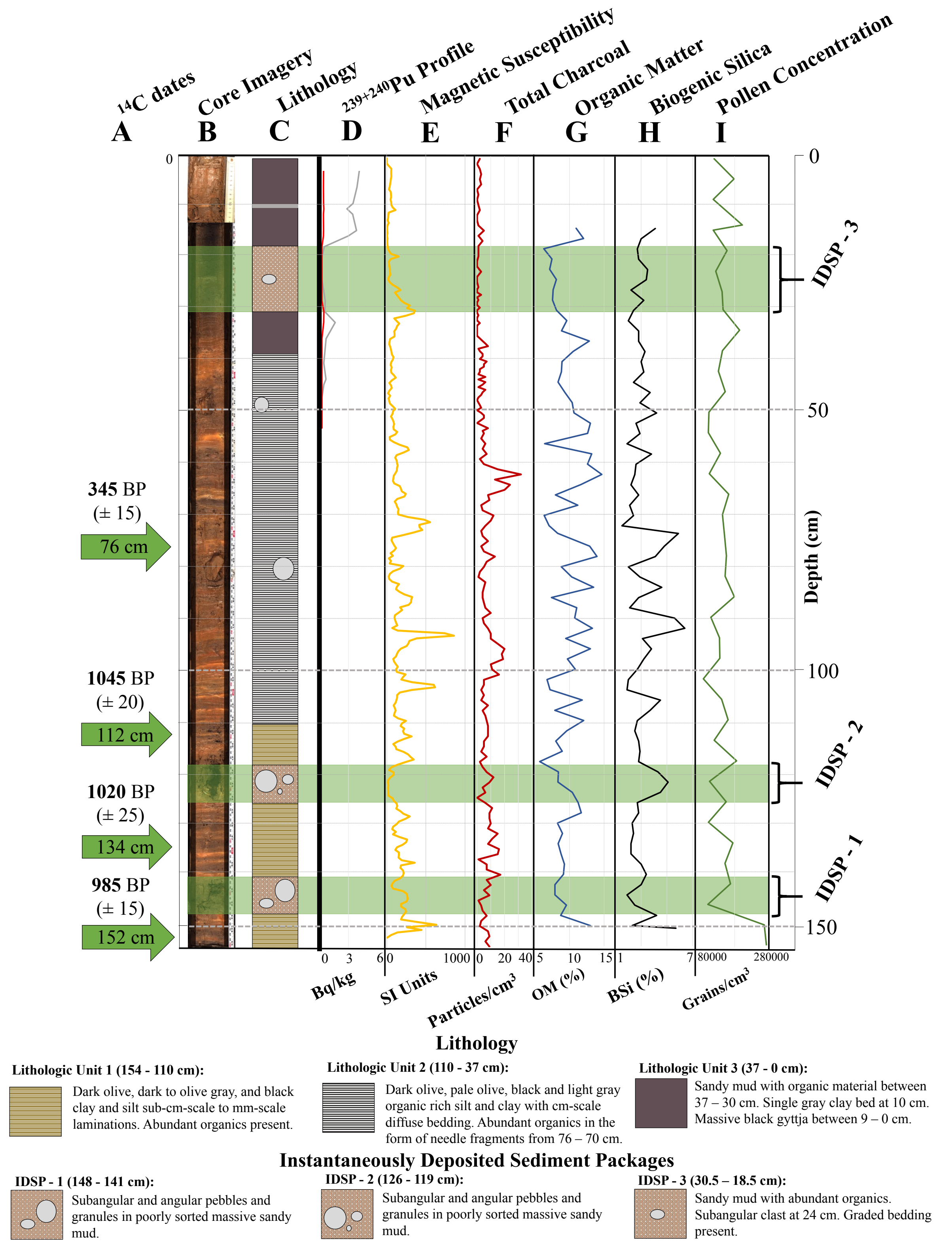

Figure 3.2: Comparison of (A) the four ^{14}C dates, (B) core imagery with (C) sediment lithology, (D) $^{239+240}$Pu profile, (E) magnetic susceptibility (MS), (F) total charcoal particles counted, (G) Organic Matter (OM) using Loss on Ignition (LOI), (H) Biogenic Silica (BSi), and (I) pollen concentration. OM, BSi, and MS data from CTR 4B are from Yackulic (2017). The horizontal green bars represent the three sections of CTR 4B that were identified as IDSPs and were not included in the final age model.

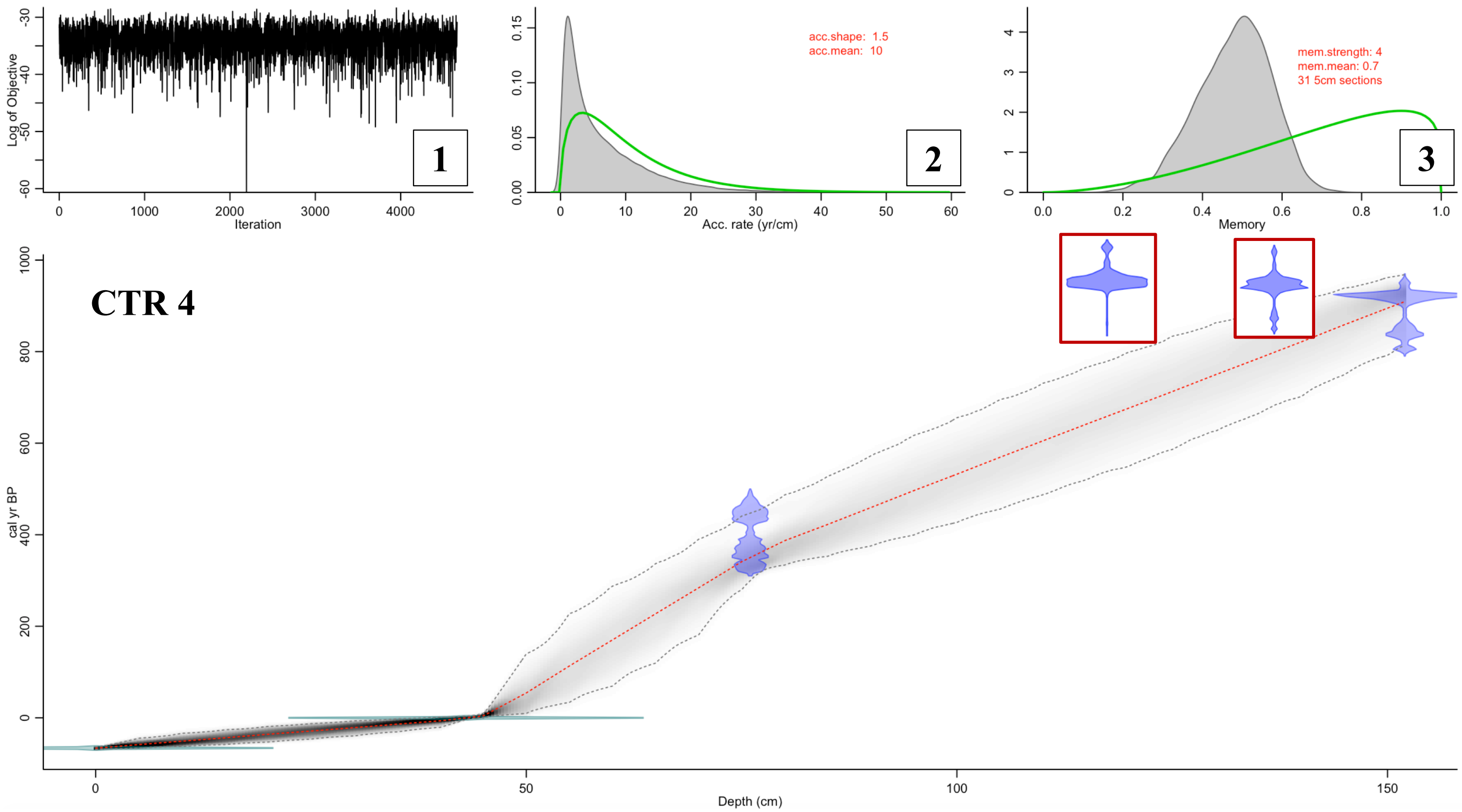

Figure 3.3: CTR 4 age model. Two excluded radiocarbon dates are in red boxes. In the large bottom panel, the single $^{239+240}Pu$ date (1950 CE) and surface of the core (2016 CE) are represented with the two horizontal lines, while the two ^{14}C dates are represented with probability density functions (dark blue). The dashed red line shows the best fit of 1000 age models run with 1-sigma errors, which are represented by the dotted grey lines. The top panel (left to right) displays (1) the number of iterations run by the program, (2) the sediment accumulation rate used by the program, and (3) the autocorrelation between sediment age and depth. The age model was generated using the age depth modeling program BACON 2.3.3 (Blaauw and Christen, 2011).

Initially, three radiocarbon samples were taken from CTR 4B. An age reversal was identified in the first three samples, with an older date (UCIAMS188313) occurring between the top (UCIAMS188312) and bottom (UCIAMS188314) samples (Table 3.2). A fourth radiocarbon sample (UCIAMS191212) was submitted to clarify the age of the middle of the section, but it also produced an age reversal (Table 3.2). It is possible that the bottom date from 152 cm is younger as a result of sample contamination, and that the two middle dates (112 and 134 cm), despite their error ranges, are correct. However, given (1) the error associated with the two reversed ^{14}C dates suggests they overlap in time (0.927 – 0.976 ka for UCIAMS188313; 0.911 – 0.975 ka for UCIAMS191212); (2) the unlikelihood that younger material would be incorporated into older sediment; and (3) that older organic material can persist in high elevation lake basins and be redeposited, the two middle ^{14}C dates were not used in the final age model. Marker layers, MS, OM, BSi, and RABD data correlating with other Crater Lake cores were helpful in confirming this decision. OM and BSi data can be found in Appendices 8 and 9.

Sample ID	Core Section	Depth (cm)	Material	^{14}C Age (BP) ± 1σ	Age (cal yr BP)
Coring Date	CTR 4A	0	-	-	-66
Ketterer MSU - Pu	CTR 4B	43	$^{239+240}$Pu	-	0
UCIAMS 188312	CTR 4B	76	unidentified twig	345 ± 15	381 (317-478)
UCIAMS 188313	CTR 4B	112	*Picea* needle fragments	1045 ± 20	excluded
UCIAMS 191212	CTR 4B	134	*Picea* needle fragments	1020 ± 25	excluded
UCIAMS 188314	CTR 4B	152	unidentified twig	985 ± 15	922 (803-934)

Table 3.2: Surface, $^{239+240}$Pu, and ^{14}C dates from CTR 4. Depth (cm) measurements were taken from the middle of each sediment sample. The calibrated ^{14}C ages in the far right column are displayed with age ranges in parentheses. The two middle ^{14}C dates (from 134 and 112 cm) were not used in the final age model. CALIB 7.1 (Stuiver et al., 2018) was used to generate calibrated ^{14}C ages and ranges.

3.1.3 Sediment Accumulation Rates

After eliminating the three identified instantaneous deposit sections, sediment accumulation rates (SAR) were calculated for CTR 4 (Figure 3.4). SARs were consistent in the lower 110.5 cm (~1035 to ~1950 CE) of the core, varying between 0.095 and 0.115 cm/yr. SARs increased ~4-5 times in the upper 43.5 cm (~1950 to 2016 CE) varying from 0.463 to 0.465 cm/yr. All SAR data can be found in Appendix 10.

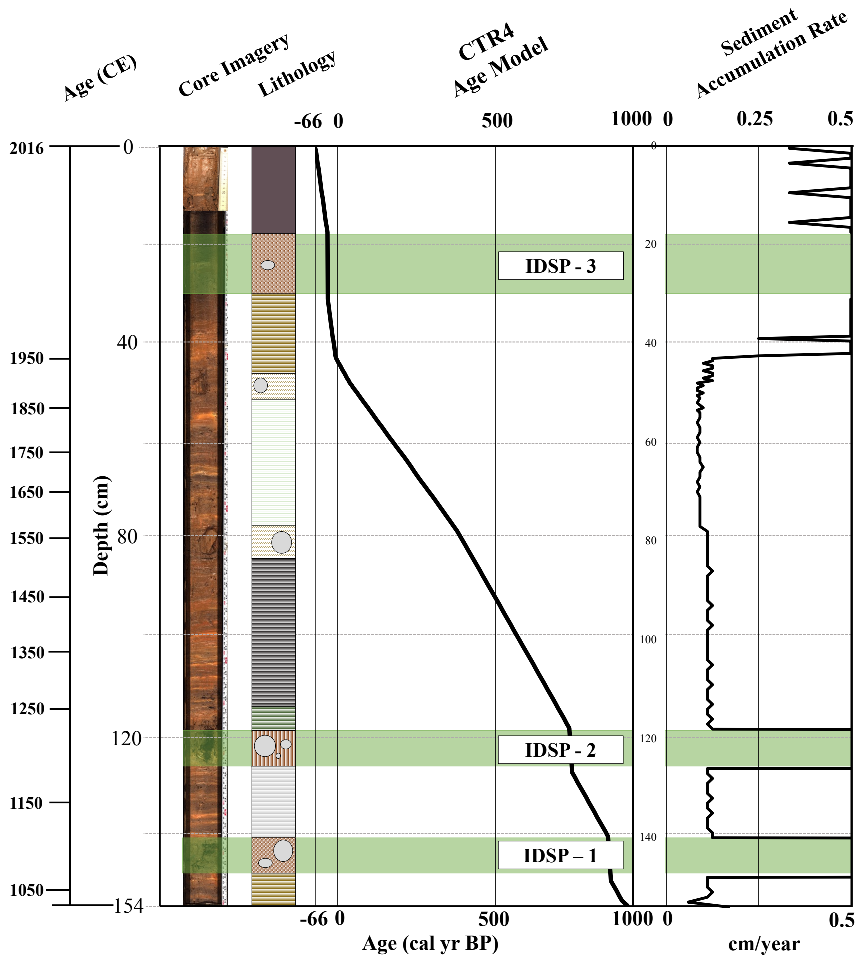

Figure 3.4: Image and lithology of CTR 4, with the three sections identified as instantaneous deposition sediment packages (IDSP) labeled and highlighted with horizontal green bars. IDSP - 1 and 2 had accumulation rates of 9 cm/year, and IDSP-3 had an accumulation rate of 13 cm/year. No other depth had a sediment accumulation rate that exceeded 0.5 cm/year. The age model was developed using the age depth modeling program BACON 2.3.3 (Blaauw and Christen, 2011). The sediment accumulation rate is displayed on the far right.

3.1.4 Magnetic Susceptibility (MS)

Magnetic susceptibility (MS) varies greatly throughout CTR 4 (Figure 3.2). Between 152 – 56 cm (~1060 to ~1820 CE) there are numerous peaks that vary by an order of magnitude. Major peaks occur at 149.5, 103.5, 93.5, and 71.5 cm depth. From 56 - 0 cm (~1820 to 2016 CE), values remain very stable and low, with no MS readings exceeding 150 SI.

3.2 Charcoal, Pyrogenic PAHs, and Pollen

3.2.1 Charcoal

Total charcoal counts throughout CTR 4 were relatively low, with no peak exceeding more than 40 particles/cm^3 (Figures 3.5 and 3.6). The concentration of 125 µm charcoal is much higher throughout the record than 250 µm charcoal (Figure 3.6). Background charcoal concentrations (average number of charcoal particles/cm^3) were higher between 154 – 58 cm (~1035 to ~1795 CE; 8.4 particles/cm^3). Average background charcoal concentrations between 58 – 0 cm (~1795 to ~2016 CE; 2.5 particles/cm^3) were lower, and total charcoal peaks are smaller, with no peaks exceeding 8 particles/cm^3.

Charcoal influx or charcoal accumulation rates (CHAR; particles/cm^2/year) were calculated to determine potential fire events (Figure 3.5 and 3.6). Between 154 – 45 cm, four CHAR peaks occur. Two CHAR peaks occur between 45 – 30 cm. These two peaks are not associated with total charcoal peaks, however. Between 17.5 – 0 cm CHAR expresses variability, but there are no prominent peaks.

Using CharAnalysis (Higuera et al., 2009) it was determined that there were five charcoal peaks at 135 cm (~1140 CE), 101 cm (~1370 CE), 78 cm (~1570 CE), 64 cm (~1725 CE), and 62 cm (~1750 CE) indicative of fire events within the lake basin (Figure 3.7). These depths closely matched CHAR peaks. CharAnalysis, however, did not determine the largest CHAR peak (41-37.5 cm) to be a fire event.

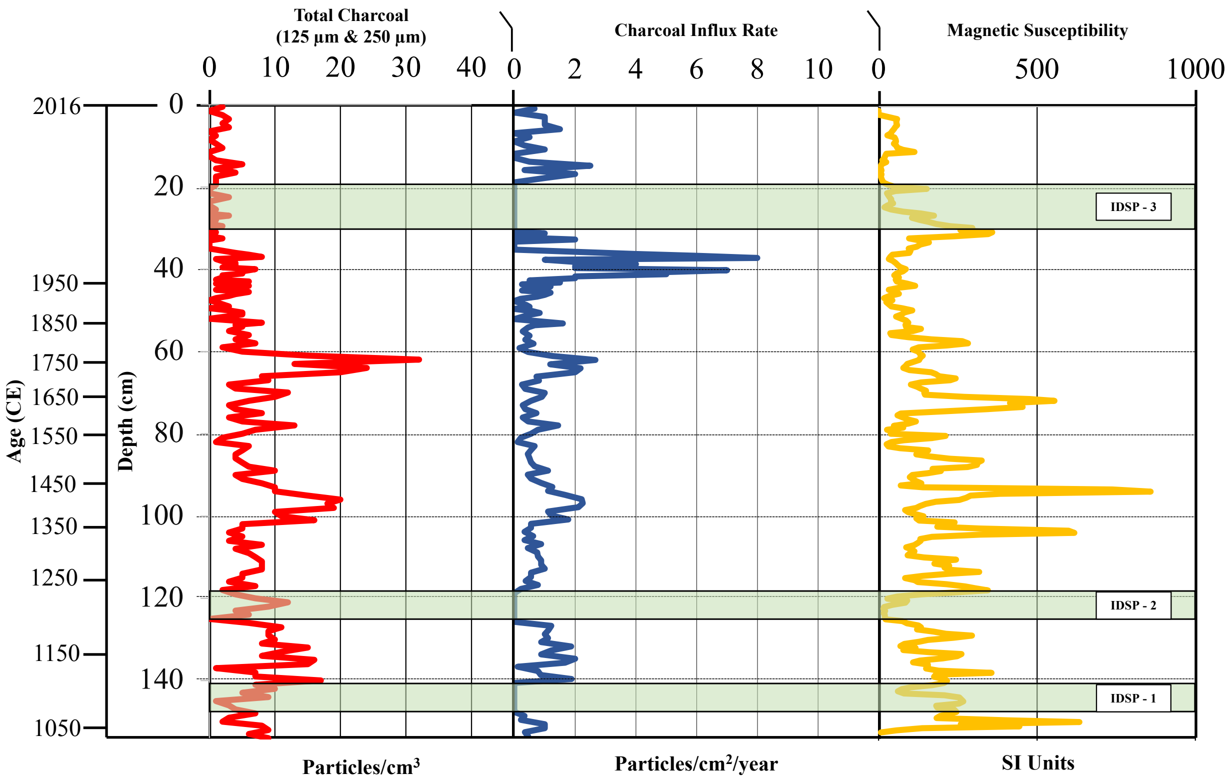

Figure 3.5: Comparison of total charcoal, charcoal influx or charcoal accumulation rate (CHAR), and magnetic susceptibility (MS) from CTR 4 after IDSP-1, 2, and 3 were excluded from the final analysis.

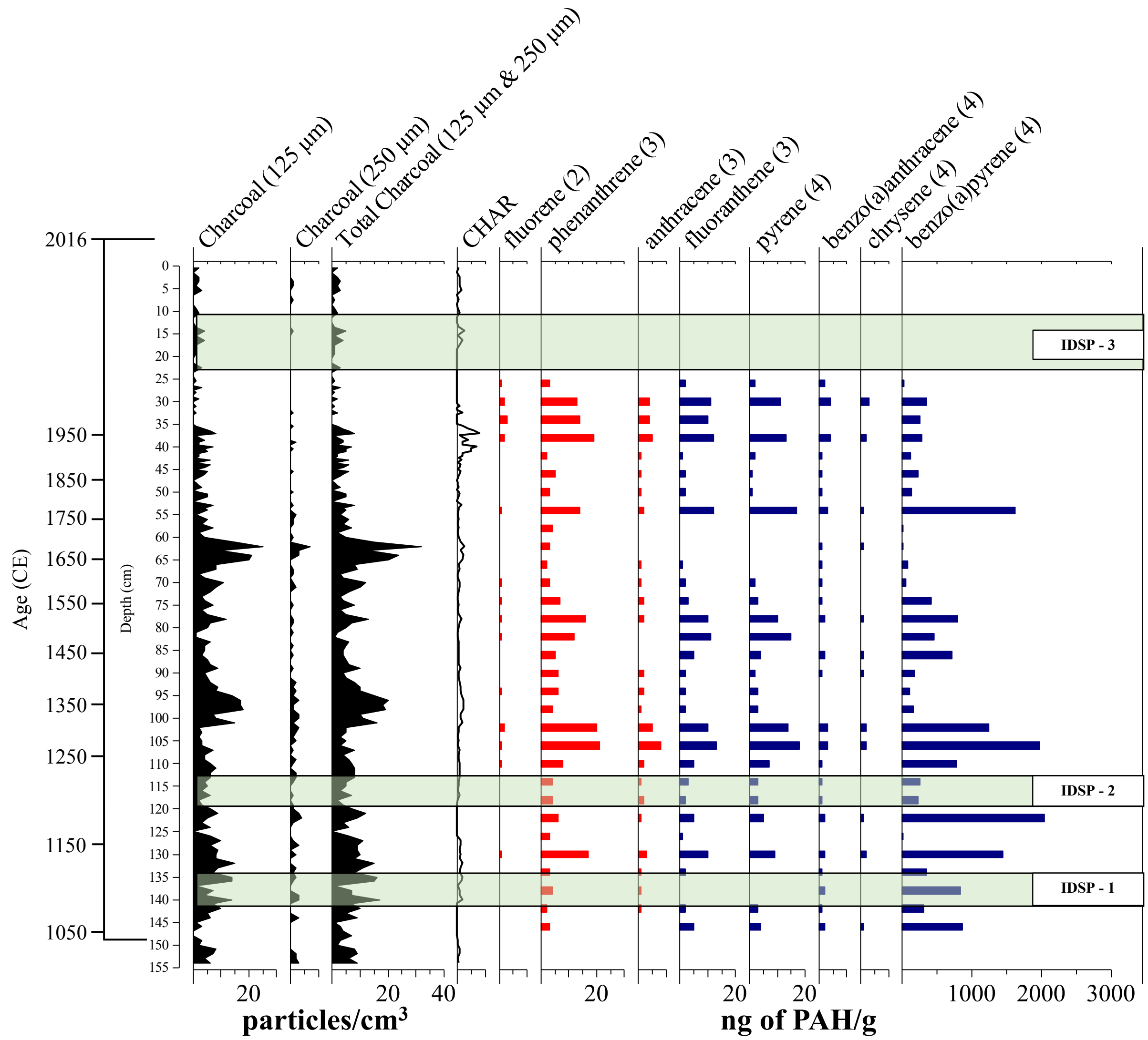

Figure 3.6: Comparison of CTR 4 total charcoal (particles/cm^3), CHAR (particles/cm^2/year), and pyrogenic PAH (ng of PAH/g) data. Sediments above 21 cm were not examined for pyrogenic PAH data. Low molecular weight (LMW) PAHs are in red, and high molecular weight (HMW) PAHs are in blue. Although 16 total PAHs were tested for in each sample, only 8 displayed significant concentrations (i.e. detected) of PAHs. IDSP-1, -2, and -3 (horizontal green bars) were excluded from the final analysis.

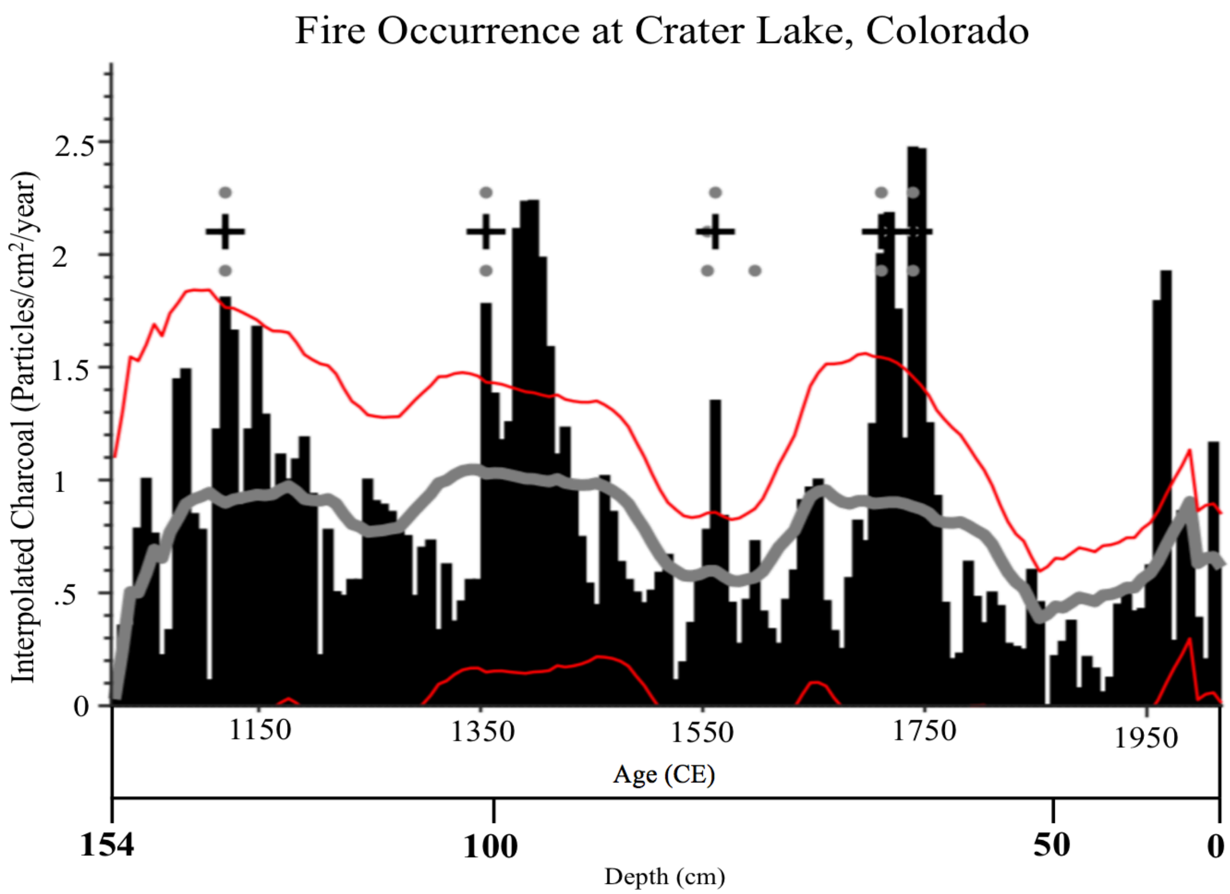

Figure 3.7: CharAnalysis (Higuera et al., 2009) determined five charcoal peaks (+) at 135 cm (~1140 CE), 101 cm (~1370 CE), 78 cm (~1570 CE), 64 cm (~1725 CE), and 62 cm (~1750 CE) to be fire events within the lake basin. The vertical black bars are interpolated charcoal concentrations based off of the raw data, the thick grey line indicates background charcoal level, and the thin red lines represent threshold charcoal concentrations calculated by the program. Small grey dots are associated with the three threshold values set in the parameters (0.95, 0.97, and 0.99; from lower to higher).

3.2.2 Pyrogenic PAHs

Following pyrogenic PAH analysis, three LMW (fluorene, phenanthrene, anthracene), and five HMW (fluoranthene, pyrene, benzo(a)anthracene, chrysene, and benzo(a)pyrene) pyrogenic PAHs of the sixteen that were initially tested for were detected in significant concentrations (Figure 3.6). Prominent peaks for both LMW and HMW pyrogenic PAHs occur at 130 cm (~1180 CE), 106 cm (~1320 CE), 78 cm (~1570 CE), and 54 cm (~1840 CE). At 38 cm (~1963 CE) there is a noticeable spike in LMW concentrations. No pyrogenic PAH data is available between 154 – 149 cm and 17.5 – 0 cm from CTR 4 because samples from these sections were not processed at the University of Glasgow in August 2016.

3.2.3 Pollen

Forty pollen samples were analyzed from CTR 4, and a total of 60 pollen types were identified. Thirteen pollen types were used to construct the CONISS analysis, including *Abies*, Cupressaceae, *Picea*, *Pinus* (total, diploxylon large [*Pinus ponderosa / P. contorta*], haploxylon small [*P. edulis*] and haploxylon large [*P. strobiformis / aristata*]), *Quercus*, Amaranthaceae, *Ephedra*, Poaceae, *Ambrosia*, and *Artemisia*. The program suggested the three pollen zones described below.

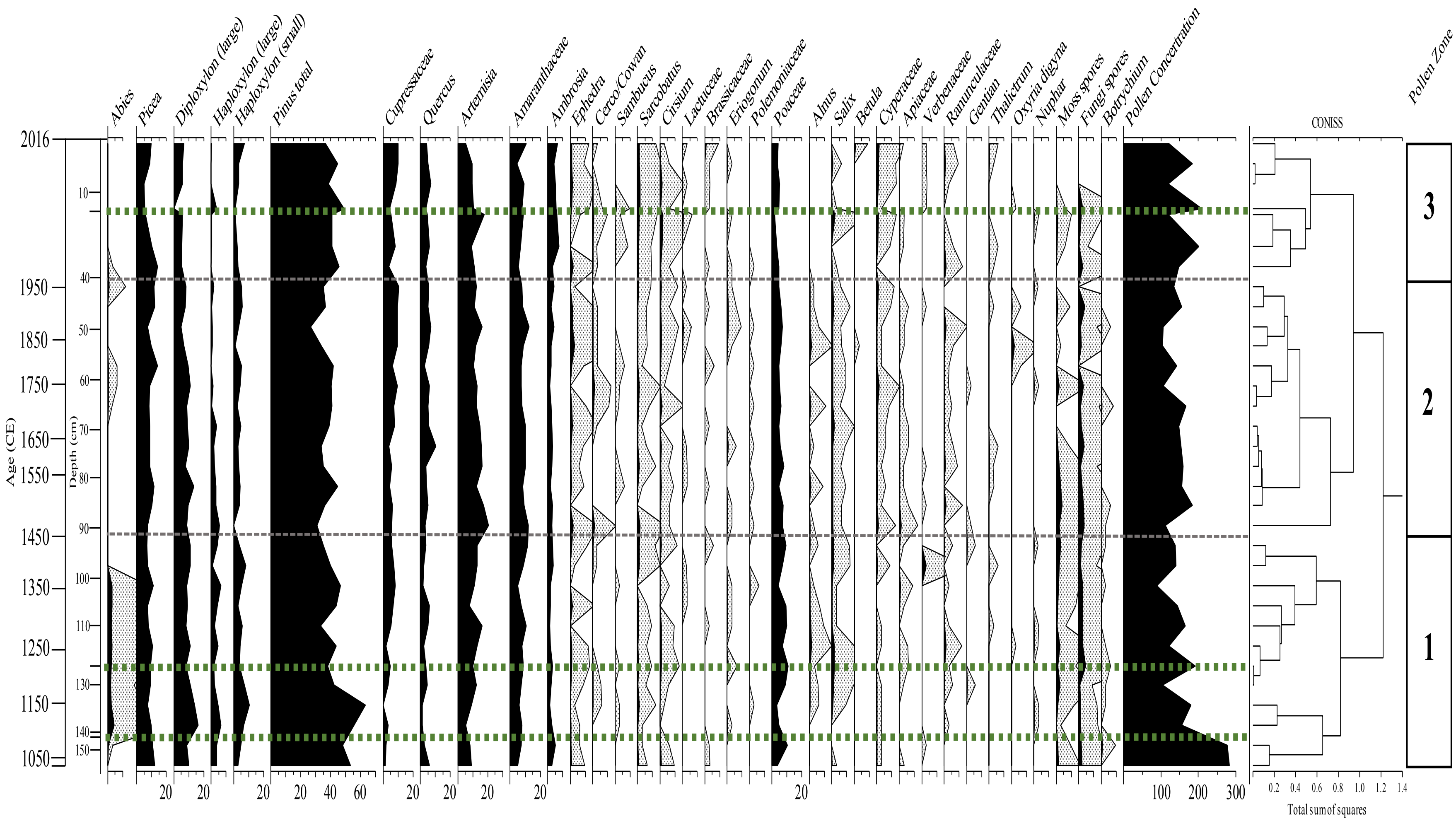

Figure 3.8: Pollen diagram from Crater Lake, Colorado, including the percentages of major pollen types identified (gray shaded outlines represent 10x exaggeration), pollen concentration, and CONISS cluster analysis (far right). Pollen zones 1-3 are defined on the far right of the diagram and demarcated by dashed grey lines. The data within the three instantaneous deposition sediment packages (IDSP – 1; 148-141 cm, IDSP – 2; 126-119 cm, and IDSP – 3; 30.5-18.5 cm) were removed, and are demarcated by dashed green lines The Pollen Concentrations are represented in grains/cm^3, and each concentration was divided by 1000.

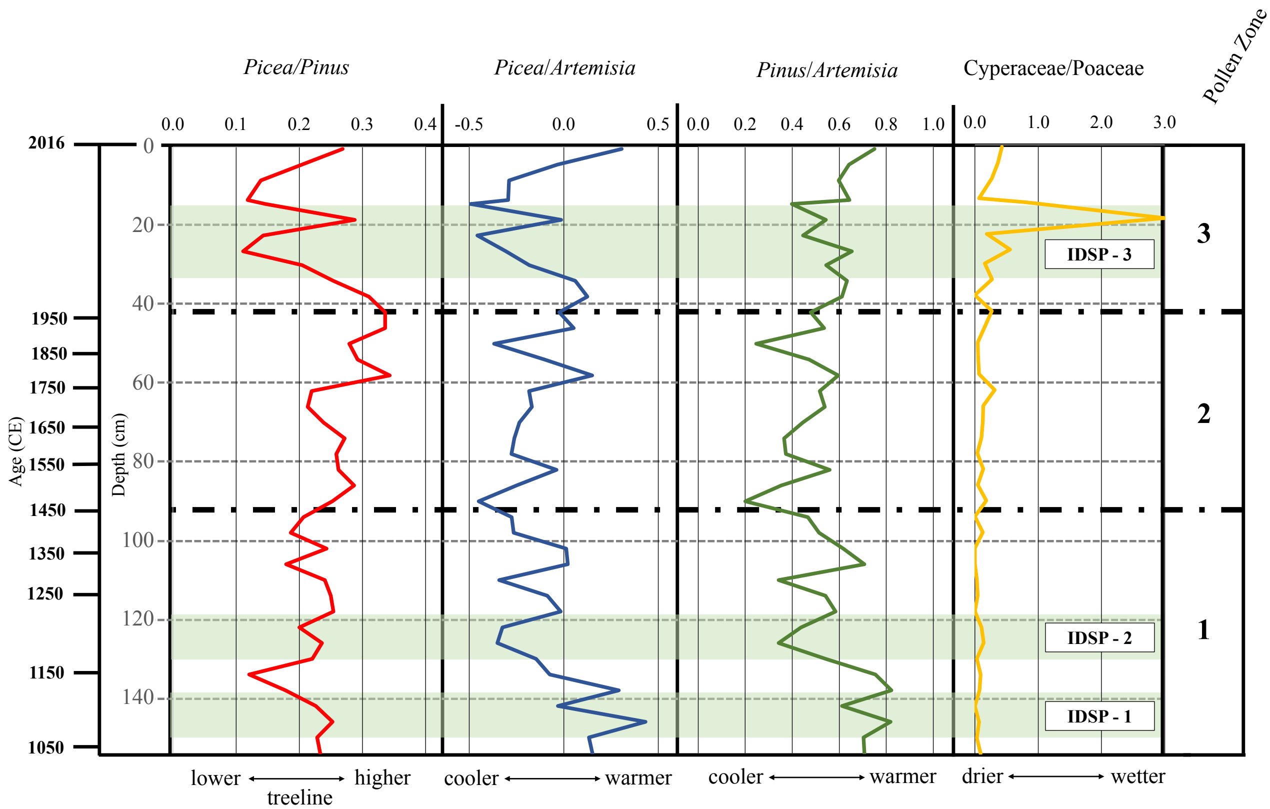

Figure 3.9: Spruce (*Picea*)/Pine (*Pinus*) (P/Pi), *Picea/Artemisia* (P/A), *Pinus/Artemisia* (Pi/A), and Cyperaceae/Poaceae (C/P) ratios were calculated using CTR 4 pollen percentages. Abbreviations adopted from Johnson et al. (2013).

Pollen Zone CTR 4-1 (~1035 to ~1450 CE; 154 to 92 cm)

Zone CTR 4-1 is characterized by high overall pollen concentrations, which fluctuate between 89 and 283 × 10^2 grains/cm^2. Dominant pollen types include *Abies* (2.5 – 3.0%), *Pinus* haploxylon small (piñon pine-type; maximum 10%; average 5.6%), *Pinus* diploxylon large (ponderosa pine-type; maximum 16%; average 10.6%), and *Pinus* total (35 – 65%), with low percentages of Cupressaceae (i.e. *Juniperus*; 0.3 - 8%) and *Quercus* (1-6%) (Figure 3.8). *Picea* remains relatively constant throughout this interval at ~10%. *Salix* (0.8%) and *Alnus* (0.5%) are most abundant in this zone, while Cyperaceae (0.3%) is at a minimum. *Poaceae* pollen averages

~8% in this zone. Verbenaceae appears abruptly at the end of the CTR 4-1 time interval, and reaches its highest value of 3% at 98 cm.

The *Picea/Pinus* (P/Pi) ratio remains stable at or near 0.2 throughout the CTR 4-1 time interval (Figure 3.9). The *Picea/Artemisia* (P/A) ratio initially increases to 0.3 during the middle of CTR 4-1, before dropping to -0.3 at the end of the zone. P/A ratio averages 0 during this interval. Similarly, the *Pinus/Artemisia* (Pi/A) ratio increases to 0.8 during the middle of CTR 4-1 time, before decreasing to 0.5, while the Pi/A ratio average is 0.46. The Cyperaceae/Poaceae (C/P) ratio remains very low, averaging 0.04.

Pollen Zone CTR 4-2 (~1450 to ~1957 CE; 92 to 40.5 cm)

CTR 4-2 is characterized by stable overall pollen concentrations (average 140×10^2 grains/cm^2). *Abies* pollen largely disappears in CTR 4-2 except between 66-58 cm (0.5%) and at 42 cm (1%). *Artemisia* percentages are highest during this zone (to 21%), along with Cupressaceae (maximum of 11%; average 7.5%), and *Quercus* (maximum of 10.5%; average of 5.3%) (Figure 3.8). During this zone, lower percentages of *Pinus edulis* (pinon pine-type, 3.7%), *P. ponderosa* (ponderosa pine-type (9%), and Poaceae (6%) occur. *Alnus* (0.4%) is less common, and more sporadic during this interval. Additionally, average *Salix* (0.8%) and Cyperaceae (0.7%) pollen percentages increase. The highest average values of Ranunculaceae (0.5%) and Apiaceae (0.5%) also occur during this time interval.

The P/Pi ratio remains stable with no values dropping below 0.2, and averages 0.3. The P/A ratio reaches a low of -0.45, and averages -0.2. The Pi/A ratio reaches a low of 0.2 at 90 cm, and averages 0.44. The C/P ratio increases substantially during this interval, and averages 0.13.

Pollen Zone CTR 4-3 (~ 1957 to 2016 CE; 40.5 cm to surface)

Zone CTR 4-3 is characterized by increased variability in overall pollen concentrations, which fluctuate between 119 and 209 × 10^2 grains/cm^2, with an average of 153 × 10^2 grains/cm^2. There is an increase in Cupressaceae (average 7.7%), which reaches its CTR 4 peak value of 10.3% at 26.5 cm. Similarly, *Ambrosia* reaches its highest value of 7.7%, averaging 5.8%. *Pinus* total also increases with an average value of 41.7%. *P. edulis* (2.7%), *P. ponderosa* (5.2%) and *Picea* (8.2%) all decline from CTR 4-1 and CTR 4-2. The Apiaceae average declines substantially to < ~0.15%. Moss spores, which are consistent throughout both the CTR 4-1 and CTR 4-2 intervals averaging 1.4%, decline to 0.3%. *Salix* declines to (0.5%), and *Alnus* disappears from the record. *Cirsium* reaches its maximum value of 2% at 14.5 cm and averages 1.1%.

The P/Pi ratio averages 0.2, with the highest value of 0.3 at 0.5 and 38 cm. P/A values average -0.1, with the highest value at 0.5 cm (.31). Pi/A values average 0.61. The C/P ratio reaches its highest value during this interval, averaging 0.2.

3.2.4 Macrofossils

Although plant remains are abundant throughout CTR 4, only *Abies* and *Picea* needle fragments were common macrofossils throughout the length of the core. The disappearance and reappearance of *Abies* pollen matches the macrofossil record. *Abies* needle fragments were found at 132, 130, 38.5, 36, and 34.5 cm (Figure 3.10). All of these depths, with the exception of 34.5 cm, correspond with the presence of *Abies* pollen in the CTR 4 pollen assemblage. The most common identified macrofossils were *Picea* needles (recovered in nearly every sample), insect chitin (including Chironomidae head capsules), and *Daphnia* (common water flea) ephippia.

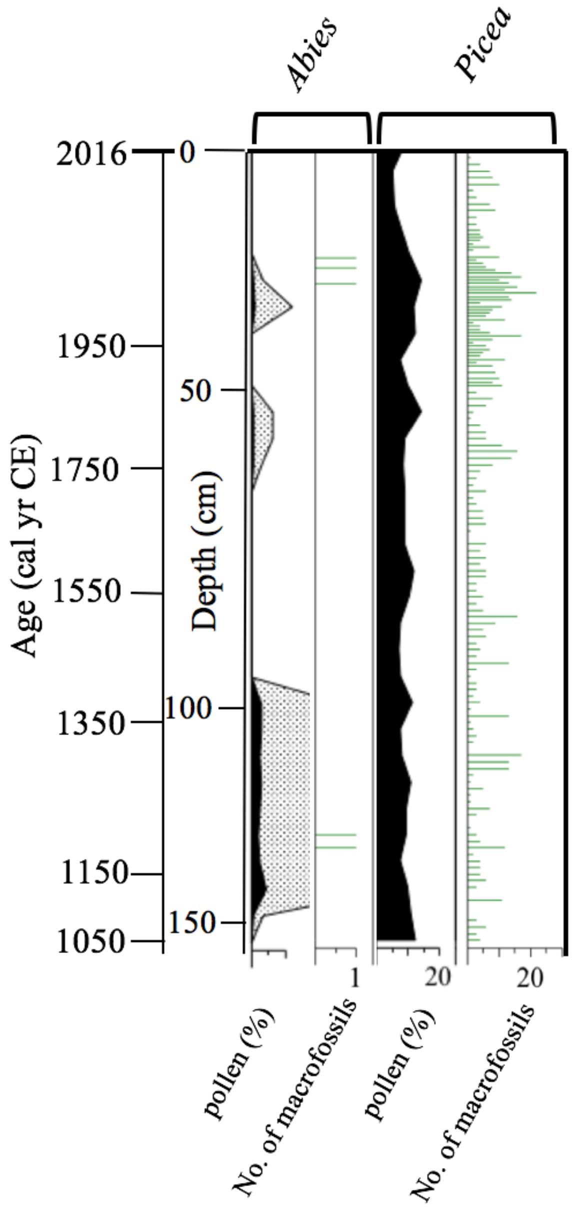

Figure 3.10: The number of macrofossils for both *Picea* and *Abies* that were identified at each depth following the removal of the three identified instantaneous deposits, paired with pollen data.

Chapter 4: Discussion

4.1 Introduction

Vegetation and fire history reconstructions from Crater Lake using pollen, charcoal and pyrogenic PAHs indicate that there have been both localized and regional ecosystem effects over the course of the last 1000 years in response to natural disturbances and climatic variability. In this section I discuss paleoenvironmental change at Crater Lake over the last 1000 years while indirectly addressing the original research questions.

4.2 Sediments and Paleoenvironments

Analysis of sediment lithology from CTR 4 reveals that at least part of the lake basin has been subject to numerous disturbances in the form of high energy deposition events over the last 1000 years. The steep slopes immediately surrounding the lake likely experience frequent avalanches in the winter and small rock slides as a result of freeze thaw action in the spring and summer. Instantaneous deposits of sediment as the result of avalanches are common in high elevation lakes surrounded by steep slopes, and these events can introduce large volumes of both organic and minerogenic debris into the lake (Fouinat et al., 2016).

As a result of the high energy deposition events, developing a chronology for the CTR 4 sediments was a challenge. CTR 4 did not have the expected plutonium profile, which made dating the upper sediments very difficult, and two of the four ^{14}C samples produced age reversals, which further complicated dating the remaining sections of the core with ^{14}C samples. Age model uncertainty undoubtedly affects the final interpretations of the CTR 4 data, particularly pollen zone constraints, FRI, SAR, and CHAR. The most recent sediments display dramatic SAR increases and could not be definitively dated using a Pu profile analysis.

The two dropstones (Figure 3.2) were likely introduced to the frozen surface of the lake by an avalanche where they remained until the summer melt. The instantaneous deposition events that were identified could also have resulted from avalanches, however, it is more likely that either (1) rockslides from the surrounding slopes were responsible when the lake was ice free, or (2) flash melt or heavy precipitation events led to pulses of sediment from the primary inflow. High energy events including avalanches, rockslides, and runoff events all have the potential to introduce large pebbles, gravels and cobbles in high elevation environments (White, 1981; Marchi and Borga, 2012; Kenner et al., 2014; Fouinat et al., 2016).

Biogenic silica (BSi) and organic matter (OM) content are both commonly used as indicators of total productivity in lake sediment studies (Birks, 2006; McKay et al., 2008; Johnson et al., 2015; Yackulic, 2017; Figure 3.2). BSi is a measurement of the total mass of siliceous organisms in a sediment sample, whereas OM is a measurement of the total amount of organic matter present in each sediment sample. Each of these methodologies was examined in great detail for the entire Holocene from multiple Crater Lake sediment cores by Yackulic (2017), who interpreted these data as indicating decreased lake productivity from ~1000 CE to ~1800 CE. These data suggest there is no distinct difference between the MCA and the LIA with regards to these productivity indicators. From ~1800 CE to present day, BSi and OM vary without any clear trend (Yackulic, 2017).

In addition to BSi and OM, Yackulic (2017) also employed hyperspectral imagery as a lake productivity indicator, specifically targeting relative absorption band depth (RABD) measurements at 615 and 660 nm. The $RABD_{615}$ and $RABD_{660}$ measurements steadily decrease through the MCA and are lowest at the beginning of the LIA. There is large increase in productivity beginning at ~1850 CE, which likely represents the dramatic response of productivity to the past century of average annual warming (Yackulic, 2017). Similar to BSi and

OM, the $RABD_{615}$ and $RABD_{660}$ measurements do not display distinct differences between the MCA and LIA.

The high-energy deposits do not exhibit elevated magnetic susceptibility in core CTR 4 (Figure 3.2). MS peaks can be indicative of increased erosion into a lake (Whitlock and Larsen, 2001), however, peaks in MS from CTR 4 are not associated with the three identified instantaneous deposition events or the two dropstones, despite the abundant minerogenic matter that is present in these sections. The most prominent peaks in MS occur between 154 and 56 cm. Sediment accumulation rates however, are relatively stable throughout this section, never exceeding 0.115 cm/year (Figure 3.4). From 56 cm to the surface, MS readings remain very low and stable, despite being associated with very high sediment accumulation rates (> 0.4 cm/year). Furthermore, peaks in MS do not correlate with increases or decreases in OM. Yackulic (2017) found similar results in his examination of multiple Crater Lake sediment cores. It is possible that peaks in MS represent deposition events that are not apparent from other proxies or lithologic examination, but there is no connection between identified deposition events or sections with high accumulation rates or changes in organic material.

4.3 Vegetation and Fire History at Crater Lake

4.3.1 Pollen, Charcoal, and Pyrogenic PAHs

Pollen Zone CTR 4-1 (~1035 to ~1450 CE; 154 to 92 cm)

During zone CTR 4-1 time, the vegetation surrounding Crater Lake was very similar in composition to the modern vegetation. However, both pollen and macrofossil evidence confirm that *Abies*, which is not part of the modern vegetation regime, was present around the lake between ~1050 to ~1375 CE. *Pinus edulis* (piñon pine; 10%) and *P. ponderosa* (ponderosa pine; ~16%) percentages both reach maximum values during this time, suggesting an expansion of these lower elevation pine species. Similarly, total *Pinus* pollen also reaches its maximum value during this interval. *Salix* and *Alnus*, both riparian indicators, are also consistently present during CTR 4-1 time. Cyperaceae, another wetland indicator species, is also present during this interval, but in its lowest percentages in the CTR 4 pollen assemblage. Poaceae (average of 7.4%) is at its highest values during the CTR 4-1 time, which indicates the presence of established grassy areas in forest openings near the lake and, potentially, increased establishment of grasslands at lower elevations.

The *Picea/Pinus* (P/Pi) ratio averages 0.2 throughout zone CTR 4-1. Although P/Pi values below 0.2 elsewhere have been interpreted as indicating the presence of alpine tundra (Anderson et al., 2014), it is unlikely treeline dropped below Crater Lake (3323 m asl) during this time interval. Rather, it is more plausible that expansion of lower elevation *Pinus* species led to the lower P/Pi values. Because ~80% of the Crater Lake basin is above treeline or not vegetated it does not contribute significantly to the sedimentary pollen record. Fall (1992) determined that *Pinus* pollen from lower elevations often overwhelms the local pollen producers above treeline. Thus it is likely that *Pinus* pollen is overrepresented in the CTR 4 record, ultimately depressing the Pi/P ratio.

Increases in *Picea/Artemisia* (P/A) values and relatively low Cyperaceae/Poaceae (C/P) values further suggest the expansion of species more characteristic of drier habitats, as a result of increased aridity and climatic warming during the early and middle stages of CTR 4-1 time (Mensing et al., 2007; Jiménez-Moreno et al., 2008, 2011). The P/A ratio shows that from ~1035 to ~1350 CE, warm arid conditions prevailed. After ~1350 CE, decreased P/A ratios indicate the climate began to cool leading into pollen zone CTR 4-2. Low C/P values throughout the CTR 4-1 time suggest drier conditions were present (Mensing et al., 2007).

During CTR 4-1 time, both the charcoal and pyrogenic PAH data show high variability. Peaks in CHAR remain well below maximum values (Figure 3.4), but background concentrations are highest during this interval. Similarly, the highest background concentrations of all eight pyrogenic PAHs occur during this interval (Figure 3.5). CharAnalysis detected two fires at 135 and 101 cm based on background charcoal concentrations (Figure 3.7). These depths match up very closely with two prominent fire peaks in the raw charcoal record during this interval at 135 and 98 cm depth. Despite the fact that (1) charcoal particle counts are very low, (2) CharAnlysis results vary greatly with small changes to input parameters, and (3) pyrogenic PAH peaks do not coincide with peak in raw charcoal (Figure 3.6), the two peaks identified by CharAnalysis appear to represent fires within the Crater Lake basin.

Although pyrogenic PAH peaks do not correspond precisely with CHAR peaks, heightened concentrations of both pyrogenic PAHs and charcoal indicate increased regional fire activity during CTR 4-1 time. Elevated fire activity was likely a product of increased regional aridity and temperature between ~950 to ~1350 CE as noted above. Both Marlon et al. (2012) and Power et al. (2012) noted increased region-wide fire event activity at multiple sites across western North America between ~950 to ~1400 CE. This is strong evidence that the record from Crater Lake fits into the larger regional reconstructions. Several dendrochronological and dust studies suggest similar trends of increased aridity and fire activity in the southern Rocky Mountains at this time (Cook et al., 2004; Meko et al., 2007; Woodhouse et al., 2010; Marlon et al., 2012; Routson et al., 2011, 2016). This interval (~1035 to ~1350 CE) generally coincides with the MCA as defined by Masson-Delmotte et al. (2013) between 950 to 1250 CE.

Slightly cooler conditions are evident during the last part of CTR 4-1 time (~1350 to ~1450 CE), as evidenced by decreasing P/A ratios (Figure 3.9), and somewhat wetter conditions may be indicated by an increase in the Cyperaceae/Poaceae ratio. *Abies* also disappears from the pollen and macrofossil records by ~1400 CE (Figure 3.10), indicating it was no longer present within the lake basin. A peak in charcoal at 98 cm and a CharAnalysis-detected fire peak at 101 cm suggests that a fire within the basin might be responsible for the disappearance of *Abies*.

Alternative explanations may include either an insect or pathogen outbreak, such as western balsam fir bark beetle (*Dryocoetes confusus*; McMillin et al., 2003; Kegley, 2006) during this climatic transition. Physical remains of biotic pests such as *Dendroctonus rufipennis* and *Dendroctonus confusus*, however, are rarely preserved in lacustrine sediments (Brunelle et al., 2008; Watt, 2008; Anderson et al., 2010; Morris et al., 2015), making this difficult to test. It is also possible that *Picea* filled in and dominated the canopy, largely eliminating *Abies*. *Picea engelmannii* will dominate forest stands over *Abies lasiocarpa* in the absence of disturbances (e.g. fire, biotic agents; Aplet, 1988; Vankat, 2013; Andrus, 2015). At least a temporary forest opening at this time is suggested by a contemporaneous peak in peak in Verbenaceae pollen (~1400 CE; Figure 3.8).

Pollen Zone CTR 4-2 (~1450 to ~1957 CE; 92 to 40.5 cm)

The CTR 4-2 time interval is characterized by the decrease of *Pinus edulis*, *P. ponderosa*, Poaceae pollen, and the P/A ratio, and increases in *Artemisia,* Cupressaceae, *Quercus* pollen and C/P ratios. Declines in both of these pines suggest a contraction of lower elevation species during this time interval. The decline in Poaceae probably indicates a closing of forest openings, and the expansion of *Artemisia*, indicates colder conditions. I interpret these as indicating a continuation of the cooling trend that began at the end of the CTR 4-1 interval. Similarly, the P/A ratio reaches its lowest values during the middle of this zone, further indicating cooling (Johnson et al., 2013). The increase in *Salix*, Apiaceae, Ranunculaceae, and Cyperaceae, in addition to the increased C/P ratio, suggests locally wetter conditions.

Quercus and Cupressaceae percentages all increase slightly over the course of CTR 4-2 time (Figure 3.8). It is notable that this occurs during and after an increase in regional fires, as indicated by the PAH data (Figure 3.6 and 4.1). *Quercus gambelii*, for example, is a fire adapted pioneer species in ponderosa pine and lower elevation mixed conifer forests (Romme et al., 2009a). Its slight expansion with a concomitant decline in ponderosa pine pollen suggests stand establishment in regionally burned areas. Cupressaceae (i.e. *Juniperus* spp.) may have responded in much the same manner, particularly in the latter part of this period (62-40.5 cm; ~1750 to ~1950 CE) by increasing its presence in forest openings as a result of disturbance, but being favored by a declining disturbance regime (e.g. Romme et al., 2009b; Margolis, 2014).

P/Pi ratios average 0.3 during zone CTR 4-2, which remain below Anderson et al.'s (2014) interpretation of presence of spruce-fir forests. Following the reasoning outlined above, however, the increase of this ratio is logical if lower elevation species of *Pinus* are no longer expanding their range. The ratio still remains below 0.4 because the majority of the catchment is not vegetated, and *Pinus* pollen remains overrepresented in the record. Although treeline may have declined slightly in elevation during the early and middle portions of zone CTR 4-2 time in response to cooler climatic conditions, it is almost certain that the *Picea* dominated spruce-fir forest remained intact around Crater Lake.

Abies reappears briefly in the pollen record during latter CTR 4-2 time, but there are no associated *Abies* macrofossils found during this interval (Figure 3.8 and 3.10). Despite the discontinuous presence of *Abies* in the pollen record and an overall low percentage (average 0.5%) during this time interval, macrofossils are present in conjunction with pollen at the beginning of CTR 4-3 time (Figure 3.10). Liepelt et al. (2009) pointed out that *Abies* has large and heavy pollen grains that are distributed discontinuously in parts of its range, suggesting that while it might not be present in the pollen record it could still be present locally. In total, this suggests that *Abies* was present in low numbers in the basin during the latter portions of CTR 4-2 time.

Average background concentrations of both charcoal, CHAR, and pyrogenic PAH concentrations are reduced from the CTR 4-1 time by ~30%. This suggests an actual decline in regional fire activity. However, the largest peak in the CTR 4 sedimentary charcoal record occurred during this period (~1750 CE; 64 to 62 cm; Figure 3.5 and 3.6), and CharAnalysis recognizes three peaks (78 cm, 64 cm, and 62 cm; Figure 3.7) as being indicative of a fire events within the Crater Lake basin.

The end of CTR 4-2 time encompasses the first potentially modern land use impacts in the region as prospectors and ranchers arrived in the mid to late 19th century (Allen, 2002). These early settlers were likely responsible for numerous fires in the region (Agee and Cuenin, 1924; Allen, 2002; Margolis et al., 2007). The Summitville mine, located about 9.5 km northeast of Crater Lake, was established in the 1870s (Margolis et al., 2007) and was nearly destroyed by a fire in 1883 (Alamosa News, 2018). The fire reported at Summitville in 1883 does not appear to have burned in the Crater Lake basin. However, a peak in pyrogenic PAHs at 54 cm may be associated with widespread fires, such as the extensive 1879 Lime Creek Burn in the western San Juan Mountains that burned 10,500 ha (Thompson, 2002; Toney and Anderson, 2006).

Based on the pollen data, zone CTR 4-2 is interpreted as an interval of increased moisture and potentially cooler and wetter climatic conditions than pollen zone CTR 4-1, particularly in the early and middle portions of this zone. Charcoal and pyrogenic PAH data suggest decreased regional fire activity similar to that suggested by Marlon et al. (2012). This interval (~1450 to ~1950 CE) largely coincides with the LIA (1450 to 1850 CE) as defined by Masson-Delmotte et al. (2013).

Pollen Zone CTR 4-3 (~ 1957 to 2016 CE; 40.5 to Surface)

The upper 40.5 cm represents the last ~59 years of vegetation and fire history at Crater Lake. It is characterized by a second reappearance of *Abies* (with plant macrofossils; Figure 3.10) and a subsequent disappearance, a decline in *Picea*, and increases in *Ambrosia*, Cupressaceae, and total *Pinus* pollen. There is also a very recent increase in *P. edulis* (Figure 3.8).

The reason for the decline in *Picea* is not clear. Based on the age model, this decline occurs prior to the current regional outbreak of spruce beetle (*Dendroctonus rufipennis*) that began in the early 2000s around Wolf Creek Pass (Andrus, 2015). The increases of *Ambrosia* and *Cirsium* may be associated with widespread human land use disturbances, particularly at lower elevations (e.g. agriculture), perhaps from as far away as the San Luis Valley (<50 km to the east). This is supported by the concurrent increase in greasewood (*Sarcobatus*), which also currently grows in the San Luis Valley. The slight increase in Cupressaceae (i.e. *Juniperus*) and in *Pinus edulis* in the most recent decades may be a function of 20th century fire suppression at lower elevations, which could have favored range expansion of piñon-juniper woodlands (Zier and Baker, 2006; Romme et al., 2009b; Margolis, 2014).

Increases in the total amount of *Pinus* and declines in the P/Pi ratio (0.2; Figures 3.8 and 3.9) also suggest the expansion of lower elevation *Pinus* species. Although pine preservation was insufficient to confirm, it is likely that this is represented by *Pinus ponderosa*, perhaps in response to 20th century fire suppression (Romme et al., 2009a). The increase of P/A ratios from CTR 4-2 time also indicates a warming during this century. These interpretations are in substantial agreement with Fink et al. (2014), who documented a continuing upward shift in treeline in Colorado over the last three decades. The C/P ratio also increases to a maximum average value despite a great deal of variability with maximum value at 14.5 cm (0.8) and minimum value at 0 cm (-0.4). The C/P ratio is in decline throughout CTR 4-3 time suggesting increasingly arid conditions over the last half century.

With the exception of the Summitville Fire (1883; Alamosa News, 2018), the Million Fire (2002; Denver Post, 2016) south of South Fork, Colorado, and the West Fork Complex Fire (2013; Denver Post, 2016), northeast of Crater Lake, no documented wildfires have burned within 40 km of the lake during the historic period (Figure 4.1). Although total charcoal from this zone is lower than in any other zone in the CTR 4 record (Figures 3.5 and 3.6), CHAR values are higher than the other two time intervals. This is because the sedimentation rates in the top 43.5 cm of the CTR 4 core are very high, which may also be a product of the uncertainty in the CTR 4 age model (Figure 3.4). The US Forest Service practice of fire suppression has not likely altered the fire regime for subalpine *Picea-Abies* forests in the southern Rocky Mountains (Margolis et al., 2007; Vankat, 2013), but because CHAR rates in the CTR 4-3 time interval are elevated, the regional impact of fire suppression in the surrounding ecosystems is not readily apparent. This is in contrast to the 20th century records of six high elevation sites from the southern Rocky Mountains (Anderson et al., 2008a) where low background charcoal concentrations were tied to fire suppression.

4.4 Using Sedimentary Charcoal and PAH Data to Determine Fires at Crater Lake

Significant differences in the average values of CHAR and pyrogenic PAH concentrations exist between pollen zones 1 and 2. Further, within each pollen zone there are also significant differences in timing between the occurrence of most CHAR and pyrogenic PAHs peaks on the order of decades to centuries (Figures 3.6 and 4.2). This suggests that the eight pyrogenic PAHs detected and analyzed in this study are either (1) not deposited simultaneously in the sediment with charcoal following the same fire events, (2) are diluted by short term increases in sedimentation following fire events causing records to appear in antiphase (negatively correlated), or (3) pyrogenic PAHs represent fire events other than those recorded by charcoal.

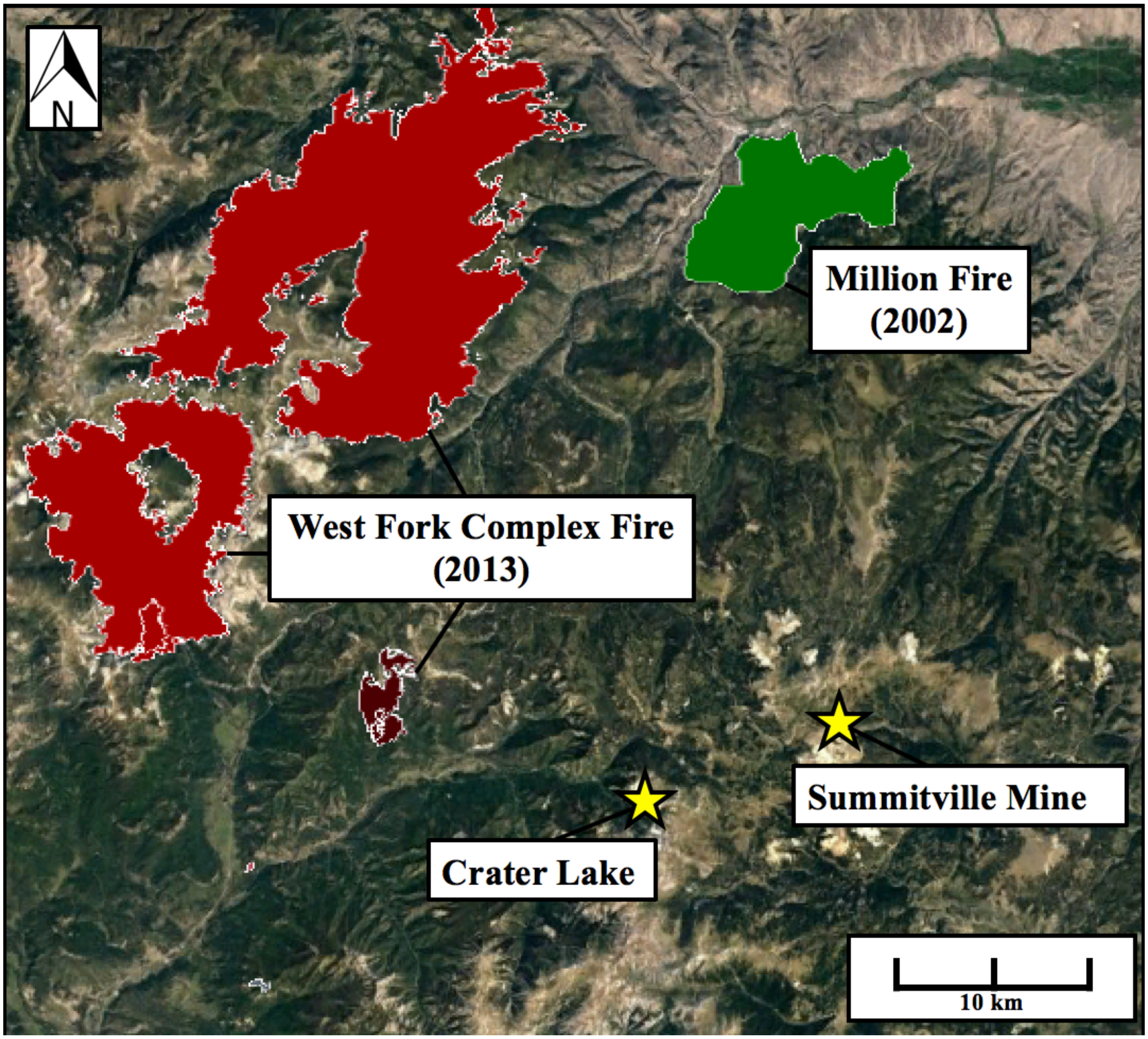

Figure 4.1: Historic fires that have burned within 40 km of Crater Lake include the Million Fire (2002) and the West Fork Complex Fire (2013; Google Earth Image, 2018 Digital Globe). Additionally, reports suggest there was a fire near the Summitville Mine in 1883 (Alamosa News, 2018). Fire perimeters inferred from satellite imagery and information provided by the National Interagency Fire Center; Rocky Mountain Insurance Information Association; U.S. Forest Service; Colorado State Forest Service; Colorado Division Emergency Management (Denver Post, 2016).

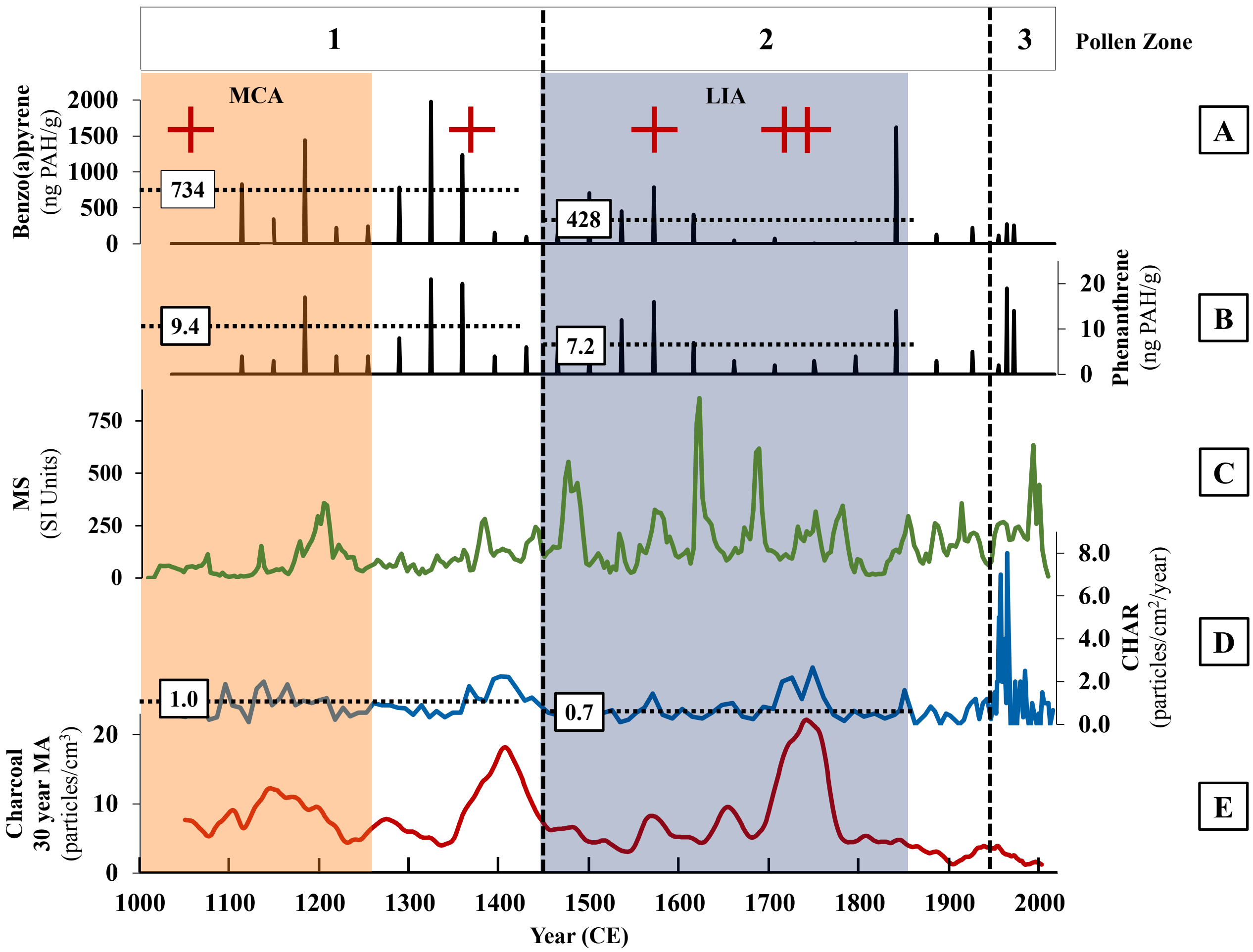

Figure 4.2 Comparison of the most prevalent (A) HMW (benzo(a)pyrene) and (B) LMW (phenanthrene) pyrogenic PAHs (ng of PAH/g) with (C) MS (SI units), (D) CHAR (particles/cm^2/year), and (E) total charcoal values (particles/cm^3) with a 30 year moving average (MA). The dashed lines and associated white boxes display the average concentration over two intervals (~1000 CE to ~1450 CE and ~1450 CE to ~1850 CE) for each proxy. CharAnalysis fire event interpretations are indicated by the five red "plus" signs. The ages of the orange (MCA) and blue (LIA) shaded boxes are defined by Masson-Delmotte et al. (2013).

Peaks in the MS record and fluctuations in sediment accumulation rates (Figure 3.4) do not coincide or occur immediately following either CHAR or pyrogenic PAH peaks (Figure 4.2). The fact that both LMW (r = -0.09, p = 0.440) and HMW (r = -0.1, p = 0.285) pyrogenic PAHs share an insignificant correlation with CHAR concentrations suggests that, if there were increases in sedimentation following fire events, they did not dilute pyrogenic PAHs (Figure 4.3). Neither the LMW nor the HMW pyrogenic PAHs detected in this study show a significant

($\alpha = 0.05$) relationship with charcoal concentrations, suggesting that these two fire proxies are unrelated and are recording different fire events throughout the record.

Working on sediments of the last 100 years, Denis et al. (2012) did not find a strong relationship between peaks in charcoal and peaks in both LMW and HMW pyrogenic PAHs. Miller et al. (2017), however, did find a strong relationship between concentrations of the pyrogenic PAH retene and peaks in charcoal over the last ~250 years. Retene concentrations were not analyzed in the CTR 4 sediments, but Miller et al. (2017) concluded that it is a good indicator of regional fire events, while chrysene, which was analyzed from the CTR 4 sediments but not detected in significant quantities, is a good indicator of the burning of fossil fuels. It is possible that the 16 pyrogenic PAH compounds analyzed in this study may not be the best indicators of forest fires. Further research is needed to confirm this.

It is also possible that additional PAHs could be identified with a different methodology. The pyrogenic PAH samples in this study were processed using GC-MS. Denis et al. (2012) found that high performance liquid chromatography with fluorescence detection (HPLC-FLD) was superior to GS-MS, with the ability to detect PAH compounds in minute quantities. Utilizing HPLC-FLD as opposed to GC-MS, might have also produced different results in this study, allowing for the detection of more pyrogenic PAH compounds across all samples.

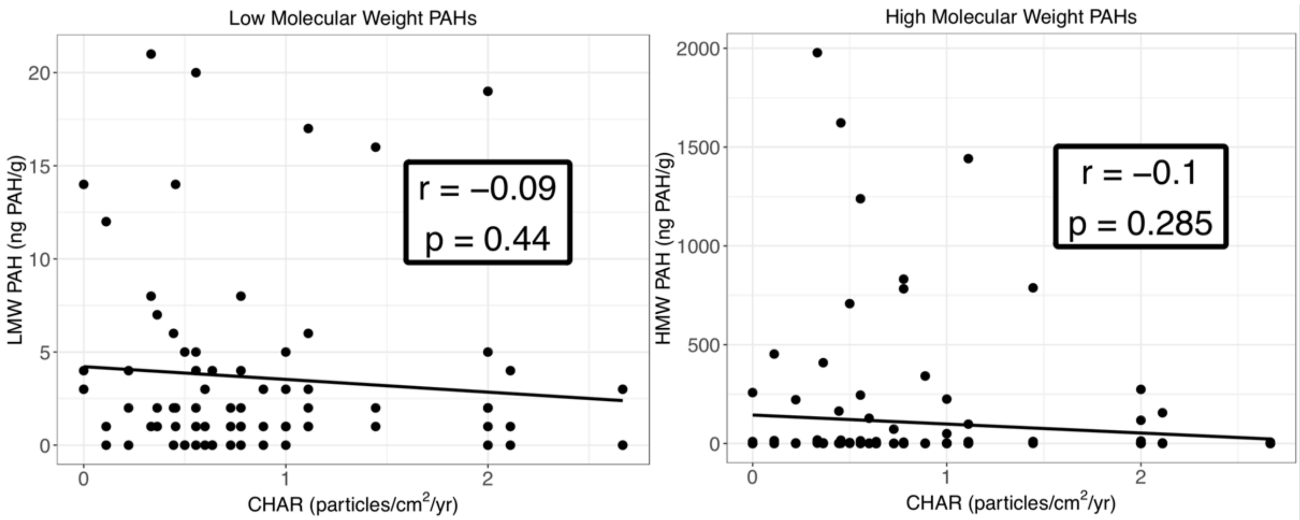

Figure 4.3: Scatter plots for LMW (left panel) and HMW (right panel) PAHs showing the relationship between pyrogenic PAH concentrations and charcoal influx rate (CHAR). The r and p values indicate correlation and significance, respectively, between the PAHs (y-axis) and CHAR (x-axis). The lines indicate the least squares linear regression.

Based on the combination of the charcoal and pyrogenic PAHs data, I deduce that the Crater Lake basin has experienced five fire events between ~1035 to 2016 CE. The CharAnalysis evaluation determined two peaks in the raw sedimentary charcoal data to be indicative of significant fire events during zone CTR 4-1 time (~1140 and ~1370 CE; Figure 3.7). The ~1370 CE fire event at 101 cm is likely responsible for the disappearance of *Abies* from the Crater Lake Basin during the end of CTR 4-1 time. Despite both average CHAR and pyrogenic PAH concentrations being lower than CTR 4-1 time (Figure 4.2), the basin experienced three fires during CTR 4-2 time (~1570 CE, ~1725 CE, and ~1750 CE). This suggests that although regional fire activity decreased during this period, the FRI was not altered substantially. Two of the fire events detected using CharAnalysis occur within ~25 years of each other, suggesting that these fires were not stand replacing around the lake basin, as the subalpine forest fire regime is typified by crown fires that require mature forests stands and ample fuel loads to carry flames (Vankat, 2013). Forest regeneration times following crown fires are typically on the order of several decades to centuries (Romme et al., 2009a), which suggests the peaks identified at 64 and

62 cm are (1) associated with the same stand replacing fire event, or (2) these were separate, non-stand replacing fire events around the Crater Lake Basin.

The five fire events identified in the CTR 4 fire history record suggest an FRI of ~200 years at Crater Lake. This closely mirrors the findings of Veblen et al. (1994) and Anderson et al. (2008a) who have suggested that fire recurrence intervals in *Picea-Abies* forests in the southern Rocky Mountains average ~100 to ~200 years throughout the Holocene. Two CharAnalysis identified fires occurred during CTR 4-1 time, while three fire events identified during CTR 4-2 time. This indicates average FRIs of ~200 years and ~170 years respectively during these two periods.

The mosaic of forested and talus areas near the lake present a significant barrier to fires burning across the basin. This has undoubtedly contributed to the observed fire regime in this study for the last 1000 years, and led to the low charcoal concentrations found throughout CTR 4. The low charcoal concentrations found in the CTR 4 sediments are comparable to those found at Little Molas Lake in an open *Picea-Abies* forest in the western San Juan Mountains (Toney and Anderson, 2006). Over the last 1000 years the FRI at Little Molas Lake was ~143 to 166 years (~6-7 fire events/1000 years). At Crater Lake, the average FRI during the combined CTR 4-1 and CTR 4-2 (~1035 to 1950) intervals was ~180 years.

4.5 The Potential for Reconstructing Spruce Beetle Infestations

Vegetation composition surrounding Crater Lake has evolved over the last 1000 years but has remained largely a *Picea* dominated spruce-fir forest. Although fire disturbances have played a distinctive role in the vegetation history at Crater Lake, other disturbances may have impacted vegetation as well. Beginning in the early 2000s, a widespread spruce beetle outbreak was detected across the eastern San Juan Mountains (CSFS, 2012; Andrus, 2015). All of the mature *Picea engelmannii* trees surrounding Crater Lake are now dead as a result. This, however, is not readily apparent in the pollen record, suggesting that similar episodes of bark beetle and/or pathogen outbreaks may have caused high mortality rates across similar mature stands of *Picea*, allowing a new cohort of understory trees to emerge and dominate the canopy in the absence of fire events (Romme et al., 2006).

Biotic pest outbreaks, such as the spruce beetle (*Dendroctonus rufipennis*; Morris et al., 2015) and the western balsam beetle (*Dendroctonus confusus*; McMillin et al., 2003; Kegley, 2006), can cause mass mortality within subalpine *Picea-Abies* forests. Yet, despite large beetle populations associated with these outbreaks, subfossil beetle remains are rarely preserved in lacustrine sediments (Brunelle et al., 2008; Watt, 2008; Anderson et al., 2010; Morris et al., 2015). A number of factors affect spruce beetle preservation including water surface characteristics, water pH, coring location, and absence or presence of fish within the lacustrine environment (Morris et al., 2015). Because of their rarity in the macrofossil record, even in sites with historically documented outbreaks, interpreting paleo-environmental changes using lake sediment proxies has been difficult (Anderson et al., 2010).

Modern and historical outbreaks both attest to the large impact biotic pests, such as beetles, can have on a forested landscape (Morris et al., 2015); beetle outbreaks have most certainly occurred naturally in subalpine ecosystems for millennia (Veblen et al., 1994). However, the frequency and scale of these events has increased considerably since European settlement of western North America (Morris et al., 2015). These trends can be linked to increased average temperatures that have stressed trees and altered and accelerated beetle life-cycles (Morris et al., 2015). As methodologies to detect the presence of beetles in lacustrine sediments improve, they will undoubtedly increase our understanding about the impacts and timing of former outbreaks, registered in lake sediments.

4.6 The MCA and LIA Intervals at Crater Lake

Previous research has suggested that during the MCA interval some areas in the southern Rockies experienced increased aridity, fire activity, and shifts in regional vegetation composition (Petersen, 1994; Woodhouse et al., 2010; Marlon et al., 2012; Routson et al., 2011, 2016), and during the LIA interval some areas experienced decreased fire activity and changes in vegetation compositions indicative of decreased aridity and cooler average temperatures (personal communication, Dr. R. Scott Anderson; Petersen, 1994; Armour et al., 2002; Anderson et al., 2008a; Bigio et al., 2010; Marlon et al., 2012; Johnson et al., 2013; Loisel et al., 2017; White, 2017). Other researchers (e.g. Grissino-Mayer and Swetnam, 2000), however, have interpreted paleo proxies as indicating a wetter MCA, and drier LIA. Still, other researchers suggest there is little, or no difference between these two intervals (Toney and Anderson, 2006; Anderson et al., 2008b; Johnson et al., 2013). The numerous and varied interpretations of climatic conditions during the MCA and LIA intervals from sites across the Southwest highlight the complexity and difficulty of identifying a distinct regional climate event across multiple paleo-proxies and sites.

Dean (1994) examined multiple proxy records from the Southwest and concluded that there is no evidence of significant difference between the MCA or LIA. The research presented in this thesis, however, suggests the MCA and LIA were distinct climate intervals in the southern Rocky Mountains as also interpreted by Petersen (1994). However, unlike Petersen (1994), who postulated a warm, wet MCA and a cool, dry LIA from the Beef Pasture site (3060 m asl, Figures 1.5 and 4.4), the CTR 4 sediments suggest a warmer, more arid MCA with lower elevation species expansion (i.e. expansion of piñon-juniper woodlands and ponderosa pine forests), and increased regional fire occurrence, and a cooler, wetter LIA with decreased lower elevation *Pinus* species expansion and regional fire occurrence. Changes in the P/Pi ratios from Beef Pasture and Crater Lake do not correspond because of the overrepresentation of *Pinus* pollen as previously discussed (Figure 4.4). The P/A ratios display similar trends at Beef Pasture and Crater Lake, but the timing of maximum ratios does not match up exactly (Figure 4.4). This may be related to differences in elevation (Crater Lake is nearly 300 m higher in elevation) and orientation (Beef Pasture is in an open spruce forest on the western slope of the La Plata Mountains) of the two sites, which causes each to experience different local climates. C/P ratios from Beef Pasture and Crater Lake, however, display similar trends over the last 1000 years (Figure 4.4), suggesting drier MCA, and a wetter LIA.

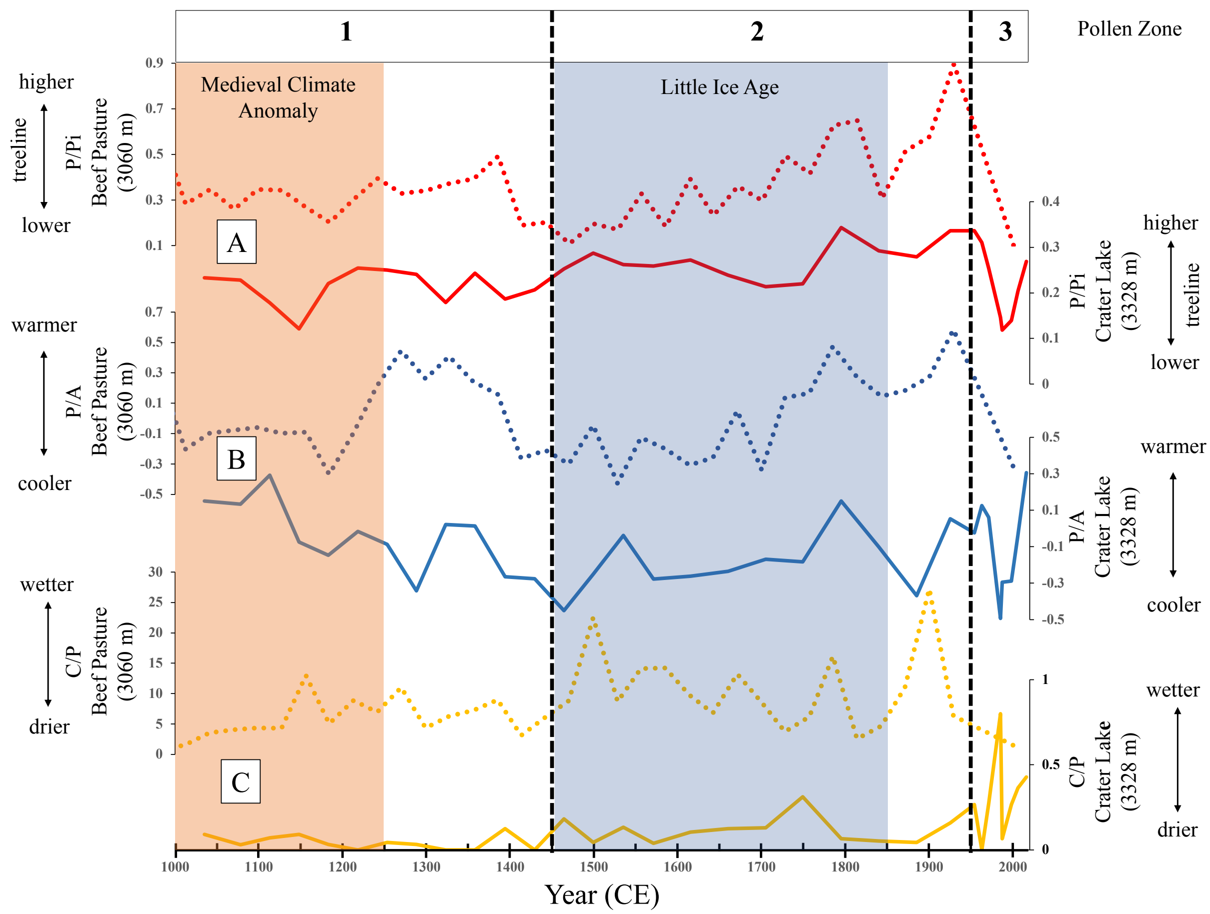

Figure 4.4: A comparison of high-resolution pollen ratio data from Beef Pasture (dotted lines; Petersen, 1994; Wright, 2006) and Crater Lake (solid lines). (A) *Picea/Pinus* (P/Pi) is indicative of changes in treeline, (B) *Picea/Artemisia* (P/A) is indicative of warmer or cooler conditions surrounding the respective coring site, and (C) Cyperaceae/Poaceae (C/P) is indicative of wetter or drier conditions. The Medieval Climate Anomaly and the Little Ice Age climate intervals as defined by Masson-Delmotte et al. (2013), are indicated by the light orange and light blue boxes respectively.

Petersen's (1994) work at Beef Pasture was later expanded upon by Wright (2006), who improved the age model. One reason both Petersen (1994) and Wright (2006) interpreted warmer, wetter regional conditions during the MCA and cooler, drier regional conditions during the MCA may be related to their exploration of Ancestral Puebloan habitation in the Four Corners region and the impact climate appears to have had on these societies. Archaeological explorations have revealed that the amount of land utilized for agricultural production increased during the MCA, and decreased during the LIA (Petersen, 1994; Wright, 2006). This has been interpreted as more favorable climate for agricultural production during the MCA timeframe, and less favorable climate during the LIA.

Although this research does not resolve the regional spatial and temporal extent of climatic conditions during the MCA and LIA, it adds a critical examination of the climatic conditions that prevailed during these intervals, and how they impacted the fire regime and vegetation communities. Drought was prevalent in the eastern San Juan Mountains throughout both the MCA and LIA climate intervals as evidenced by the Routson et al. (2016) study of Fish Lake ~15 km to the south of Crater Lake (Figures 1.5 and 4.5). More arid conditions prevailed during the MCA, and moisture availability increased over the course of the LIA climate interval, however, climatic variability also appears to have increased during the LIA as evidenced by periods of extreme drought that are readily apparent in regional dendrochronology studies (e.g. Routson et al., 2011). This may be associated with increased variability in solar irradiance that began around ~1250 CE (Steinhilber et al., 2009; Figure 4.5, panel J). Loisel et al. (2017) suggest that the extremes in moisture availability experienced during the LIA, and warm, dry conditions similar to that which were experienced during the MCA at Crater Lake, serve as appropriate climate analogues for future climatic conditions across the Southwest as average annual temperatures continue to increase.

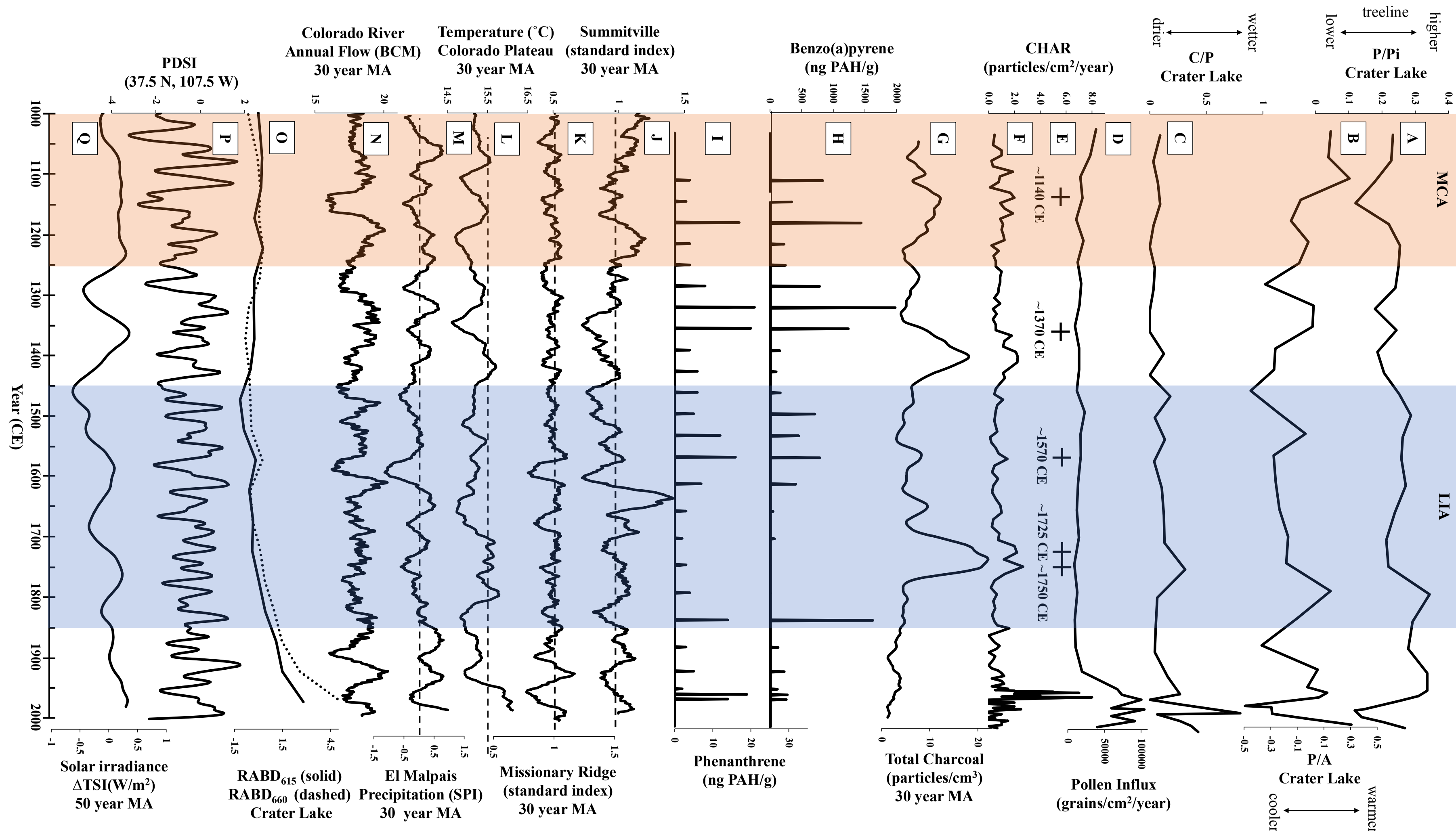

Figure 4.5: From the top, (A) P/Pi, (B) P/A, (C) C/P pollen ratios, (D) pollen influx, (E) CharAnalysis fire event interpretations indicated by the five "plus" signs and their respective ages, (F) CHAR, (G) total raw charcoal data smoothed with a 30 year moving average (MA), (H) benzo(a)pyrene (HMW) and (I) phenanthrene (LMW) pyrogenic PAH concentrations, (J) Summitville (Routson et al., 2011) and (K) Missionary Ridge (Bigio et al., 2010) dendrochronology moisture records, (L) southern Colorado Plateau temperature reconstruction (Salzer and Kipfmueller, 2005) with a 30 year MA, (M) El Malpais, New Mexico, precipitation reconstruction (SPI; Grissino-Mayer, 1995), Colorado River flow reconstruction from Lee's Ferry, Arizona, in billions of m^3 (BCM; Meko et al., 2007), (O) $RABD_{615}$ (solid line) and $RABD_{660}$ (dashed line) data from Crater Lake (Yackulic, 2017), (P) PDSI from 37.5 N, 107.5 W with 20 year smoothing (Cook and Krusic, 2004), (Q) and solar irradiance with a 50 year moving average (Steinhilber et al., 2009). The ages of the MCA (orange) and LIA (blue) shaded boxes are defined by Masson-Delmotte et al. (2013).

4.7 Policy Considerations

One increasingly important function of paleoecological studies, such as the research presented in this thesis, is to provide baseline information for understanding contemporary ecosystems (Dietl and Flessa, 2011; Wingard et al., 2017). High-resolution documentation of past climatic fluctuations and the associated effects on vegetation, fire, and other disturbance regimes provide researchers, land managers, and policy makers with critical information about the processes that have and will continue to shape and influence ecosystem changes in the future (Anderson et al., 2015). Past environmental changes as recorded by paleoecologic and paleoclimate proxies are not perfect analogues for future changes but do provide a better understanding of how climatic changes and disturbance regime will affect modern ecosystems. Armed with the wealth of information paleorecords provide, researchers, resource managers, and policy makers will have a more thorough understanding of how future climate changes will affect regional ecosystems and will ultimately be able to formulate more effective and meaningful strategies to deal with these changes (Anderson et al., 2000; Birks, 2003; Jackson et al., 2009; Denis et al., 2012; Wingard et al., 2017).

As the Southwest becomes increasingly arid as a result of anthropogenically induced climate change, the research presented in this thesis suggests that we will likely see an upward elevational expansion of vegetation communities. This has already been documented with treeline by researchers in the southern Rocky Mountains (Fink et al., 2014). Land managers, such as the U.S. Forest Service should carefully monitor changes to treeline, as well as vegetation composition changes in ecotones.

We will also see increases in both frequency and areal extent of wildland fires in ecosystems at all elevations (Marlon et al., 2012). In mature subalpine forest stands that have not experienced fire in the last two centuries, many sites will likely see large, stand replacing fires, or significant biotic pest outbreaks, in the next half century. Following large-scale disturbances (e.g. fires, beetle outbreaks), land managers should carefully monitor forest regeneration rates, and what species are returning. It has already been observed that some forested ecosystems across the Southwest are not recovering to pre-disturbance compositions (Hayes and Robeson, 2011).

It is already projected that annual snowpack will decrease and dramatically by the middle of the 21st century and spring melt will start earlier in the season (Nydick et al., 2012). Increases in average annual temperature and decreases in moisture will undoubtedly have a major impact on the high elevation ecosystems that harbor the majority of the moisture that human populations in the Southwest utilize. Future climatic changes foreshadow a major water crisis for the large human populations that now inhabit the region, and a major ecological crisis for high elevation vegetation communities. Properly monitoring and managing forested ecosystems in the Southwest is critical for the water security of future generations.

Chapter 5: Conclusions

The pollen, plant macrofossil, sedimentary charcoal, and pyrogenic polycyclic aromatic hydrocarbon PAH records developed from Crater Lake add additional important pieces of information to the larger network of studies from the southern Rocky Mountains. The objectives of this research were to (1) reconstruct the vegetation and fire histories of the Crater Lake basin for the last ~1000 years, in order to explore how the subalpine ecosystem surrounding Crater Lake has changed as a result of climatic variability and natural disturbance regimes (e.g. fire), (2) to investigate the undefined relationship between sedimentary charcoal and pyrogenic Polycyclic Aromatic Hydrocarbons (PAHs) in long term sediment records and how each of these proxies record fire events, and (3) determine whether the high-resolution pollen and sedimentary fire histories presented in this thesis reveal anything unique about the last 1000 years, such as centennial scale climate phenomena like the MCA and LIA, compared to previous studies from mixed conifer to subalpine lakes and bogs in the southern Rocky Mountains. Although it has remained a largely *Picea* dominated subalpine forest, high-resolution pollen, macrofossil, charcoal, and pyrogenic PAH records derived from CTR 4 have revealed distinct changes to the ecosystem surrounding Crater Lake over the last 1000 years.

5.1 Addressing the Research Questions

5.1.1 Vegetation Changes at Crater Lake Over the Last 1000 Years

The pollen assemblages revealed numerous vegetation changes and three distinct pollen zones between ~1035 to ~1450 CE (CTR 4-1), ~1450 to ~1950 CE (CTR 4-2), and ~1950 to present (CTR 4 -3). CTR 4-1 and CTR 4-2 are contemporaneous with the MCA and LIA climate intervals, respectively. Between ~1035 to ~1350, the eastern San Juan Mountains, as typified by the Crater Lake record, experienced increased aridity and higher temperatures, as well as an increase in regional fire activity. The local forest consisted of both *Picea* and *Abies* trees. Based on well-defined pollen ratios, evidence suggests an expansion of lower elevation *Pinus* forest and woodland (P/A ratio), and an increase in subalpine treeline near the lake (P/Pi ratio) and a general increase in forest openings (C/P ratio).

By ~1350, however, the disappearance of *Abies* from the pollen and macrofossil record as the result of a fire event signals a climatic shift. Between ~1350 to ~1850, the region experienced cooler, wetter conditions. The expansion of lower elevational *Pinus* species tapers off, and there is an overall decrease in regional fire activity, and a likely decrease in treeline. The historical period in the region began around ~1850 with the arrival of prospectors and ranchers (Allen, 2002). Historic land use practices and the beginning of fire suppression across the western United States have notable impacts particularly on lower elevational environments. There is no evidence of historic or modern livestock grazing at the Crater Lake site, nor are there any grazeable meadows within the Crater Lake watershed. It is unlikely that there have been any significant or lasting alterations to the ecosystems surrounding the lake as a result of human land use activity.

5.1.2 The Relationship Between the Sedimentary Charcoal and Pyrogenic PAH Records

Analysis of sedimentary charcoal and pyrogenic PAHs revealed five fire events at Crater Lake of the last 1000 years (FRI ~200 years). Multi-century-scale trends in the average concentrations of PAHs and charcoal correspond and show that fire was more common during the MCA interval than during the LIA interval. Peak concentrations of charcoal and pyrogenic PAHs, however, do not correspond. This suggests that charcoal and the 16 pyrogenic PAHs analyzed from CTR 4 do not record the same fire events. The lack of an apparent relationship between peak concentrations of charcoal and pyrogenic PAHs may also be the result of the specific pyrogenic PAHs that were analyzed in this study, and the detection sensitivity of the laboratory methods that were employed.

Despite similarities in general patterns between charcoal and pyrogenic PAHs, the data from Crater Lake suggest that these two proxies record different fire events. Future studies should analyze for a broader range of pyrogenic PAHs, including retene, and utilize more sensitive sample detection methodologies, such as using HPLC-FLD as opposed to GC-MS, to detect pyrogenic PAHs that may be present in lower concentrations. Field methodologies, such as selecting a sediment core from a lake with a well-developed and known charcoal chronology, and avoiding lakes that are surrounded by a broken forested ecosystem with natural fire buffers that might have experience few fire events, should also be considered. Future studies will undoubtedly shed more light on the unresolved relationship between pyrogenic PAHs and charcoal.

5.1.3 The Record from Crater Lake vs. Other Records from the Southern Rocky Mountains

Unlike Dean (1994) who suggested there was no indication of distinct centennial-scale climate events over the last 1000 years, the high-resolution pollen, charcoal, and pyrogenic PAH record developed in this thesis suggest there were distinct climate intervals associated with both the MCA and the LIA as defined by Masson-Delmotte et al. (2013). Several records from across the region are in agreement with the interpretations developed in this thesis, suggesting increased aridity during the MCA (Cook et al., 2004; Salzer and Kipfmueller, 2005; Meko et al., 2007; Woodhouse et al., 2010; Marlon et al., 2012; Routson et al., 2011, 2016), however, only a few (e.g. Petersen, 1994; Anderson et al., 2015) attribute this to the MCA interval. Similarly, few studies (e.g. Petersen, 1994; Anderson et al., 2015) have suggested a distinct LIA interval in

Colorado.

Although the ecosystem surrounding Crater Lake has remained a *Picea* dominated spruce-fir forest over the last 1000 years, distinct changes, such as the disappearance of *Abies* following a fire event, the expansion of lower elevational arboreal species, and responses to climatic intervals, such as the MCA and LIA, were captured by this high-resolution study. These data show distinct MCA and LIA intervals in the southern Rocky Mountains. Because the general trends of vegetation and fire history are well resolved across the southern Rocky Mountains since the LGM, future vegetation studies should focus on specific intervals with high-resolution approaches, similar to this study.

References

Abolt, R.A.P., 1997. Fire histories of upper elevation forests in the Gila Wilderness, New Mexico, via fire scar and stand age structure analyses. MS Thesis, University of Arizona, Tucson, Arizona.

Adams, D.K., Comrie, A.C., 1997. The North American monsoon. Bulletin of the American Meteorological Society 78, 2197-2213.

Agee, F.K., Cuenin, J.M., 1924. History of Cochetopa National Forest: Historical report of the forest supervisor. USDA Forest Service, Salida, Colorado.

Alamosa News, 2018. Summitville tour and dedication ceremony set July 14-15, Valley Courier. https://alamosanews.com/article/summitville-tour-and-dedication-ceremony-set-july-14-15 (accessed 4 April 2018).

Allen, C.D., 2002. Lots of lightning and plenty of people: an ecological history of fire in the upland Southwest, in: Vale, T.R. (Ed.), Fire, Native peoples, and the Natural Landscape. Island Press, Washington, D.C., pp. 143-193.

Allen, C.D., Anderson, R.S., Jass, R.B., Toney, J.L., Baisan, C.H., 2008. Paired charcoal and tree-ring records of high frequency Holocene fire from two New Mexico bog sites. International Journal of Wildland Fire 17, 115-130.

Allen, C.D., Betancourt, J.L., Swetnam, T.W., 1998. Landscape changes in the southwestern United States: Techniques, longterm datasets, and trends, in: Sisk, T.R. (Ed.), Perspectives on the Land use History of North America: A Context for Understanding our Changing Environment. U.S. Geological Survey Biological Science Report 1998-03, pp. 71–84.

Anderson, L., Brunelle, A., Thompson, R.S., 2015. A multi-proxy record of hydroclimate, vegetation, fire, and post-settlement impacts for a subalpine plateau, central Rocky Mountains, USA. The Holocene 25, 1-12.

Anderson, R.S., Feiler, E., 2009. Holocene vegetation and climate change on the Colorado Great Plains, USA, and the invasion of Colorado pinyon (*Pinus edulis*). Journal of Biogeography 36, 2279-2289.

Anderson, R.S., Betancourt, J.L., Mead, J.I., Hevly, R.H., Adam, D.P., 2000. Middle- and late-Wisconsin paleobotanic and paleoclimatic records from the southern Colorado Plateau, USA. Paleogeography, Paleoclimatology, Paleoecology 155, 31-57.

Anderson, R.S., Allen, C.D., Toney, J.L., Jass, R.B., Bair, A.N., 2008a. Holocene vegetation and fire regimes in subalpine and mixed conifer forests, southern Rocky Mountains, USA. International Journal of Wildland Fire 17, 96-114.

Anderson, R.S., Jass, R.B., Toney, J.L., Allen, C.D., Cisneros-Dozal, L.M., Hess, M., Heikoop, J., Fessenden, J., 2008b. Development of the mixed conifer forest in northern New Mexico and its relationship to Holocene environmental change. Quaternary Research 69, 263-275.

Anderson, R.S., Smith, S.J., Lynch, A.M., Geils, B.W., 2010. The pollen record of a 20th century spruce beetle (*Dendroctonus rufipennis*) outbreak in a Colorado subalpine forest, USA. Forest Ecology and Management 260, 448-455.

Anderson, R.S., Jiménez-Moreno, G., Ager, T., Porinchu, D.F., 2014. High-elevation paleoenvironmental change during MIS 6-4 in the central Rockies of Colorado as determined from pollen analysis. Quaternary Research 82, 542-552.

Andres, H.J., Peltier, W.R., 2016. Regional influences of natural external forcings on the transition from the Medieval Climate Anomaly to the Little Ice Age. Journal of Climate 29, 5779-5800.

Andrus, R.A., 2015. Influences of an active spruce beetle outbreak on fire severity in spruce-fir forests in southern Colorado. MS Thesis, University of Colorado, Boulder, Colorado.

Aplet, G.H., Laven, R.D., Smith, F.W., 1988. Patterns of community dynamics in Colorado Engelmann spruce-subalpine fir forests. Ecology 62, 312-319.

Armour, J., Fawcett, P.J., Geissman, J.W., 2002. 15 k.y. paleoclimatic and glacial record from northern New Mexico. Geology 30, 723-726.

Barron, J.A., Metcalfe, S.E., Addison, J.A., 2012. Response of the North American monsoon to regional changes in ocean surface temperature. Paleoceanography 27, 1-17.

Benedict, J.B., Benedict, R.J., Lee, C.M., Staley, D.M., 2008. Spruce trees from a melting ice patch: evidence for Holocene climatic change in the Colorado Rocky Mountains, USA. The Holocene 18, 1067-1076.

Beniston, M., Diaz, H.F., Bradley, R.S., 1997. Climate change at high-elevation sites: an overview. Climatic Change 36**,** 233-251.

Benson, L., Berry, M.S., 2009. Climate change and cultural response in the prehistoric Southwest. KIVA 75, 89-119.

Betancourt, J.L., 1990. Late Quaternary biogeography of the Colorado Plateau, in: Betancourt, J.L., Van Devender, T.R., Martin, P.S. (Eds.), Packrat middens: The last 40,000 years of Biotic Change. University of Arizona Press, Tucson, Arizona, pp. 259-293.

Bigio, E., Swetnam, T., Baisan, C., 2010. A comparison and integration of tree-ring and alluvial records of fire history at the Missionary Ridge Fire, Durango, CO, USA. The Holocene 20, 1047-1061.

Birks, H.H., 2003. The importance of plant macrofossils in the reconstruction of lateglacial vegetation and climate: examples from Scotland, western Norway, and Minnesota, USA. Quaternary Science Reviews 22, 453-473.

Birks, H.H., 2006. Plant macrofossils, in: Smol, J.P., Birks, B., Last, W.M. (Eds.), Tracking Environmental Change Using Lake Sediments: Terrestrial, Algal, and Siliceous Indicators. Kluwer Academic Publishers, Dordrecht, Netherlands, pp. 49-74.

Blaauw, M., Christen, J.A., 2011. Flexible paleoclimate age-depth models using an autoregressive gamma process. Bayesian Analysis 6, 457-474.

Bradley, R.S., 1999. Dating methods I, in: Bradley, R.J. (Ed.), Paleoclimatology, third edition. Elsevier/Academic Press, pp. 55-100.

Brunelle, A., Rehfeldt, G.E., Bentz, B., Munson, A.S., 2008. Holocene records of *Dendroctonus* bark beetles in high-elevation pine forests of Idaho and Montana, USA. Forest Ecology and Management 255, 836-846.

Brunner-Jass, R.M., 1999. Fire occurrence and paleoecology at Alamo Bog and Chihuahueños Bog, Jemez Mountains, New Mexico, USA. MS Thesis, Northern Arizona University, Flagstaff, Arizona.

Carrara, P.E., 2011. Deglaciation and postglacial treeline fluctuation in the northern San Juan Mountains, Colorado. U.S. Geological Survey Professional Paper 1782, 1-48.

Carrara, P.E., Mode, W.N., Rubin, M., 1984. Deglaciation and postglacial timberline in the San Juan Mountains, Colorado. Quaternary Research 21, 42-55.

Chambers, C.L., Holthausen, R.S., 2000. Montane ecosystems used as rangelands, in: Jemison, R., Raish, C. (Eds), Livestock Management in the American Southwest: Ecology, Society, and Economics. Elsevier, New York, pp. 213-280.

Chylek, P., Manvendra, D., Lesins, G., Li, J., Hengartner, N., 2014. Imprint of the Atlantic multi-decadal oscillation and Pacific decadal oscillation on southwestern US climate: past, present, and future. Climate Dynamics 43, 119-129.

Colorado River Water Users Association (CRWUA), 2017. Agriculture. https://www.crwua.org/colorado-river/uses/agriculture (accessed 17 December 2017).

Colorado State Forest Service (CSFS), 2012. 2012 Report on the health of Colorado's forests. Colorado State Forest Service, Fort Collins, Colorado.

Conedera, M., Tinner, W., Neff, C., Meurer, M., Dickens, A.F., Krebs, P., 2009. Reconstructing past fire regimes: methods, applications, and relevance to fire management and conservation. Quaternary Science Reviews 28, 555-576.

Cook, E.R., Krusic, P.J., 2004. The North American Drought Atlas. Lamont-Doherty Earth Observatory and the National Science Foundation.

Cook, E.R., Woodhouse, C.A., Eakin, C.M., Meko, D.M., Stahle, D.W., 2004. Long term aridity changes in the western United States. Science 306, 1015-1018.

Costigan, K.R., Bossert, J.E., Langley, D.L., 2000. Atmospheric/hydrologic models for the Rio Grande Basin: simulations of precipitation variability. Global and Planetary Change 25, 83-110.

Cour, P., Zheng, Z., Duzer, D., Calleja, M., Yao, Z., 1999. Vegetational and climatic significance of modern pollen rain in northwestern Tibet. Review of Palaeobotany and Palynology 104, 183-204.

Daubenmire, R.F., 1938. Merriam's life zones of North America. The Quarterly Review of Biology 13, 327-332.

Dean, J.S., 1994. The Medieval Warm Period on the southern Colorado Plateau. Climatic Change 26, 225-241.

Dearing, J.A., 1999. Holocene environmental change from magnetic proxies in lake sediments, in: Maher, B.A., Thompson, R. (Eds.), Quaternary Climates, Environments and Magnetism. Cambridge University Press, Cambridge, UK, pp. 231-278.

Denis, E.H., Toney, J.L., Tarozo, R., Anderson, R.S., Roach, L.D., Huang, Y., 2012. Polycyclic aromatic hydrocarbons (PAHs) in lake sediments record historic fire events: validation using HPLC-fluorescence detection. Organic Geochemistry 45, 7-17.

Denver Post, 2016. Colorado's largest wildfires (burn area). https://www.denverpost.com/2012/06/25/colorados-largest-wildfires-burn-area/ (accessed 5 April 2018).

DeRose, R. J., Long, J. N., 2007. Disturbance, structure, and composition: spruce beetle and Engelmann spruce forests on the Markagunt Plateau, Utah. Forest Ecology and Management 244, 16-23.

Dietl, G. P., Flessa, K. W., 2011. Conservation paleobiology: putting the dead to work. Trends in Ecology and Evolution 26, 30-37.

Eddy, J.E., 1976. The Maunder Minimum. Science 192, 1189-1202.

Elias, S.A., 2007. Plant macrofossil methods and studies: Rodent middens, in: Elias, S.A. (Ed.), Encyclopedia of Quaternary Science. Elsevier Science Publishers, Amsterdam, Netherlands, pp. 2356-2367.

Elias, S.A., Carrara, P.E., Toolin, L.J., Jull, J.T., 1991. Revised age of deglaciation of Lake Emma based on new radiocarbon and macrofossil analyses. Quaternary Research 36, 307-321.

Faegri, K., Iversen, J., 1989. Textbook of Pollen Analysis. Wiley, New York, New York.

Fall, P.L., 1992. Pollen accumulation in a montane region of Colorado, USA: a comparison of moss polsters, atmospheric traps and natural basins. Review of Palaeobotany and Palynology 72, 169-197.

Fall, P.L., 1997. Timberline fluctuations and late Quaternary paleoclimates in the southern Rocky Mountains, Colorado. Geological Society of America Bulletin 109, 1306-1320.

Fink, M., Rondeau, R., Decker, K., 2014. Treeline monitoring in the San Juan Mountains. Colorado Natural Heritage Program. http://www.cnhp.colostate.edu/download/documents/2014/Final_Treeline_report_2014.pdf (accessed 12 December 2017).

Finkelstein, D.B., Pratt, L.M., Curtin, T.M., Brassell, S.C., 2005. Wildfires and seasonal aridity recorded in late Cretaceous strata from southeastern Arizona, USA. Sedimentology 52, 587-599.

Flint, R., Flint S.C., 2005. Documents of the Coronado expedition, 1539-1542: "They were not familiar with his majesty, nor did they wish to be his subjects." Southern Methodist University Press, Dallas, Texas.

Forman, S.L., Spaeth, M., Marín, L, Pierson, J., Gómez, J., Bunch, F., Valdez, A., 2006. Episodic late Holocene dune movements on the sand-sheet area, Great Sand Dunes National Park and Preserve, San Luis Valley, Colorado, USA. Quaternary Research 66, 97-108.

Fouinat, L., Sabatier, P., Poulenard, J., Reyss, J., Montet, X., Arnaud, F., 2016. A new methodology exploring the record of snow avalanches in lake sediments. Earth Surface Dynamics 5, 199-209

Friedman, I., Carrara, P., Gleason, J., 1988. Isotopic evidence of Holocene climate change in the San Juan Mountains, Colorado. Quaternary Research 30, 350-353.

Fulé, P.Z., Crouse, J.E., Heinlein, T.A., Moore, M.M., Covington, W.W., Verkamp, G., 2003. Mixed-severity fire regime in a high-elevation forest of Grand Canyon, Arizona, USA. Landscape Ecology 18, 465-486.

Gabos, S., Ikonomou, M.G., Schopflocher, D., Fowler, B.R., White, J., Prepas, E., Prince, D., Chen, W., 2001. Characteristics of PAHs, PCDD/Fs and PCBs in sediment following forest fires in northern Alberta. Chemosphere 43, 709-719.

Goosse, H., Crepin, E., Dubinkina, S., Loutre, M., Mann, M.E., Renssen, H., Sallaz-Damaz, Y., Shindell, D., 2012. The role of forcing and internal dynamics in explaining the “Medieval Climate Anomaly”. Climate Dynamics 39, 2847-2866.

Grace, J., Berninger, F., Nagy, L., 2002. Impact of climate change on the tree line. Annals of Botany 90, 537-544.

Grimm, E.C., 2005. TILIA and TILIA GRAPH. PC spreadsheet and graphics software for pollen data. Illinois State Museum, Springfield, IL.

Grissino-Mayer, H.D., 1995. The climate and fire history of El Malpais National Monument, New Mexico. Ph.D. Dissertation, University of Arizona, Tucson, Arizona.

Grissino-Mayer, H.D., Swetnam, T.W., 2000. Century scale climate forcing of fire regimes in the American Southwest. The Holocene 10, 213-220.

Grissino-Mayer, H.D., Romme, W.H., Floyd, M.L., Hanna, D.D., 2004. Climatic and human influences on fire regimes of the southern San Juan Mountains, Colorado, USA. Ecology 85, 1708-1724.

Grove, J.M., Switsur, R., 1994. Glacial geological evidence for the Medieval Warm Period. Climatic Change 26, 143-169.

Guido, Z.S., Ward, D.J., Anderson, R.S., 2007. Pacing the post-Last Glacial Maximum demise of the Animas Valley glacier and the San Juan Mountain ice cap, Colorado. Geology 8, 739-742.

Hayes, J.J., Robeson, S.M., 2011. Relationships between fire severity and post-fire landscape pattern following a large mixed-severity fire in the Valle Vidal, New Mexico, USA. Forest Ecology and Management 261, 1392-1400.

Herring, E.M., Anderson, R.S., San Miguel, G.S., 2014. Fire, vegetation, and Ancestral Puebloans: A sediment record from Prater Canyon in Mesa Verde National Park, Colorado, USA. The Holocene 24, 853-863.

Higgins, R.W., Yao, Y., Wang, X.L., 1997. Influence of the North American monsoon system on the United States summer precipitation regime. Journal of Climatology 10, 2600-2622.

Higuera, P.E., Brubaker, L.B., Anderson, P.M., Hu, F.S., Brown, T.A., 2009. Vegetation mediated the impacts of postglacial climate change on fire regimes in the south-central Brooks Range, Alaska. Ecological Monographs 79, 201-219.

Hughes, M.K., Diaz, H.F., 1994. Was there a "Medieval Warm Period", and if so, where and when? Climatic Change 26, 109-142.

Husar, R.B., Sullivan, T.J., Charles, D.F., 1991. Historical trends in atmospheric sulfur deposition and methods for assessing long-term trends in surface water chemistry, in: Charles, D.F. (Ed.), Acidic Deposition and Aquatic Ecosystems. Springer, New York, New York, pp. 65-82.

International Boundary and Water Commission (IBWC), 2016. About the Rio Grande. https://www.ibwc.gov/CRP/riogrande.htm (accessed 7 December 2016).

Jackson, S.T., Gray, S.T., Shuman, B., 2009. Paleoecology and resource management in a dynamic landscape: Case studies from the Rocky Mountain headwaters, in: Dietl, G.P., Flessa, K.W. (Eds), Conservation Paleobiology: Using the Past to Manage the Future. Paleontological Society short course, The Paleontological Society papers 15, pp. 67-86.

Jiang, C., Alexander, R., Kagi, R.I., Murray, A.P., 1998. Polycyclic aromatic hydrocarbons in ancient sediments and their relationships to palaeoclimate. Organic Geochemistry 29, 1721-1735.

Jiménez-Moreno, G., Anderson, R.S., 2012. Pollen and macrofossil evidence of late Pleistocene and Holocene treeline fluctuations from an alpine lake in Colorado, USA. The Holocene 23, 68-77.

Jiménez-Moreno, G., Fawcett, P.J., Anderson, R.S., 2008. Millennial- and centennial-scale vegetation and climate changes during the late Pleistocene and Holocene from northern New Mexico, USA. Quaternary Science Reviews 27, 1442-1452.

Jiménez-Moreno, G., Anderson, R.S., Desprat, S., Grigg, L.D., Grimm, E.C., Heusser, L.E., Jacobs, B.F., López-Martínez, C., Whitlock, C.L., Willard, D.A., 2010. Millennial-scale variability during the last glacial in vegetation records from North America. Quaternary Science Reviews 29, 2865-2881.

Jiménez-Moreno, G., Anderson, R.S., Atudorei, V., Toney, J.L., 2011. A high-resolution record of vegetation, climate, and fire regimes in the mixed conifer forest of northern Colorado USA. Geological Society of America Bulletin 123, 240-254.

Johnsen, AR. Wick, L.Y., Harms, H., 2005. Principles of microbial PAH-degradation in soil. Environmental Pollution 133, 71-83.

Johnson, B.G., 2012. Holocene landscape evolution of alpine areas in the southern San Juan Mountains, Colorado. Vignettes: Key Concepts in Geomorphology. http://serc.carleton.edu/vignettes/collection/42895.html (accessed 5 March 2016).

Johnson, B.G., Eppes, M.C., Diemer, J.A., Jiménez-Moreno, G., Layzell, A.L., 2011. Post-glacial landscape response to climate variability in the southeastern San Juan Mountains of Colorado, USA. Quaternary Research 76, 352-362.

Johnson, B.G, Jiménez-Moreno, G., Eppes, M.C., Martha, Diemer, J.A., Stone, J.R., 2013. A multiproxy record of postglacial climate variability from a shallowing, 12-m deep subalpine bog in the southeastern San Juan Mountains of Colorado, USA. The Holocene 23, 1028-1038.

Johnson, B.G., Layzell, A.L., Eppes, M.C., 2015. Chronosequence development and soil variability from a variety of sub-alpine, post-glacial landforms and deposits in the southeastern San Juan Mountains of Colorado. Catena 127, 222-239.

Kegley, S.J., 2006. Western balsam bark beetle, ecology and management, in: U.S. Department of Agriculture, Forest Service. Forest Insect and Disease Identification and Management Guide of Northern and Central Rocky Mountain Conifer and Hardwood. U.S. Department of Agriculture, Forest Service, Forest Health Protection, Region 1 and 4. http://www.fs.fed.us/r1-r4/spf/fhp/mgt_guide/western_balsambark_beetle/index.html. (accessed 3 April 2018).

Kenner, R., Bühler, Y., Delaloye, R., Ginzler, C., Phillips, M., 2014. Monitoring of high alpine mass movements combining laser scanning with digital airborne photogrammetry. Geomorphology 206, 492-504.

Killops, S.D., Massoud, M.S., 1992. Polycyclic aromatic hydrocarbons of pyrolytic origin in ancient sediments: evidence for Jurassic vegetation fires. Organic Geochemistry 18, 1-7.

Kulakowski, D., Veblen, T.T., 2007. Effect of prior disturbances on the extent and severity of wildfire in Colorado subalpine forests. Ecology 88, 759-769.

Lamb, H.H., 1965. The early medieval warm epoch and its sequel. Palaeogeography, Palaeoclimatology, Palaeoecology 1, 1-13.

Legg, T.E., Baker, R.G., 1980. Palynology of Pinedale sediments, Devlins Park, Boulder County, Colorado. Arctic and Alpine Research 12, 319-333.

Lekson, S.H., 1999a. The Chaco Meridian: Centers of political power in the ancient Southwest. Altamira Press/Sage Publications, Thousand Oaks, California, USA.

Lekson, S.H., 1999b. Chapter one: Great towns in the Southwest, in: Neitzel, J.E. (Ed.), Great Towns and Regional Polities in the Prehistoric American Southwest and Southeast. An Amerind Foundation Publication, Dragoon, AZ. University of New Mexico Press, Albuquerque, New Mexico.

Liepelt, S., Cheddadi, R., Beaulieu, J., Fady, B., Gömöry, D., Hussendörfer, E., Konnert, M., Litt, T., Longauer, R., Terhürne-Berson, R., Ziegenhagen, B., 2009. Postglacial range expansion and its genetic imprints in *Abies alba* (Mill.) – A synthesis from palaeobotanic and genetic data. Review of Palaeobotany and Palynology 153, 139-149.

Lipman, P.W., 1975. Evolution of the Platoro Caldera Complex and Related Volcanic Rocks, Southeastern San Juan Mountains, Colorado. U.S. Geological Survey Professional Paper 852, 1-128.

Lipman, P.W., Dungan, M.A., Brown, L.L., Deino, A., 1996. Recurrent eruption and subsidence at the Platoro caldera complex, southeastern San Juan volcanic field, Colorado: New tales from old tuffs. Geological Society of America Bulletin 8, 1039-1055.

Loisel, J., MacDonald, G.M., Thomson, M.J., 2017. Little Ice Age climate erraticism as an analogue for future enhanced hydroclimatic variability across the American Southwest. PLoS ONE 12, e0186282.

Lynch, E.A., 1996. The ability of pollen from small lakes and ponds to sense fine-scale vegetation patterns in the central Rocky Mountains, USA. Review of Palaeobotany and Palynology 94, 197-210.

Maher, L., 1961. Pollen analysis and postglacial vegetation history in the Animas Valley region, southern San Juan Mountains, Colorado. Unpublished Ph.D. Dissertation, University of Minnesota, Saint Paul, Minnesota.

Maher, L., 1972. Nomograms for computing 0.95 limits of pollen data. Review of Palaeobotany and Palynology 13, 85-93.

Mann, M.E., 2002a. Little Ice Age, in: Munn, T., MacCracken, M.C., Perry, J.S. (Eds.), Vol 1, The Earth System: Physical and Chemical Dimensions of Global Environmental Change, Encyclopedia of Global and Environmental Change. John Wiley and Sons, Ltd, Chichester, pp. 504-509.

Mann, M.E., 2002b. Medieval Climatic Optimum, in: Munn, T., MacCracken, M.C., Perry, J.S. (Eds.), Vol 1, The Earth System: Physical and Chemical Dimensions of Global Environmental Change, Encyclopedia of Global and Environmental Change. John Wiley and Sons, Ltd, Chichester, pp. 514-516.

Mann, M.E., Bradley, R.S., Hughes, M.S., 1998. Global-scale temperature patterns and climate forcing over the past six centuries. Nature 392, 779–787.

Mann, M.E., Zhang, Z., Rutherford, S., Bradley, R.S., Hughes, M.K., Shindell, D., Ammann, C., Faluvegi, G., Ni, F., 2009. Global signatures and dynamical origins of the Little Ice Age and Medieval Climate Anomaly. Science 27, 1256-1260.

Marchi, L., Borga, M., 2012. Flash Floods in Alpine Basins, in: Krecek, J., Haigh, M.J., Hofer, T., Kubin, E. (Eds.), Management of Mountain Watersheds. Springer, Dordrecht, Netherlands, pp. 83-92.

Margolis, E.Q., 2014. Fire regime shift linked to increased forest density in a piñon-juniper savanna landscape. International Journal of Wildland Fire 23, 234-245.

Margolis, E.Q., Swetnam, T.W., Allen, C.D., 2007. A stand-replacing fire history in upper montane forests of the southern Rocky Mountains. Canadian Journal of Forest Restoration 37, 2227-2241.

Margolis, E.Q., Swetnam, T.W., Allen, C.D., 2011. Historical stand-replacing fire in upper montane forests of the Madrean sky islands and the Mogollon Plateau, southwestern USA. Fire Ecology 7, 88-107.

Markgraf, V., Scott, L., 1981. Lower timberline in central Colorado during the past 15,000 years. Geology 9, 231-234.

Marlon, J.R., Bartlein, P.J., Gavin, D.G., Long, C.J., Anderson, R.S., Briles, C.E., Brown, K.J., Colombaroli, D., Hallett, D.J., Power, M.J., Scharf, E.A., Walsh, M.K., 2012. Long-term perspective on wildfires in the western USA. Proceedings of the National Academy of Science 109, 535-543.

Masson-Delmotte, V., Schulz, M., Abe-Ouchi, A., Beer, J., Ganopolski, A., González Rouco, J.F., Jansen, E., Lambeck, K., Luterbacher, J., Naish, T., Osborn, T., Otto-Bliesner, B., Quinn, T., Ramesh, R., Rojas, M., Shao, X., Timmermann, A., 2013. Information from Paleoclimate Archives, in: Stocker, T.F., Qin, D., Plattner, G.-K., Tignor, M., Allen, S.K., Boschung, J., Nauels, A., Xia, Y., Bex, V., Midgely, P.M. (Eds.), Climate Change

2013: the physical science basis. Contribution of Working Group I to the Fifth Assessment Report of the Intergovernmental Panel on Climate Change. Cambridge University Press, Cambridge, UK and New York, NY, USA, pp. 383-464.

Mateo, E.I., 2017. Rock glacier hydrology in the San Juan Mountains, Colorado. MS Thesis, University of Denver, Denver, Colorado.

Matthes, F. E., 1939. Report of Committee on Glaciers, April 1939. Transactions, American Geophysical Union 20, 518-523.

McGrath, T.E., Chan, W.G., Hajaligol, M.R., 2003. Low temperature mechanism for the formation of polycyclic aromatic hydrocarbons from the pyrolysis of cellulose. Journal of Analytical and Applied Pyrolysis 66, 51-70.

McKay, N.P., Kaufman, D., Michelutti. N., 2008. Biogenic silica concentration as a high-resolution, quantitative temperature proxy at Hallet Lake, south-central Alaska. Geophysical Research Letters 35, 4-9.

McMillin, J.D., Allen, K.K., Long, D.F., Harris, J.L., Negron, J.F., 2003. Effects of western balsam bark beetle on spruce-fir forests of north-central Wyoming. Western Journal of Applied Forestry 18, 259-266.

Meko, D. M., Woodhouse, C., Baisan, C., Knight, T., Lukas, J., Hughes, M., Salzer, W., 2007. Medieval drought in the upper Colorado River basin. Geophysical Research Letters 34, 1-5.

Mensing, S.A., Smith, J., Allan, M., Norman, K.B., 2007. Extended drought in the Great Basin western North America in the last two millennia reconstructed from pollen records. Quaternary International 188, 79-89.

Miller, D.R., Castañeda, I.S., Bradley, R.S., MacDonald D., 2017. Local and regional wildfire activity in central Maine (USA) during the past 900 years. Journal of Paleolimnology 58, 455-466.

Mitchell, V.L., 1976. The regionalization of climate in the western United States. Journal of Applied Meteorology 15, 920-927.

Mock, C.J., 1996. Climate controls and spatial variations of precipitation in the western United States. Journal of Climate 9, 111-1125.

Monastersky, R., 2015. And then there were none: seven centuries ago, tens of thousands of people mysteriously fled their homes in the American Southwest. Archaeologists are trying to work out why. Nature 527, 26-29.

Moore, P.D., Webb, J.A., 1978. An illustrated guide to pollen analysis. Hodder Arnold, London, UK.

Morris, J.L., Mustaphi, C.J., Carter, V., Watt, J., Derr, K., Pisaric, M., Anderson, R.S., Brunelle, A.R., 2015. Do bark beetle remains in lake sediments correspond to severe outbreaks? A review of published and ongoing research. Quaternary International 387, 72-86.

Nabbefeld, B., Grice, K., Summons, R.E., Hays, L.E., Cao, C., 2010. Significance of polycyclic aromatic hydrocarbons (PAHs) in Permian/Triassic boundary sections. Applied Geochemistry 25, 1374-1382.

Neff, J.M., 1979. Polycyclic Aromatic Hyrdrocarbons in the Aquatic Environment: sources, fates, and biological effects. Applied Science Publishers Ltd., London, U.K.

Nydick, K., Crawford, J., Bidwell, M., Livensperger, C., Rangwala, I., Cozetto, K., 2012. Climate change assessment for the San Juan Mountain regions, southwestern Colorado, USA: a review of scientific research. Mountain Studies Institute, U.S. Department of Agriculture, Forest Service, San Juan National Forest Service, and U.S. Department of the Interior, Bureau of Land Management Tres Rios Field Office, Durango, CO. https://static1.squarespace.com/static/53bc5871e4b095b6a42949b4/t/54c68f8ae4b062b0cea8b189/1422299018785/ClimateResearchReview_SJMs_FINAL.pdf (accessed 7 November, 2015).

Olivier, S., Bajo, S., Fifield, L.K., Gäggeler, H., Papina, T., Santschi, P.H., Ulrich, S., Schwikowski, M., Wacker, L., 2004. Plutonium from global fallout recorded in an ice core from the Belukha Glacier, Siberian Altai. Environmental Science and Technology 38, 6507-6512.

Page, D.S., Boehm, P.D., Douglas, G.S. Bence, A.E., Burns, W.A., Mankiewicz, P.J., 1999. Pyrogenic polycyclic aromatic hydrocarbons in sediments record past human activity: a case study in Prince William Sound, Alaska. Marine Pollution Bulletin 38, 247-260.

PAGES 2k Consortium, 2013. Continental-scale temperature variability during the past two millennia. Nature Geoscience 6, 339-346.

Pampanin, D.M., Sydnes, M.O., 2013. Polycyclic Aromatic Hydrocarbons a constituent of petroleum: presence and influence in the aquatic environment, in: Kutcherov, V. (Ed.), IntechOpen, pp. 83-118.

Pase, C.P., Brown, D.E., 1994. Rocky Mountain (Petran) subalpine conifer forest, in: Brown, D.E. (Ed.), Biotic Communities: southwestern United States and northwestern Mexico. University of Utah Press, Salt Lake City, Utah, pp. 43-48.

Pepin, N., Bradley, R.S., Diaz, H.F., Baraer, M., Caceres, E.B., Forsythe, N., Fowler, H., Greenwood, G., Hashmi, M.Z., Liu, X.D., Miller, J.R., Ning, L., Ohmura, A., Palazzi, E., Rangwala, I., Schöner, W., Severskiy, I., Shahgedanova, M., Wang, M.B., Williamson, S.N., Yang, D.Q., 2015. Elevation-dependent warming in mountain regions of the world. Nature Climate Change 5, 424-430.

Petersen, K.L., 1994. A warm and wet Little Climatic Optimum and a cold and dry Little Ice Age in the southern Rocky Mountains, USA. Climatic Change 26, 243-269.

Pfister, R.D., 1972. Vegetation and soils in the subalpine forest of Utah. Ph.D. Dissertation, Washington State University, Pullman, Washington.

Pierce, J.L., Meyer, G.A., 2008. Long-term fire history from alluvial fan sediments: the role of drought and climate variability, and implications for management of Rocky Mountain forests. International Journal of Wildland Fire 17, 84-95.

Pierce, K.L., 2003. Pleistocene glaciations of the Rocky Mountains, in: Gillespie, A.R., Porter, S.C., Atwater, B.F. (Eds.), The Quaternary Period in the United States. Developments in Quaternary Science, Elsevier, Amsterdam, Netherlands, pp. 63-76.

Plog, S., 1997. Ancient peoples of the Southwest. Thames and Hudson Ltd., London, UK.

Power, M.J., Mayle, F.E., Bartlein, P.J., Marlon, J.R., Anderson, R.S., Behling, H., Brown, K.J., Carcaillet, C., Colombaroli, D., Gave, D., Hallett, D., Horn, S., Kennedy, L., Lane, C., Long, C., Moreno, P., Paitre, C., Robinson, G., Taylor, Z., Walsh, M.K., 2012. Climatic control of the biomass-burning decline in the Americas after AD 1500. The Holocene 23, 2-13.

Rangwala, I., Sinsky, E., Miller, J.R., 2013. Amplified warming projections for high altitude regions of the northern hemisphere mid-latitudes from CMIP5 models. Environmental Research Letters 8, 1-9.

Reasoner, M.A., Jodry, M.A., 2000. Rapid response of alpine timberline vegetation to the Younger Dryas climate oscillation in the Colorado Rocky Mountains, USA. Geology 28, 51-54.

Romme, W.H., Clement, J., Hicke, J., Kulakowski, D., MacDonald, L.H., Schoennagel, T.L., Veblen, T.T., 2006. Recent forest insect outbreaks and fire risk in Colorado forests: a brief synthesis of relevant research. Colorado Forest Restoration Institute, Colorado State Forest Service, Fort Collins, Colorado.

Romme, W.H., Allen, C.D., Bailey, J.D., Baker, W.L., Bestelmeyer, B.T., Brown, P.M., Eisenhart, K.S., Floyd, L.M., Huffman, D.W., Jacobs, B.F., Miller, R.M., Muldavin, E.H., Swetnam, T.W., Tausch, R.J., Weisberg, P.J., 2009b. Historical and modern disturbance regimes, stand structures, and landscape dynamics in piñon-juniper vegetation of the western United States. Rangeland Ecology Management 62, 203-222.

Romme, W. H., Floyd, M. L., Hanna, D., Bartlett., E.J., 2009a. Historical range of variability and current landscape condition analysis: south central highlands section, southwestern Colorado and northwestern New Mexico. Colorado Forest Restoration Institute, Colorado State University, Fort Collins, Colorado.

Routson, C., Woodhouse, C., Overpeck, J., 2011. Second century megadrought in the Rio Grande headwaters, Colorado: how unusual was medieval drought? Geophysical Research Letters 38, 1-5.

Routson, C., Overpeck, J.T., Woodhouse, C.A., Kennedy, W.F., 2016. Three millennia of southwestern North American dustiness and future implications. PLoS ONE 11, e0149573.

Salzer, M.W., Kipfmueller K.F., 2005. Reconstructed temperature and precipitation on a millennial timescale from tree-rings in the southern Colorado Plateau, USA. Climatic Change 70, 465-487.

Sandgren, P., Snowball, I., 2001. Application of mineral magnetic techniques to paleolimnology, in: Last, W.M, Smol, J.P. (Eds.), Tracking Environmental Change Using Lake Sediments: Physical and Chemical Techniques, developments in paleoenvironmental research, Vol. 2. Kluwer Academic Publishers, Dordrecht, Netherlands, pp. 217-237.

Schwindt, D., Bocinsky, R.K., Ortman, S.G., Glowacki, D.M., Varien, M.D., Kohler, T.A., 2016. The social consequences of climate change in the central Mesa Verde region. American Antiquity 81, 74-96.

Seager, R., Vecchi, G.A., 2010. Greenhouse warming and the 21st century hydroclimate of southwestern North America. Proceedings of the National Academy of Sciences 107, 21277-21282.

Seppä, H., 2007. Pollen analysis, principles, in: Elias, S.A. (Ed.), Encyclopedia of Quaternary Science. Elsevier, pp. 2486-2498.

Short, S.K., Elias, S.A., 1987. New pollen and beetle analyses at the Mary Jane site, Colorado: evidence for late glacial tundra conditions. Geological Society of America Bulletin 98, 540-548.

Shuman, B.N., Henderson, A.K., Colman, S.M., Stone, J.R., Fritz, S.C., Steven, L.R., Power, M.J., Whitlock, C., 2009. Holocene lake-level trend in the Rocky Mountains, USA. Quaternary Science Reviews 28, 1861-1879.

Sibold, J.S., Veblen, T.T., Gonzalez., M.E., 2006. Spatial and temporal variation in historic fire regimes in subalpine forests across the Colorado Front Range in Rocky Mountain National Park, Colorado, USA. Journal of Biogeography 33, 631–647.

Smeardon, J.E., Pollack, H.N., 2016. Reconstructing Earth's surface temperature over the past 2000 years: the science behind the headlines. WIREs Climate Changes, Advanced Review 7, 746-771.

Steinhilber, F., Beer, J., Fröhlich, C., 2009. Total solar irradiance during the Holocene. Geophysical Research Letters 36, 1-5.

Steven, T.A., Lipman, P.W., Hail, W.J., Barker, F., Luedke, R.G., 1974. Geologic map of the Durango quadrangle, southwestern Colorado. U.S. Geological Survey, Miscellaneous Investigations Series Map I-764, scale 1:250,000.

Stogiannidis, E., Laane, D., 2015. Source characterization of Polycyclic Aromatic Hydrocarbons by using their molecular indices: an overview of possibilities, in: Whitacre, D.M. (Ed.), Reviews of Environmental Contamination and Toxicology 234, Springer Nature, Cham, Switzerland, pp. 49-133.

Stuiver, M., Reimer, P.J., Reimer, R.W., 2018. CALIB 7.1. http://calib.org (accessed 24 January 2018).

Taylor, R.E., 1987. Chapter 2 – Definition of Major Anomalies, in: Taylor, R.E. (Ed.), Radiocarbon Dating an Archaeological Perspective. Academic Press, Cambridge, MA, pp. 15-38.

Thompson, J., 2002. Lime Creek Burn, 1879. San Juan Mountain Journal 3, 7-9.

Thompson, R., Oldfield, F., 1986. Environmental magnetism. George Allen and Unwin Ltd., Crows Nest, New South Wales, Australia, pp. 1-183.

Thompson, R.S., Anderson, K.H., 2013. Past climate and vegetation changes in the southwestern United States, impact of climate change and land use in the southwestern United States. http://geochange.er.usgs.gov/sw/impacts/biology/pastclim/ (accessed 23 January 2016).

Toney, J.L., 2004. A postglacial paleoecological record from Little Molas Lake, San Juan Mountains, Colorado. MS Thesis, Northern Arizona University, Flagstaff, Arizona.

Toney, J.L., Anderson, R.S., 2006. A postglacial palaeoecological record from the San Juan Mountains of Colorado USA: fire, climate and vegetation history. The Holocene 16, 505-517.

Turney, C.S.M., Kershaw, A.P., Clemens, S.C., Branch, N., Moss, P.T., Fifield, L.K., 2004. Millennial and orbital variations of El Niño/Southern Oscillation and high-latitude climate in the last glacial period. Nature 428, 306-310.

United States Department of the Interior – Bureau of Reclamation (USDI), 2012. Colorado River basin water supply and demand study – executive summary. https://www.usbr.gov/watersmart//bsp/docs/finalreport/ColoradoRiver/CRBS_Executive_Summary_FINAL.pdf (accessed 10 October 2017).

van der Plicht, J., 2007. Variation in atmospheric ^{14}C, in: Elias, S.A. (Ed.), Encyclopedia of Quaternary Science. Elsevier, pp. 2923-2931.

Vankat, J.L., 2013. Spruce-fir forest, in: Vankat, J.L. (Ed.), Vegetation Dynamics on the Mountains and Plateaus of the American Southwest. Springer, New York, New York, pp. 72-123.

Veblen, T.T., Hadley, K.S., Reid, M.S., Rebertus, A.J., 1989. Blowdown and stand development in a Colorado subalpine forest. Canadian Journal of Forest Research 19, 1218-1225.

Veblen, T.T., Hadley, K.S., Nel, E.M., Kitzberger, T., Reid, M., Villalba, R., 1994. Disturbance regime and disturbance interactions in a Rocky Mountain subalpine forest. Journal of Ecology 82, 125-135.

Vierling, L.A., 1998. Palynological evidence for late- and postglacial environmental change in central Colorado. Quaternary Research 49, 222-232.

Walker, M.J.C., Berkelhammer, M., Björck, S., Cwynar, L.C., Fisher, D.A., Long, A.J., Lowe, J.J., Newnham, R.M., Rasmussen, S.O., Weiss, H., 2012. Formal subdivision of the Holocene series/epoch: a discussion paper by a work group of INTIMATE (Integration of ice-core, marine and terrestrial records) and the subcommission on Quaternary Stratigraphy (International Commission on Stratigraphy). Journal of Quaternary Science 27, 649-659.

Waters, C.N., Syvitski, J.P.M., Galuszka, A., Hancock, G.J., Zalasiewicz, J., Cearreta, A., Grinevald, J., Jeandel, C., McNeill, J.R., Summerhayes, C., Barnosky, A., 2015. Can nuclear weapons fallout mark the beginning of the Anthropocene Epoch? Bulletin of the Atomic Scientists 71, 46-57.

Watt, J.H., 2008. A Late-Holocene reconstruction of spruce beetle (*Dendroctonus rufipennis*) disturbance from Antler Pond, Colorado, USA. MS Thesis, Northern Arizona University, Flagstaff, Arizona.

Weber, W.A., Wittman, R.C., 2012. Colorado Flora – Western Slope, fourth ed. University Press of Colorado, Boulder, Colorado.

White, S., 2017. A cold welcome, the Little Ice Age and Europe’s encounter with North America. Harvard University Press, Cambridge, Massachusetts.

White, S.E., 1981. Alpine mass movement forms (non-catastrophic): classification, description, and significance. Arctic and Alpine Research 13, 127-137.

Whitlock, C., Larsen C., 2001. Charcoal as a fire proxy, in: Smol, J.P., Birks, B., Last, W.M. (Eds.), Tracking Environmental Change Using Lake Sediments: Terrestrial, Algal, and Siliceous Indicators. Kluwer Academic Publishers, Dordrecht, Netherlands, pp. 75-97.

Wingard, G.L., Bernhardt, C.E., Wachnicka, A.H., 2017. The role of paleoecology in restoration and resource management – The past as a guide to future decision-making: review and example from the greater Everglades ecosystem, USA. Frontiers in Ecology and Evolution 5, 1-11.

Winship, G.P., 1896. The Coronado expedition, 1540-1542, historical introduction, in: Powell, J.W. (Ed.), The Fourteenth Annual Report of the Bureau of Ethnology, part I. Government Printing Office Smithsonian Institution, Washington, D.C., pp. 393-599.

Wisconsin Department of Health Services (WDHS), 2015. Polycyclic Aromatic Hydrocarbons (PAHs). https://www.dhs.wisconsin.gov/chemical/pah.htm (accessed 23 January 2016).

Woodhouse, C.A., Meko, D.M., MacDonald, G.M., Stahle, D.W., Cook, E.R., 2010. A 1200-year perspective of 21st century drought in southwestern North America. Proceedings of the National Academy of Sciences 107, 21283-21288.

Wright, A.M., 2006. A low-frequency paleoclimatic reconstruction from the La Plata Mountains, Colorado, and its implications for agricultural productivity in the Mesa Verde region. MA Thesis, Washington State University, Pullman, Washington.

Yackulic, E., 2017. Productivity and temperature variability over the past 1500 years at a small alpine lake in the southern San Juan Mountains, Colorado. MS Thesis, Northern Arizona University, Flagstaff, Arizona.

Young, N.E., Schweinsberg, A.D., Briner, J.P., Schaefer, J.M., 2015. Glacier maxima in Baffin Bay during the Medieval Warm Period coeval with Norse settlement. Science Advances 1, e1500806.

Yuan, F., Koran, M.R., Valdez, A., 2013. Late glacial and Holocene record of climatic change in the southern Rocky Mountains from sediments in San Luis Lake, USA. Palaeogeography, Palaeoclimatology, Palaeoecology 392, 146-160.

Zheng, J., Wu, F., Yamada, M., Liao, H., Liu, C., Wan, G., 2008. Global fallout Pu recorded in lacustrine sediments in Lake Hongfeng, SW China. Environmental Pollution 152, 314-321.

Zier, J.L., Baker, W.L., 2006. A century of vegetation change in the San Juan Mountains, Colorado: an analysis using repeat photography. Forest Ecology and Management 228, 251-262.